PHENOTYPIC ANALYSIS OF STEM CELL MICROENVIRONMENTS WITHIN THE CONDUCTING AIRWAY EPITHELIUM

by

Adam Giangreco

Bachelor of Science, University of Rochester, 1999

Master of Science, University of Rochester, 2001

Submitted to the Graduate Faculty of

School of Medicine in partial fulfillment

of the requirements for the degree of

Doctor of Philosophy

University of Pittsburgh

2004

UNIVERSITY OF PITTSBURGH

FACULTY OF SCHOOL OF MEDICINE

This dissertation was presented

by

Adam Giangreco

It was defended on

April 12, 2004

and approved by

_____

Sergio A. Onate, Ph.D.

_____

Joseph M. Pilewski, M.D.

_____

Bruce R. Pitt, Ph.D.

_____

Simon C. Watkins, Ph.D.

_____

Barry R. Stripp, Ph.D.
Dissertation Director

PHENOTYPIC ANALYSIS OF STEM CELL MICROENVIRONMENTS WITHIN THE CONDUCTING AIRWAY EPITHELIUM

Adam Giangreco, PhD

University of Pittsburgh, 2004

The elucidation of mechanisms for epithelial maintenance and renewal after injury are central to understanding aspects of normal airway diversity and the pathobiology of lung diseases including asthma, chronic obstructive pulmonary disease, idiopathic pulmonary fibrosis, and cancer. Due to the low steady state turnover of the airway epithelium, it has been proposed that epithelial remodeling following chronic lung injury or disease may be the result of aberrant epithelial stem cell activation. Previous results indicated that intrapulmonary conducting airways contain rare populations of stem cells that localized to neuroepithelial body (NEB) microenvironments, and that these cells are activated following injury involving depletion of airway Clara cells. These airway cells were uniquely pollutant resistant, exhibited robust mitotic and differentiation potential, and exhibited the molecular property of Clara cell secretory protein (CCSP) expression. Despite this recent progress, many aspects of airway stem cell maintenance, initiation, and regulation remain elusive.

Studies presented in this dissertation were undertaken (1) to investigate the existence of alternate, regionally distinct airway stem cell populations, (2) to elucidate mechanisms of airway stem cell pollutant resistance, and (3) to identify signaling pathways associated with stem cell-associated repair. Results of these studies demonstrate the existence of unique, NEB microenvironment-independent CCSP expressing stem cells restricted to airway bronchoalveolar

duct junction (BADJ) microenvironments. Results also identify likely mechanisms of CCSP expressing stem cell pollutant resistance that include reduced levels of Cytochrome P450 expression and robust drug / pollutant efflux systems. Finally, results of these studies indicate that activation of the β-catenin signaling pathway and definitive downstream target genes occurs within NEB and BADJ microenvironments during airway regeneration. Together, these findings demonstrate that regionally distinct, pollutant resistant airway stem cell populations are responsible for the maintenance of appropriate epithelial diversity and facilitate renewal processes after injury. Furthermore, these studies support the notion that β-catenin signaling and downstream target gene activation are important mediators of stem cell-associated epithelial renewal.

DEDICATION

The work presented in this thesis is dedicated to my father Tom and my late mother, Janet Giangreco. Their love and support has been an unwavering source of encouragement in all that I've done.

ACKNOWLEDGEMENTS

"When the going gets weird, the weird turn pro." - HST

There are a number of people that need to be acknowledged who've helped me in some way or another to maintain perspective and focus on my journey into bat country and back again.

To my committee: Thank you for the helpful suggestions and comments over the past few years. You have all provided valuable insights in guiding my studies of airway epithelial stem cells.

Barry: in addition to providing scientific advice in the planning and execution of my work, I particularly appreciate your ability to maintain and encourage balance between "life" and "science life."

Sue: your daily advice and encouragement helped my projects to maintain critical focus and scientific rigor.

Greg, Kyung, and Tenea: thanks for the help and the examples you set for me as fellow Stripp lab graduates!

Charlotte, Candace, Fadra, and Carlos: thank you for your help and friendship in the lab these past few years and notably for sticking by during my more colorful moments.

And especially Dawn: Your encouragement and love for the past three years has been a constant source of joy. Every day I feel lucky to have someone as wonderful as you in my life. But I'm still not calling you Dr. Giangreco before me.

There are many other people, too numerous to mention who have helped and encouraged me on this journey through graduate school at both the University of Rochester and currently at the University of Pittsburgh. Thank you all.

ABBREVIATIONS

[3H]-TdR	Tritiated thymidine
ABC	ATP-binding cassette
ACT	Acetylated tubulin
APC	adenomatous polyposis coli
Ash1	Achaete scute homologue 1
BADJ	Broncho-alveolar duct junction
Bcrp1	Breast cancer resistance protein 1
BMP4	Bone morphogenic protein 4
BrdU	Bromodeoxyuridine
CCSP	Clara cell secretory protein
CCTK	CCSP promoter driven HSVtk transgenic mice
CE	CCSP Expressing
CGRP	Calcitonin gene related peptide
CYP2F2	Cytochrome P450 isoform 2F2
CYP450	Cytochrome P450
DAB	Diaminidobenzidine
DAPI	4, 6, diamidino-2-phenylindole
FGF	Fibroblast growth factor
GSI-β4	*Griffonia simplicifolia* isolectin-B4
GSK3β	Glycogen synthase kinase-3 beta
Hes1	Hairy enhancer of split 1

HSC	Hematopoietic stem cell
IP	Immuno-positive
IPF	Idiopathic pulmonary fibrosis
Lef	Lymphoid enhancer factor
LRC	Label retaining cell
MUC5AC	Mucin 5AC
NEB	Neuroepithelial body
NSCLC	Non-small cell lung carcinoma
PAS	Periodic acid schiff
PECAM	Platelet endothelial cell adhesion molecule
PI3K	Phosphatidyl inositol 3 phosphate kinase
PNEC	Pulmonary neuroendocrine cell
RT-PCR	Reverse transcription-polymerase chain reaction
Sca-1	Stem cell antigen 1
SCLC	Small cell lung carcinoma
Shh	Sonic Hedgehog
S-HRP	Streptavidin Horseradish peroxidase
SMG	Submucosal gland
SP	Side population
SP-C	Surfactant protein C
TA	Transit amplifying
Tcf	T-cell factor
TOPgal	TCF/ Lef optimal promoter β-galactosidase

vCE	Variant CCSP Expressing
Wnt	Inhibitor of Wingless
X-gal	5-bromo-4-chloro-3-indolyl-β-D-galactosidase

TABLE OF CONTENTS

LIST OF TABLES

LIST OF FIGURES

1. Introduction

1.1. Overview

The current chapter is an introduction to concepts in airway epithelial biology, progenitor cell biology, and identified airway-specific progenitor cells that are germane to subsequent studies proposed in Chapter 2 and presented in Chapters 3-5. Chapter 2 outlines the rationale and hypotheses of this project. Chapter 3 presents studies in which airway-specific Clara cell injury was used to investigate alternate airway stem cell microenvironments. Results indicate that the broncho-alveolar duct junction (BADJ) represents a niche for the maintenance of tissue-specific stem cells. Chapter 4 examines possible mechanisms for airway pollutant resistance within identified CCSP-expressing (CE) airway stem cells. This study demonstrates that Neuroepithelial body (NEB) microenvironment-associated CE stem cells contain reduced levels of the phase I metabolizing enzyme CYP2F2 (CYP2F2). Rare, drug-effluxing airway side population cells that maintain a molecular phenotype consistent with that of airway stem cells were also characterized. Chapter 5 presents β-catenin signaling activation during airway repair and its effects on stem cell proliferation, migration, and differentiation. Results presented in this chapter suggest that β-catenin signaling is preferentially activated within NEB and bronchoalveolar duct junction (BADJ) microenvironments concomitant with airway epithelial cell regeneration. Chapter 6 presents a summary and discussion of these results and provides future directions for the study of airway epithelial stem cells. Overall, studies presented in this dissertation characterize important aspects of airway stem cell-mediated renewal. These findings also highlight associations between chronic airway injury and microenvironment-associated renewal, epithelial remodeling, and the generation of airway disease.

1.2. Lung Injury and Disease

The conducting airway serves a number of functions in the maintenance of overall lung homeostasis and prevention of disease. Airways are lined by a highly specialized epithelium that serves to facilitate removal of respiratory byproducts, clear and detoxify inhaled pollutants, prevent loss of essential proteins / extracellular lining fluids, and modulate reparative and inflammatory processes following injury [104, 140, 161, 286, 287, 294, 295]. Changes to airway composition and function due to injury have the potential to disrupt lung homeostasis. Typically, resolution of airway injury is accompanied by transient or persistent epithelial cell hyperplasia [73, 74, 76, 108, 202, 203, 235, 242, 274]. Persistent epithelial hyperplasia is considered a risk factors in both small cell and non-small cell lung cancer development [18, 40, 41, 123, 127, 151, 152, 168, 255, 267]. Most frequently chronic patterns of lung injury, epithelial repair, and subsequent airway hyperplasia are self-induced due to heavy cigarette smoking [3, 246] However, numerous epidemiological studies also demonstrate an association between airway diseases or chronic pollutant exposures and the predisposition towards formation of lung cancer [53, 67, 174, 246, 264]. Many of the pathologic changes associated with cancer risk in human airways are also apparent in lungs of experimental animals.

1.2.1. Pollutant Injury and Chronic Lung Disease

The lung is highly susceptible to injury from a range of environmental pollutants that may be deposited in the lung either through inhalation or systemic routes depending on their physico-chemical properties [201, 203]. Airborne diesel exhaust particulate matter, residual oil fly ash, and numerous other fine and ultrafine particulates lodge within airways and induce varying degrees of epithelial injury. Prolonged exposure to these ubiquitous environmental

particulates is associated with decreased airway function and is considered a risk factor for chronic lung disease. Exposure to oxidant pollutants such as ozone results in predominately ciliated cell damage and is followed by cellular repair and hyperplasia [74, 75, 131, 214, 219]. Exposure to systemic lipophilic pollutants results in bioactivation-dependent toxicity among other subsets of airway cells [27, 83, 89, 147, 210, 211, 241, 277]. While short term affects of pollutant exposure may prove beneficial by tolerizing lungs against further injury, chronic exposures result in significant alterations to normal airway heterogeneity [202, 203, 212, 213, 302, 304]. Importantly, changes in murine conducting airways following chronic pollutant exposure and injury are often pathognomic to early events in neoplastic transformation [127, 151, 202, 212, 256].

In addition to repeated toxicant exposures, numerous chronic airway diseases including chronic obstructive pulmonary disease and idiopathic pulmonary fibrosis are associated with airway remodeling and increased cancer risk [40, 41, 65, 108, 263, 271]. Asthma is increasingly recognized as a disease of airway inflammation resulting in chronic epithelial injury, repair, and remodeling. Here, excessive activation of the immune system due to allergen sensitization results in high concentrations of airway-associated proteases and subsequent epithelial damage [108, 140, 263, 271]. Chronic stimulation of the airway immune response results in continuous cycling between epithelial injury and renewal processes, eventually resulting in changes to the normal airway cellular diversity and proximal-distal heterogeneity.

1.2.2. Lung Cancer

Despite significant evidence linking persistent airway injury / repair cycles with susceptibility and progression of lung disease, little is currently known regarding specific

mechanisms regulating epithelial renewal and cancer presdisposition. Additionally, few studies have successfully identified specific airway cell types or stem cell microenvironments that facilitate normal and dysregulated epithelial renewal. Lung cancer studies have previously implicated Clara and pulmonary neuroendocrine cells as progenitors of non-small cell lung carcinoma (NSCLC) and SCLC, respectively [100, 123, 134, 151, 152, 168, 254, 255, 267]. Importantly, several types of lung injury that result in persistent Clara and neuroendocrine cell proliferation are identified lung cancer risk factors [119, 202, 212, 241, 243, 249]. Also, genetically identical mutations indicative of early neoplastic transformation have been observed within multifocal, widely dispersed epithelial zones [91]. Together, these data point to the likely involvement of microenvironment-associated Clara and neuroendocrine cell subsets as initiators of NSCLC and SCLC. The studies presented in this dissertation define mechanisms regulating airway stem cell microenvironment activation within normal and injured lungs. It is anticipated that an understanding of mechanisms regulating stem cell maintenance and activation following acute injury will prove beneficial in designing therapies for chronically injured, and potentially neoplastic airways.

1.3. The Airway Epithelium

1.3.1. Adult Airway Cell Types

At least forty distinct cell types exist within mammalian lungs, many of which are specific to conducting airways [163, 286, 287]. Overall, the abundance of airway specific cell types varies according to developmentally established proximal-distal heterogeneity. Well-characterized airway specific cell types include goblet cells, serous cells, ciliated cells, basal cells, pulmonary neuroendocrine cells, and Clara cells (Figure 1.1). These cells regulate luminal salt concentrations, secrete bactericidal proteins, facilitate mucous clearance, provide appropriate epithelial barriers, and function as airway oxygen chemosensors [1, 38, 47, 80, 81, 143, 161, 189, 262, 306, 314]. Transient alterations to airway cellular diversity due to injury or disease results in activation of endogenous airway progenitor cells and restoration of normal epithelial cellular phenotypes [54, 74-76]. Expansions, alterations, and loss of airway cellular diversity results from chronic lung injury and subsequent aberrant progenitor cell activation. These changes result in decrements to lung function including inappropriate luminal protein secretions, failure of mucociliary clearance, loss of epithelial barrier function, and increased sensitivity to continued airway injury [33, 45, 65, 108, 146, 258]. To appreciate alterations in epithelial diversity associated with chronic injury and airway remodeling it is important to understand functions associated with normal airway epithelial cells.

Goblet cells are considered to be a terminally differentiated cell population located primarily in tracheas and large airways (Figure 1.1, light blue cells, trachea). These cells contain significant glycoprotein and produce most airway mucins. Mucin proteins remain associated with Goblet cell apical membranes or are secreted into the airway lumen. Extracellular Goblet

cell mucins enable efficient mucociliary clearance and inhibit bacterial adherence [189]. Goblet cells are identified by periodic acid-schiff (PAS) histochemical staining and immunohistochemical detection of Mucin 5AC (MUC5AC). While Goblet cells are terminally differentiated and incapable of cellular proliferation, asthma-associated Goblet cell hyperplasia occurs via Clara and basal cell metaplasia. As a result of metaplasia, some nascent Goblet cells express markers specific to both Clara and Goblet cell lineages (e.g., CCSP and PAS reactivity) [103, 139, 282]. Thus, while Goblet cells themselves are not a mitotic population responsible for altering normal epithelial diversity, the presence of ectopic Goblet cell phenotypes is strongly correlated with disease-associated airway injury and aberrant repair processes.

Ciliated cells are located throughout conducting airways and have been identified in all mammalian species studied (Figure 1.1, green cells). Ciliated cells are characterized by their cuboidal to columnar morphology and apically localized, synchronously beating cilia. These cells function to clear microbes and other harmful agents trapped within extracellular airway mucous. Efficient mucociliary clearance is critical for preventing airway infection [160, 208]. Ciliated cells have not been demonstrated to be capable of proliferation and are generated by Clara or basal cell progenitor cells [76, 143]. Ciliated cells are sensitive to oxidant injury and Paramyxoviral infection but appear resistant to injury by most Clara cell-specific toxicants [156]. Numerous studies demonstrate that unresolved ciliated cell injury results in increased airway morbidity. Cystic fibrosis patients who display ineffective ciliary mucous clearance are prone to recurrent mucous plugging, airway infection, and epithelial remodeling [307].

Airway basal cells are small, triangular cells with an elongated morphology and close contact with the airway basal lamina / basement membrane. These cells are normally restricted to tracheas and mainstem bronchi, but are detected in primary bronchioles following certain

types of injury (Figure 1.1, yellow cells) [111]. Basal cells exhibit a high nuclear-to-cytoplasmic ratio, significant levels of intracellular keratin filaments, and numerous integrin-associated desmosomes and hemidesmosomes. Molecular markers for basal cells include keratin 14 and Griffonia simplicifolia isolectin-B4 (GSI-B4) [29, 80, 81, 111, 112, 163]. Basal cells provide attachment points for proximal epithelial cell adhesion. In addition to their structural role in airways, basal cells function as proximal airway progenitors capable of proliferation and epithelial renewal. Tritiated thymidine or BrdU incorporation studies have shown that basal cells represent the most abundant mitotic cell type within proximal airways. Additionally, studies involving a scrape injury model comparable to aspiration-type injuries determined that basal cell proliferation and migration occurs following tracheal wounding. Despite their robust mitotic potential, airway basal cells are not frequently identified as progenitors responsible for airway remodeling or carcinogenesis [168, 267]. Thus, it appears that while most tracheal basal cells are definitive airway progenitors, the majority of these cells do not contribute to chronic airway remodeling diseases and neoplastic transformation.

Pulmonary neuroendocrine cells (PNECs) are rare cells located intermittently throughout conducting airways (Figure 1.1, maroon cells). They exist either as individual PNECs or small innervated PNEC clusters termed neuroepithelial bodies (NEBs) [10, 46, 172, 272]. NEBs are typically, but not exclusively, localized at airway branch points and their frequency does not vary between proximal and distal airways. Individual neuroendocrine cells are small, basally located cuboidal epithelial cells that contain numerous dense-core secretory granules. Neuropeptides produced by PNECs include calcitonin, calcitonin gene related peptide (CGRP), gastin-related peptide (GRP) / bombesin, leuenkephalin, and PGP9.5 [10, 42, 193]. Despite their neuroendocrine phenotype, PNECs do appear to originate within primitive foregut endoderm

along with other airway cell types [120]. These are the earliest differentiated cell types observed during lung development and may function as airway oxygen chemosensors [272, 286] [314]. Additionally, PNECs can function as airway progenitor cells, although they do not frequently proliferate in the absence of injury and are too rare to maintain overall epithelial diversity. Hyperplasia of PNECs / NEBs occurs following exposure to injurious chemicals including diethylnitrosamine, 4-nitroquinoline, naphthalene, tobacco smoke, ozone, and hypoxia exposure. Significant NEB hyperplasia is associated with several chronic lung diseases including bronchopulmonary dysplasia and COPD [119, 121, 172, 193, 249, 257]. Despite these findings, there has been no direct evidence linking PNEC / NEB proliferation with functional epithelial renewal. PNECs are widely considered as major progenitors of airway SCLC, and these tumors commonly exhibit markers consistent with neuronal and neuroendocrine cell origins [37, 100, 152, 254].

Clara cells are an abundant airway cell type found throughout airways of virtually all mammalian species. Maxfield von Clara initially described these cells in 1937 as cuboidal, non-ciliated bronchiolar epithelial cells with abundant smooth endoplasmic reticula and numerous dense-core granules localized within cytoplasmic apical projections. Today, Clara cells are defined by the molecular criteria of Clara-cell secretory protein (CCSP) expression [161, 205, 208, 306]. CCSP expressing Clara cells are found in varying abundance throughout human conducting airways and are most prevalent within terminal bronchioles (Figure 1.1, orange cells). Clara cells defined by CCSP expression are first detected in human airways by 15 weeks gestation and increase in abundance through 24 weeks [13, 160, 208, 209, 226]. In mice and rats, Clara cells are the predominant airway cell type and account for 50% of proximal and up to 70% of distal airways [189, 206]. Several functions have been attributed to Clara cells based on

their molecular and biochemical properties. Clara cells are thought to help maintain an appropriate ELF through their secretion of proteins such as CCSP, surfactant proteins A, B, and D, tryptase Clara, and Uteroglobin gene related protein [104, 286]. Together, these proteins serve immunoregulatory, anti-inflammatory, and anti-oxidant roles within airways [161]. CCSP itself also contains a xenobiotic binding pocket that appears to facilitate binding of polychlorinated biphenyl (PCB)-like airway pollutants [180, 181, 251]. Also, Clara cells are an abundant source of numerous Cytochrome P450 (CYP450) enzymes and glutathione production. Together, these compounds facilitate xenobiotic metabolism and detoxification of lipophilic pollutants. CYP450s are phase I metabolizing enzymes that decrease the hydrophobicity and increase the reactivity of lipid compounds for subsequent glutathione conjugation / phase II pollutant metabolism [89, 90, 210, 211, 215, 238, 288]. At low doses, these lipophilic compounds elicit morphologic changes to Clara cells and may result in enhanced glutathione production and establishment of pollutant tolerance [302, 304]. Administration of high doses results in exhaustion of Clara cell glutathione stores, acute Clara cell-specific toxicity, and severe airway epithelial necrosis. In mice, expression of Cytochrome P450 isoenzymes 2F2 and 2B2 render Clara cells uniquely sensitive to naphthalene [215, 288]. This Clara cell-specific property has been used to elicit severe airway injury and is an accepted model of epithelial injury and repair.

In addition to major roles in secretion and pollutant metabolism, Clara cells function as a major progenitor within intrapulmonary bronchioles. In the absence of injury, experiments performed to identify proliferating airway cells demonstrate that Clara cells account for most proliferation within airway bronchioles [74, 76]. Oxidant exposure studies of Evans and colleagues demonstrated that, upon injury, Clara cells de-differentiate to a morphologically

variant, Type A Clara cell [76, 79]. These "Type A" Clara cells then function as preferred airway progenitors and account for 73% of proliferating cells within intrapulmonary bronchioles. Similar results have been obtained in our laboratory using ozone-mediated oxidant lung injury that preferentially targets airway ciliated cells [131-133]. Importantly, Type A Clara cell proliferation in response to oxidant injury occurs broadly throughout the airway epithelium, indicating the broad distribution of this progenitor pool. Taken together, these observations indicate that most Clara cells only function as transiently amplifying (TA) progenitor cells. However, the observation that Clara cells may also infrequently function as progenitors of NSCLCs raises the possibility that a subpopulation of CCSP expressing cells maintain enhanced mitotic and differentiation potential [151, 187, 254]. Characteristics of these CCSP expressing airway stem cells are discussed in section 1.6.3.

1.3.2. Airway Heterogeneity

Significant proximal- distal, location-dependent differences in epithelial cell height and cellular representation exist throughout conducting airways and it is this airway heterogeneity that enables critical functional diversity. Proximal-distal differences in airways include variability in epithelial cell height, cell representation, and composition of extracellular lining fluid [129, 209, 239]. Morphologically, three easily distinguished airway regions are defined: the trachea and mainstem bronchi, intrapulmonary midlevel bronchioles, and terminal bronchioles (see Figure 1.1). Loss of appropriate epithelial heterogeneity occurs in many lung diseases including asthma, chronic obstructive pulmonary disease, cystic fibrosis, and idiopathic pulmonary fibrosis. While origins of these diseases are highly varied (and include factors such as inherent genetic mutations, pollutant / tobacco smoke exposures, and dysregulated Th1 / Th2

immunity), the outcomes of altered proximal-distal heterogeneity appear similar [33, 40, 41, 45, 140, 319]. Within each disease, chronic epithelial injury results in dysregulated epithelial cell regeneration or repair, airway remodeling, and fixation of irreversible phenotypic changes. To better appreciate airway changes associated with chronic injury it is important to understand aspects of normal proximal-distal airway heterogeneity.

The trachea and mainstem bronchi are the largest diameter and most proximal conducting airways. The trachea is composed of a pseudo-stratified columnar epithelium with a large epithelial cell height and size. Typically, tracheas are composed of ciliated, Clara, serous, mucous, and goblet cell types [81, 160, 163, 189, 215, 239]. Tracheas contain specialized anatomical structures known as submucosal glands (SMGs) that (1) normally secrete several fluids and mucous proteins with known antimicrobial effects, and (2) that contain abundant cellular CFTR proteins [57, 69, 70]. The trachea and mainstem bronchi secrete greater quantities of antimicrobial-containing extracellular proteins and mucous than distal airways. These large airways maintain the highest velocity airflow and allow passage of much fine and all ultrafine sized particulate matter. The trachea is also susceptible to direct traumatic injury and airborne microbial infection [215]. Also, the tracheal epithelium proliferates ten to twenty times more frequently than that of intrapulmonary conducting airways [73, 74, 81, 316]. Despite these continued insults and frequent proliferation, cells of the trachea and mainstem bronchi are not frequent targets of neoplastic transformation or epithelial remodeling. One notable exception to this finding is the development of hypertrophic, hyperplastic SMGs in cystic fibrosis and other lung diseases [28, 307]. Here, SMGs expand into more distal airway regions resulting in changes to the local cellular milieu.

Midlevel conducting airways (bronchioles) are smaller in diameter than tracheas or mainstem bronchi, and contain the majority of airway bifurcations. There is significantly less extracellular lining fluid present within intrapulmonary bronchioles and no measurable extracellular mucous [104]. Intrapulmonary bronchioles maintain a simple columnar to cuboidal morphology and lack basal and goblet cell phenotypes common within larger airways [286, 287]. Instead, intrapulmonary bronchioles are comprised predominately of ciliated, Clara, and rare pulmonary neuroendocrine cells. Neuroepithelial bodies (NEBs) containing neuroendocrine and Clara cells frequently localize to airway branch points where they function as oxygen chemosensors and airway stem cell microenvironments [224, 314]. Airflow within bronchioles is reduced compared to proximal airways and flow is often disrupted at these bifurcations resulting in branchpoint-associated particulate impaction. As such, intrapulmonary bronchioles are targets of particulate matter deposition, but are protected from the majority of airborne pathogens [201, 203]. Under normal conditions, less than 0.1% of bronchiolar cells proliferate per day. However, exposure to agents including tobacco smoke, oxidant gases, and some particulate matter can trigger intrapulmonary branch-point associated injury and subsequent hyperplasia [108, 129, 278] [219]. Following branch point-associated injury, NEBs exhibit decreased cohesiveness and transient hyperplasia [10, 193, 224, 249]. Chronic intrapulmonary injury and continuous epithelial renewal results in branch point-associated epithelial remodeling and is associated with formation of neuroendocrine and non-neuroendocrine tumors. It is increasingly accepted that NEB-associated Clara and neuroendocrine cell populations are the predominant intrapulmonary progenitor cells and that these cell types likely contribute to the formation of NSCLC and SCLC.

Terminal bronchioles adjacent to broncho-alveolar duct junctions are the most distal conducting airways. Due to their protected environment, airway terminal bronchioles contain little extracellular lining fluid and no detectable airway mucous. In most species, Clara and ciliated cells represent 100% of terminal bronchiolar cell types. Airflow rate in terminal bronchioles is quite low, allowing this airway region to evade most pathogen exposures [2, 129, 286]. Not surprisingly, this region of conducting airways exhibits very low cellular turnover / proliferation in the absence of injury [76]. Despite these findings, experiments have determined that terminal bronchioles are particularly susceptible to oxidant-mediated injuries. While the severity of injury is related to exposure duration and concentration of airborne pollutants, ciliated cells are clearly the most susceptible cell population. After oxidant injury, subsets of terminal bronchiolar Clara cells proliferate to function as ciliated cell progenitors. Chronic exposure to oxidant gases such as ozone is associated with expansion of Clara cell phenotypes within airway terminal bronchioles / adjacent alveoli and formation of NSCLC-like hypertrophic lesions [54, 127, 151, 202, 212].

Interestingly, evidence suggests that airways with the highest epithelial proliferation rates (trachea and mainstem bronchi) are the least susceptible to permanent epithelial alterations resulting from injury and dysregulated cellular renewal. In contrast, terminal bronchioles / bronchoalveolar ducts proliferate infrequently and are highly susceptible to phenotypic alterations following chronic pollutant exposure or injury. These observations raise the possibility that phenotypically distinct populations of regenerative cells with variable endogenous repair capacity exist within each airway region, and that these progenitor cells themselves are primarily responsible for establishing normal or dysregulated epithelial repair processes. It is therefore critically important to understand mechanisms of epithelial injury and

repair not only within airways as a whole, but also with respect to regionally distinct differences in repair capacity.

1.4. Cellular and Molecular Regulation of Epithelial Cell Composition

1.4.1. Airway Development

Recent evidence suggests that specific mechanisms regulating development and establishment of conducting airways are also relevant in the pathogenesis of diseases associated with chronic lung injury [23-25, 175]. Therefore, studies that have identified mechanisms of airway development may provide important clues regarding regulation of epithelial repair processes. In order to form a functionally and phenotypically diverse epithelium, the primitive foregut endoderm undergoes extensive branching morphogenesis followed by distal airway alveolarization [107, 196, 287]. Many aspects of branching morphogenesis and the establishment of airway heterogeneity are evolutionarily conserved between species. Human lungs originate as a primitive laryngo-tracheal groove at 5 weeks gestation; an analogous process occurs at embryonic day 9.5 in mouse. Human conducting airways undergo extensive branching morphogenesis eventually resulting in 23 distinct airway generations. Human distal lung alveolarization begins at approximately 20 weeks gestation and is completed postnatally. Mouse lung development contains four distinct stages of airway / alveolar morphogenesis. These are (1) the pseudoglandular stage of primary airway branch formation (embryonic days 9.5-16.5), (2) the canalicular stage during which time terminal bronchiolar sacs develop (embryonic days 16.5-17.4), (3) the saccular stage of alveolar type 1 and type 2 cell differentiation (embryonic day 17.4 – postnatal day 5), and (4) the alveolar stage when lungs become fully mature (postnatal days 5-20). During each of these stages, there is progressive growth and differentiation resulting in the proximal-distal heterogeneity observed in adult airways [107, 196, 287].

Differentiated airway cell phenotypes appear in a proximal-to-distal fashion during the early pseudoglandular stage. Pulmonary neuroendocrine cells are the first cell types to differentiate within conducting airways and result in early establishment of neuroepithelial body microenvironments (NEBs) [272]. Clara cells defined by Clara cell secretory protein (CCSP) expression are detectable in proximal airways during the later pseudoglandular stage, and progressily differentiate in a proximal-to-distal fashion concomitant with ciliated cell differentiation [286, 287]. Regional differences in CCSP expression and Clara cell morphology are evident throughout development and may denote establishment of functionally variant CCSP expressing cell populations [129, 209, 303]. Specific transcription factors induced during development (and their effects) include Nkx2.1/TTF-1 mediated branching morphogenesis and Clara cell differentiation [35], Foxp1 and Foxp2-dependent down regulation of Clara cell secretory protein (CCSP) expression in distal lungs [236], HNF-3β signaling inducing CCSP [232], ASH1 dependent induction of neuroendocrine cells [26], and HFH-4 dependent induction of ciliogenesis [38, 101]. Signaling pathways or molecules involved in airway development and differentiation include FGF's, Shh, EGF, TGF-β, and BMPs (particularly BMP-4) [15, 17, 105, 114, 166, 167, 195, 273, 287, 305]. As expected, aberrant activation of several of these pathways / transcription factors in adults is associated with uncontrolled epithelial proliferation and lung cancer formation.

In addition to the aforementioned signaling pathways, a number of recent studies have begun to elucidate roles for Wnt / β-catenin signaling in establishment of airway cell fate. Numerous Wnt proteins, including Wnt2, Wnt2b, Wnt5a, Wnt7b, and Wnt11 are expressed in spatially discrete patterns during airway development [15, 171]. Specifically, Wnt7b and Wnt5a expression is restricted to distal airway buds. Wnt5a knockout mice display defects in terminal

airway differentiation, while Wnt7b knockout mice exhibit significant lung defects and prenatal lethality [149, 237, 298]. While these data do not definitively identify the involvement of β-catenin signaling in Wnt-mediated airway development, nuclear β-catenin (indicative of signaling) and numerous β-catenin cofactors have been detected within embryonic distal conducting airways [64, 244, 260]. In addition, Lef1 expression is critical for formation of tracheal submucosal glands [57, 58, 228]. Recently, Mucenski et. al. provided direct evidence of the importance of β-catenin signaling during lung maturation. In this study, Surfactant protein-C-dependent ablation of β-catenin resulted in alveolar hypoplasia and disrupted airway branching morphogenesis. These malformed airways expressed CCSP but were significantly enlarged and lungs lacked appropriate gas exchange [173]. Taken together, these data are highly suggestive of the importance of β-catenin signaling in establishment of airway proximal-distal heterogeneity.

1.5. Properties of Progenitor Cells in Other Systems

1.5.1. Stem and Transit Amplifying Cells

Cellular regeneration is of significant interest due to its relevance to chronic disease, tissue remodeling, and neoplastic progression. Progenitor cells capable of proliferation are subdivided into two distinct categories: stem cells and transit amplifying (TA) cells. Significant differences exist between stem and TA cells, and include variable mitotic capacity, differentiation potential, and frequency within a given tissue or organ [240]. Stem cells are rare, exist throughout the life of an organism, maintain robust proliferative capacity, and can contribute to numerous different cell types [240, 291]. Additionally, stem cells exhibit a slow rate of cycling in steady state tissues and typically express few lineage-commmitted phenotypic markers [21, 43]. In contrast, TA cells represent the bulk of mitotic cells within a given tissue and exhibit a more differentiated cellular phenotype [72, 148]. Stem cells have been identified in all regenerative tissue types studied to date including intestine, skin, liver, hematopoietic lineages, bone, lung, mammary gland, nervous system, prostate, testis, and ovary. Of these, only a subset has been well characterized in terms of stem cell location, regulation, and potency. Tissues with well-characterized stem cell populations include intestine [14, 141, 269], skin [4, 113, 176, 177, 266, 290, 292, 293], and cells of the hematopoietic lineage.

Recent studies of well-characterized stem cell populations have revealed phenotypic similarities raising the possibility that a defined set of global stem cell characteristics exists. Identified similarities include several dominant signaling pathways and functional paradigms. These findings are also significant as they have highlighted numerous correlations between normal stem cell populations and cancers. Signaling pathways including Wnt / β-catenin, Sonic

Hedghog (Shh), and Notch-Delta are emerging as potentially global regulators of stem cell maintenance and activation [222, 240, 261, 291]. Strong evidence indicates that these pathways that are transiently activated within normal stem cells are aberrantly activated in many cancers, and may induce unregulated proliferation [191, 222]. Specific examples of this phenomenon include continual β-catenin signaling in most intestinal or colon cancers [269, 284], unregulated Shh signaling in nervous system medulloblastomas [297], and uncontrolled Notch signaling due to chromosomal alterations in T-cell leukemias [66, 85, 194]. Specifics regarding each of these pathways and their role in airway epithelial renewal or carcinogenesis are discussed in Section 1.7 of this Chapter.

1.5.2. Stem Cell Pollutant Resistance

Numerous stem cell populations exhibit inherent resistance to effects of harmful toxicants or pollutants. Potential mechanisms include enhanced glutathione biosynthesis, reduced phase I metabolizing enzyme activity, enhanced cellular DNA repair mechanisms, and efficient ATP-dependent xenobiotic removal [197, 200, 233, 283, 317]. Like stem cells, cancer cells are frequently more resistant to toxicants due to enhanced pollutant resistance. Additionally, stem cells and cancer cells are resistant to radiation-induced DNA damage due to enhanced DNA repair mechanisms and suppression of apoptotic signaling [191, 222]. Toxicant efflux has been demonstrated following incubation of cells with the lipophilic toxicant mimetic Hoechst 33342. In bone marrow, this widely used Hoechst fluorescent dye incubation assay defines a "side population" (SP) of cells with low Hoechst 33342 red / blue fluorescence that are functionally and phenotypically analogous to hematopoietic stem cells (HSC) [32, 97, 318]. Subsequent studies demonstrated that ATP-dependent small lipophilic molecule transporters including

Multidrug resistance proteins (Mrps), P-glycoproteins (Pgps), and Breast cancer resistance protein 1 (Bcrp1 / ABCG2) enable the observed HSC side population phenotype [233, 317, 318].

1.5.3. Stem Cell Microenvironments

Despite differences among stem cells from multiple tissues with regards to differentiation potential, mitotic capacity, and differentiated characteristics, it is now becoming apparent that microenvironment-association is an important feature of most stem cell populations [245, 291]. Typically, microenvironments are localized within physically isolated regions of tissue, a property which may provide some protection to local stem cell populations: (1) In epidermis, interfollicular stem cell microenvironments are located in the deep rete ridges of nonhairy skin [126, 293]. (2) In hairy skin, stem cell microenvironments are restricted to the lowest permanent portion of the hair follicle, termed the follicular bulge [30, 155, 185, 259, 266]. (3) In intestine, stem cells are restricted to the relatively protected intestinal crypt regions [44, 141]. Several lines of evidence also indicate that the local microenvironment influences stem cell phenotype. Activation of common stem cell signaling pathways is often controlled by the local cellular microenvironment. For example, evidence suggests that β-catenin signaling within follicular stem cells is due in large part to local Wnt protein secretions [4, 176, 177, 185]. Also, recent findings indicate that local microenvironment interactions (such as integrin adhesion and matrix metalloprotease secretion) regulate aspects of asymmetric stem cell division necessary for maintenance of stem cell number and mobilization following injury [93, 136, 179, 245, 291]. In addition to regulating the fate of normal stem cells, local microenvironmental influences affect the phenotype and outcome of various stem cell-derived tumors [188]. While studies thus far

have provided significant evidence of the influence of the microenvironment over many stem cell populations, many aspects regarding the understanding of how stem cell microenvironments function remains poorly defined.

1.6. Airway Stem Cell Microenvironments

1.6.1. Overview

The characterization of airway stem cells has been difficult due to low cellular turnover rates within conducting airways. Using BrdU or tritiated thymidine labeling techniques, researchers determined that approximately 10% of the tracheal epithelium proliferates each day [55]. This rate drops to 0.2% - < 1% per day within intrapulmonary conducting airways [11]. From these studies, several putative airway progenitor cells have been identified. These include basal cells of proximal airways, Clara cells, and pulmonary neuroendocrine cells [31, 78, 249]. Additionally, previous studies excluded airway ciliated cells as potential airway progenitors [76]. Overall, these studies determined that most airway progenitor cells were analogous to transit amplifying (TA) cells identified in other tissues. Recently, studies involving selective depletion of airway TA cells demonstrate that airways contain several distinct, microenvironment-associated stem cell populations [29, 71, 110-112, 224, 250]. Evidence supports the existence of phenotypically distinct, regio-specific stem cell microenvironments within trachea, intrapulmonary airways, and terminal bronchioles that are critical for epithelial renewal following severe lung injury. Importantly, regionally distinct airway stem cells localized within submucosal glands, neuroepithelial bodies, and terminal bronchioles appear capable of re-establishing appropriate proximal-distal heterogeneity following TA cell depletion. Additionally, these microenvironment-associated stem cells bear strong phenotypic resemblance to airway cancers, and are spatially located in sites of frequent neoplastic transformation. As such, the further characterization of airway stem cell molecular and functional phenotypes is of clinical importance.

1.6.2. Tracheal Stem Cell Microenvironments

In addition to studies identifying most basal cells as a TA cell population, several *ex vivo* and recent *in vivo* studies have identified subpopulations of basal cells with stem cell-like characteristics. Initial experiments studied populations of isolated, purified basal or secretory cells transplanted into host denuded rat tracheas or cultured in vitro [51, 60, 116, 117, 154, 313, 316]. These purified cell populations were then allowed to proliferate and differentiate, and their relative proliferative capacity and differentiation potential was assessed. Results indicated that a subset of isolated basal cells maintained significant mitotic capacity and multipotent differentiation potential [51, 60]. These basal cells generated large differentiated colonies containing basal, secretory, and ciliated cell populations after several weeks. In contrast, purified bronchial secretory cells were only capable of generating colonies containing secretory and ciliated cell lineages [116, 117]. From these results, the investigators concluded that subsets of basal cells maintain properties consistent with tracheal stem cells. There are several caveats to this interpretation. First, these studies did not appropriately address the potential of incomplete host tracheal epithelial denudation. Second, there remains a strong possibility that impure cell populations were grafted into host tracheas. Finally, these studies also failed to define any tracheal microenvironmental conditions necessary for endogenous basal stem cell activity. Nonetheless, these results indicate that basal cells include a subset with properties of tracheal stem cells.

Recently, several *in vivo* studies from our laboratory and others have identified tracheal microenvironments that may support basal stem cell populations [29, 68, 71, 112]. Studies by Borthwick, et. al. describe the presence of slow cycling, label retaining cells within submucosal

glands (SMG) that were activated following sulphur dioxide-mediated epithelial injury [29]. These cells were defined as basal cells based on their expression of keratin 5 and GSI-B4 lectin. Studies performed by Hong et. al. confirmed the existence of multipotent tracheal basal cells using a bi-transgenic ligand-regulated Cre-loxP lineage tagging system [112]. Here, a subset of keratin 14 expressing basal cells generated very large cell colonies 45 days after epithelial injury. These basal cell-derived colonies contained basal, secretory, and ciliated cell phenotypes. Under low magnification, these large keratin 14 expressing cell-derived colonies appeared to localize preferentially at intercartilagenous borders. Together, these data support the existence of tracheal basal-like stem cells.

1.6.3. Intrapulmonary Neuroepithelial Body Stem Cell Microenvironments

To definitively identify whether subsets of CCSP expressing cells exhibit stem cell-like properties, previous studies in our laboratory used selective TA / Clara cell depletion to induce airway stem cell activation [250]. This type of TA cell-selective injury has been used successfully in other tissues and organs to reveal otherwise quiescent stem cell populations [82]. As previously described, Clara cells are uniquely susceptible to naphthalene exposure through Cytochrome P450 mediated bioactivation to a toxic epoxide [238, 274, 288]. This property was exploited to achieve >95% Clara cell ablation throughout conducting airways. Two days after naphthalene exposure epithelial repair was restricted to airway branch points and terminal bronchioles (Figure 1.1) [250]. Subsequent studies determined that regeneration at these sites was mediated by pollutant resistant CCSP expressing cells thatwere associated with pulmonary neuroepithelial body microenvironments [224, 249]. Within NEBs, both pollutant resistant CE cells and PNECs contributed to epithelial proliferation (Figure 1.2) [224]. Nine days after

naphthalene administration, significant epithelial renewal was evident immediately adjacent to NEB microenvironments (Figure 1.3A). These domains of epithelial renewal expanded to several hundred microns in diameter within 45 days (Figure 1.3B) [110]. Additional studies revealed that subsets of both NEB-associated CCSP and CGRP expressing cells exhibited a slow cycling, label retaining phenotype indicative of stem cells [110].

To determine whether CCSP or CGRP expressing cells represent NEB microenvironment-associated stem cells, Hong et al used transgenic mice in which the *Herpes simplex* virus gene thymidine kinase (HSVtk) was regulated by the murine CCSP promoter to achieve conditional ablation of airway cell subsets (designated CCtk mice; Figure 1.4A) [110, 225]. Expression of this HSVtk transgene has previously been used to elicit cell-specific toxicity following administration of the nucleoside analog gancyclovir (GCV). Use of this trangene-mediated CCSP ablation model overcame any inherent pollutant resistance among Clara cell subsets and allowed for the unambiguous assessment of whether CGRP expressing neuroendocrine cells functioned as airway stem cells capable of epithelial regeneration. Airways of CCtk mice immunostained for CCSP and HSVtk revealed Clara cell-specific expression of thymidine kinase throughout conducting airways but not within any other airway, alveolar, or mesenchymal cell populations (Figure 1.4B) [225]. Lung sections stained for CCSP + HSVtk 0, 1, 2, 3, 6, and 10 days after acute GCV exposure revealed immediate and progressive loss of CCSP/HSVtk immunoreactive cells throughout the 10 day recovery period (Figure 1.5A-F) [110]. No changes in the number of acetylated tubulin reactive airway ciliated cells were observed at this time, eliminating the possibility of bystander toxicity effects (data not shown). Airways of GCV-exposed CCtk mice failed to demonstrate epithelial renewal, exhibited progressive alveolar inflammation, a decline in overall health, and death several weeks after

GCV exposure. These results indicated that despite extensive neuroendocrine cell proliferation and NEB hyperplasia, there was no evidence of epithelial renewal or restoration of a CCSP expressing epithelium (Figure 1.6) [110]. This suggested that CGRP expressing pulmonary neuroendocrine cells were unable function as multipotent airway stem cells.

Taken together, these findings suggest that NEB-associated, pollutant resistant CCSP expressing cells are airway-specific stem cells activated to faciliate epithelial renewal following TA cell depletion (Figure 1.7) [110]. Additionally, the definitive identification of stem cells associated with NEB microenvironments is intriguing in the context of chronic airway remodeling and cancer predisposition. As stated previously, CE and PNECs are widely regarded as the major progenitors of NSCLC and SCLC, respectively. The discovery that NEB microenvironments harbor airway stem cells would seem to indicate that these CE airway stem cells are the most likely candidates for neoplastic transformations.

1.7. Signaling Pathways Implicated in Stem Cell Maintenance and Function

1.7.1. Overview

A number of potential airway stem cell signaling pathways have begun to be elucidated. Studies of stem cells in other tissues now indicate that Hedgehog, Notch, and β-catenin signaling pathways are conserved among different stem cell populations. In addition, each of these pathways is involved in aspects of lung development and maturation, further supporting their roles in airway epithelial renewal [16, 20, 122, 125, 173, 195, 228, 260]. Finally, evidence is growing implicating each of these signaling pathways in the pathogenesis of stem cell derived cancers [191, 222]. Data summarized below highlights aspects of airway Hedgehog, Notch, and β-catenin signaling that support their identification as potential stem cell signaling pathways.

1.7.2. Hedgehog Signaling

Sonic hedgehog (Shh) signaling is a critical component of airway development and mediates appropriate epithelial-mesenchymal interactions [16, 195]. Sonic Hedgehog is a member of the Hedgehog family of secreted signaling proteins whose members include Sonic, Indian, and Desert Hedgehog. Hedgehog proteins interact with Patched receptors to induce gene transcription by disinhibiting Gli family transcription factors [182]. Loss of Shh during development results in failure of both branching morphogenesis and airway maturation. Studies in other tissues have also identified roles for Hedgehog signaling proteins as regulators of stem cell activity and inhibitors of terminal differentiation [44, 178, 270]. Furthermore, it is increasingly accepted that aberrant Hedgehog protein expression accelerates tissue remodeling and cancer formation in several tissues [59, 178, 192, 297]. For these reasons, Watkins et. al.

have investigated roles for Shh signaling in airway injury and repair [289]. Results of these studies indicated that acute airway injury rapidly induced widespread, NEB microenvironment-associated Shh expression that was repressed following epithelial renewal and neuroendocrine cell differentiation. Additionally, most murine SCLC and all human SCLC neuroendocrine-like cell lines expressed detectable Shh protein. Within SCLC, Shh expression was necessary to maintain cell survival and proliferation. A minority of murine NSCLC lines also expressed significant Shh. Taken together, these data indicate the likely involvement of Shh proteins in regulating NEB-associated neuroendocrine cell differentiation and proliferation. The observation that only a minority of NSCLC required Shh signals suggests that this signaling pathway is not centrally involved in maintenance of NEB-associated, CCSP expressing progenitor / stem cells.

1.7.3. Notch Signaling

Studies of hematopoietic and skin stem cell populations indicate that Notch signaling regulates important aspects of stem cell differentiation and microenvironment association [52, 158, 184, 293]. Multiple roles for Notch signaling in the pathogenesis of numerous types of cancer are also well established [221]. The mechanisms of Notch-Delta signaling and downstream effector gene regulation are fairly complex. Membrane-associated Notch activation by its ligands triggers activation of basic helix-loop-helix (bHLH) transcription factors. These transcription factors then act as fate determinants by inducing selective downstream target genes while concomitantly suppressing other transcription factor activities. In adjacent cells, expression of Notch ligands and interaction with Notch receptors may have the opposite effect, preventing expression of Notch proteins / downstream bHLH transcription factors and thereby

favoring an alternate differentiation pathway [7, 52, 190]. To determine whether Notch signaling might be involved in aspects of lung epithelial development, normal stem cell mediated repair, or airway neoplastic transformation, several studies have investigated the consequences of either disrupting or enhancing Notch signaling through manipulation of downstream target gene expression. Genetic ablation of the Notch bHLH transcription factor Hairy enhancer of split 1 (Hes1) resulted in overexpression of the proneural transcription factor Achaete-scute homologue 1 (Ash1) and ectopic development of PNEC / NEBs within embryonic conducting airways [122]. The pathophysiology of these airways was similar in appearance to lungs containing preneoplastic SCLC-type lesions. This link between Hes1 disruption, Ash1 induction, and excessive NEB formation was supported by the observation that numerous human SCLCs express Ash1 [26, 37, 152]. Disruption of the Mash1 gene resulted in the development of airways devoid of PNEC / NEBs but did not display any other overt airway abnormalities [26]. These findings, while somewhat confusing, appear to indicate that Notch functions as a tumor suppressor of neuroendocrine cell-derived SCLC by inhibiting Ash1 and other pro-neuronal, promitotic genes [247, 248]. These data also raise the possibility that mutated Notch may may function as an oncogene in NSCLC by priming non-neuroendocrine airway cells to undergo unregulated proliferation [48, 221]. Unfortunately, studies of stem cell-mediated airway injury and repair that may have helped formalize these conclusions are not currently possible due to the early postnatal lethality observed in both Hes1 -/- and Ash1 -/- mice.

1.7.4. β-catenin Signaling

Many studies from numerous tissues have determined that β-catenin signaling has profound affects on stem cell proliferation, differentiation, and migration [113, 223, 252, 293,

308, 312, 315]. There is also strong evidence from multiple organs that aberrant β-catenin signaling is associated with tissue remodeling and cancer formation [170, 269, 284]. β-catenin signaling can occur through Wnt-dependent (canonical), or Wnt-independent (non-canonical) mechanisms [62, 102, 218, 280]. In the absence of Wnt or other stimuli, cytoplasmic GSK3β forms functionally active protein complexes with APC, Axin, and Disheveled that can rapidly phosphorylate free β-catenin. Cytoplasmic phospho-β-catenin is then targeted for degradation through the ubiquitin / proteasome pathway. However, Wnt signaling through Frizzled receptors direct activities of FGF-2, epidermal growth factors, and other growth-promoting signals can inhibit GSK3β activity and thus prevent phosphorylation of cytoplasmic β-catenin. Free cytoplasmic β-catenin undergoes nuclear translocation where it heterodimerizes with TCF family transcriptional cofactors for the formation of a bipartite transcriptional activator and stimulation of downstream target gene expression. Typical downstream target genes of β-catenin signaling include matrix metalloproteinase 7 (MMP7), cyclin D1, c-myc, Axin2, and bone morphogenic protein 4 (BMP4). There is growing evidence for the involvement of β-catenin signaling in establishment of proximal-distal airway heterogeneity and establishment of potential airway stem cell microenvironments (see section 1.4.1) [173, 228, 260]. Additionally, studies have demonstrated strong nuclear / cytoplasmic β-catenin localization within hyperproliferative epithelial lesions. Specifically, recent evidence indicates that idiopathic pulmonary fibrosis (IPF)-associated airway remodeling and epithelial cell hyperplasia may involve aberrant activation of the β-catenin pathway [41, 183, 244]. In IPF, extensive nuclear / cytoplasmic localization of β-catenin is observed within regions of abnormal epithelial cell phenotypes, and is associated with activation of promitotic (cyclin D1) and promigratory (MMP7) gene expression [40, 41]. The involvement of β-catenin signaling in airway stem cell-mediated epithelial renewal

is the subject of Chapter 5 of this dissertation. Implications regarding the involvement of β-catenin in airway neoplastic transformation are also discussed.

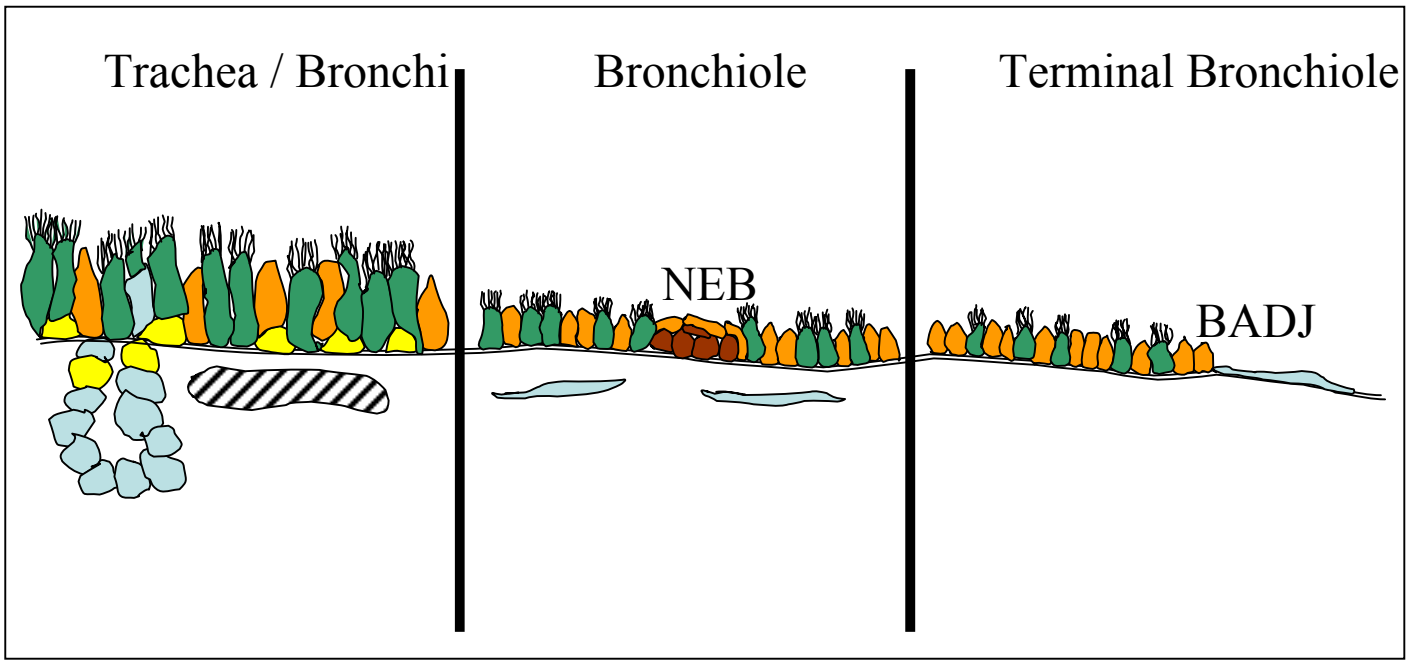

Figure 1.1 Cellular heterogeneity within normal conducting airways.

Conducting airway epithelium is comprised of three regionally, functionally, and morphologically distinct zones: the proximal trachea and mainstem bronchi, midlevel intrapulmonary bronchioles, and distal airway terminal bronchioles. Clara cells, defined by the molecular criterion of CCSP expression, are present throughout conducting airways of mice and humans but are most abundant within terminal bronchioles (orange). Ciliated cells (green) are also present throughout conducting airways. Additionally, proximal conducting airways maintain a significant population of airway basal cells (yellow) as well as other cell types including Goblet and serous cells (light blue cells in trachea / bronchi). Midlevel bronchioles also contain rare pulmonary neuroendocrine cells (maroon) that are frequently observed in 4-6 cell clusters termed neuroepithelial bodies (NEBs). Terminal bronchioles contain the broncho-alveolar duct junction (BADJ) border between conducting airway and alveolar epithelial lung regions.

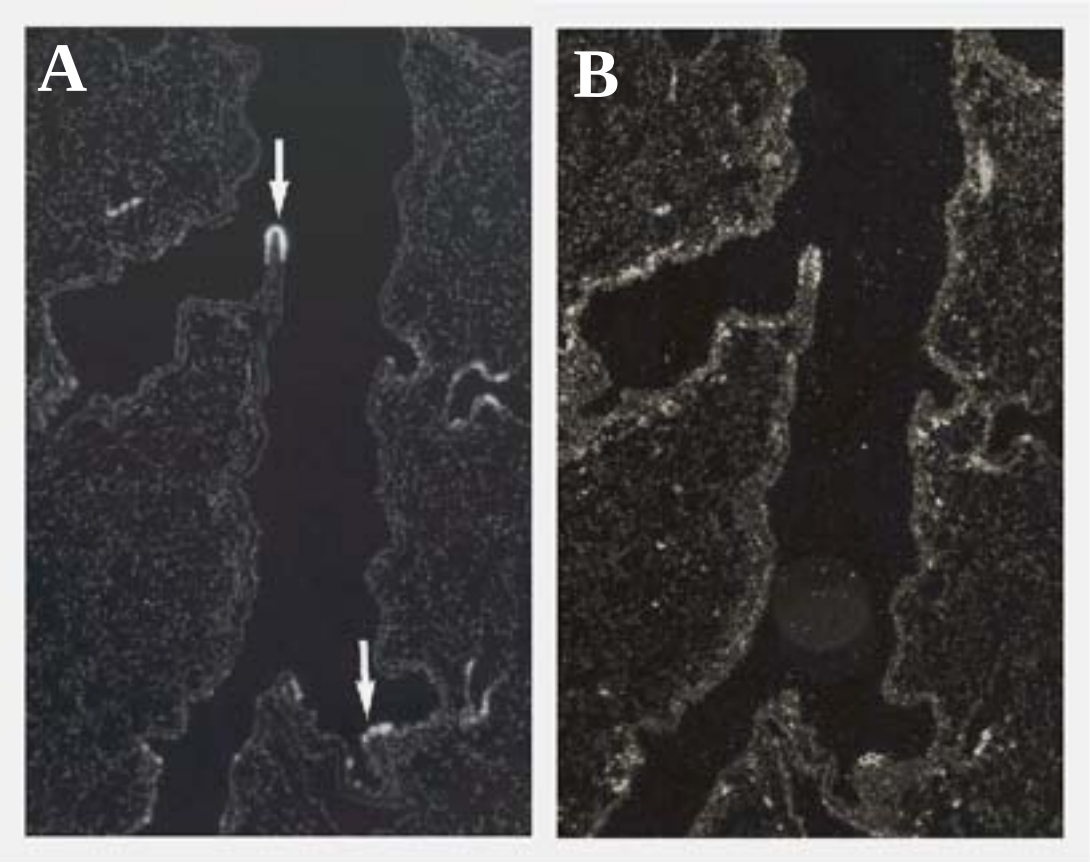

Figure 1.2 Focal epithelial cell renewal following naphthalene mediated Clara cell depletion.

In situ localization of mRNAs for CCSP (A) and CDK1 (B) in adjacent serial sections of lung tissue from mice treated with 200mg / kg naphthalene and recovered for 72 hours. Arrows in (A) indicate airway branch points expressing CCSP mRNA and (B) CDK1 mRNA.

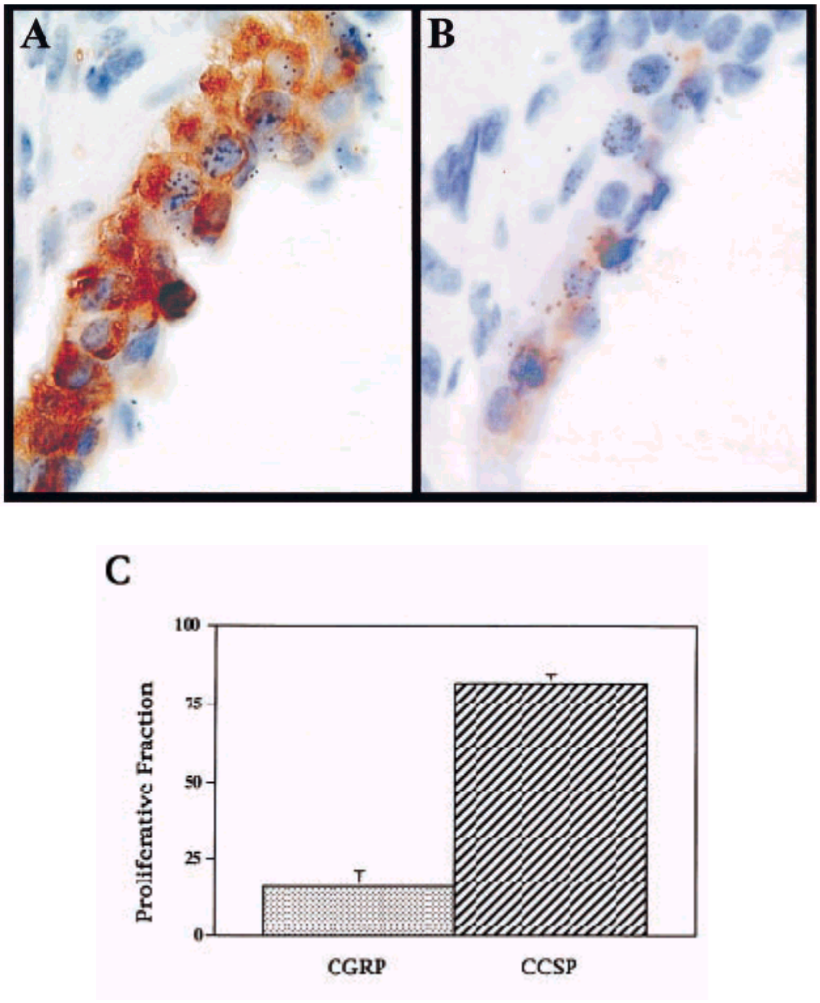

Figure 1.3 Epithelial cell proliferation is restricted to neuroepithelial bodies following naphthalene.

Adjacent serial sections from animals 72 hours post-naphthalene treatment were stained for CCSP (A) or for CGRP (B), using standard immunohistochemical techniques and DAB detection of antigen-antibody complexes. Slides were then dipped in emulsion, and grains (black dots over nuclei) developed after one week. (C) The percent of all mitotic airway cells expressing either CGRP or CCSP was 16.06 ± 5.53% or 81.47 ± 3.00% , respectively.

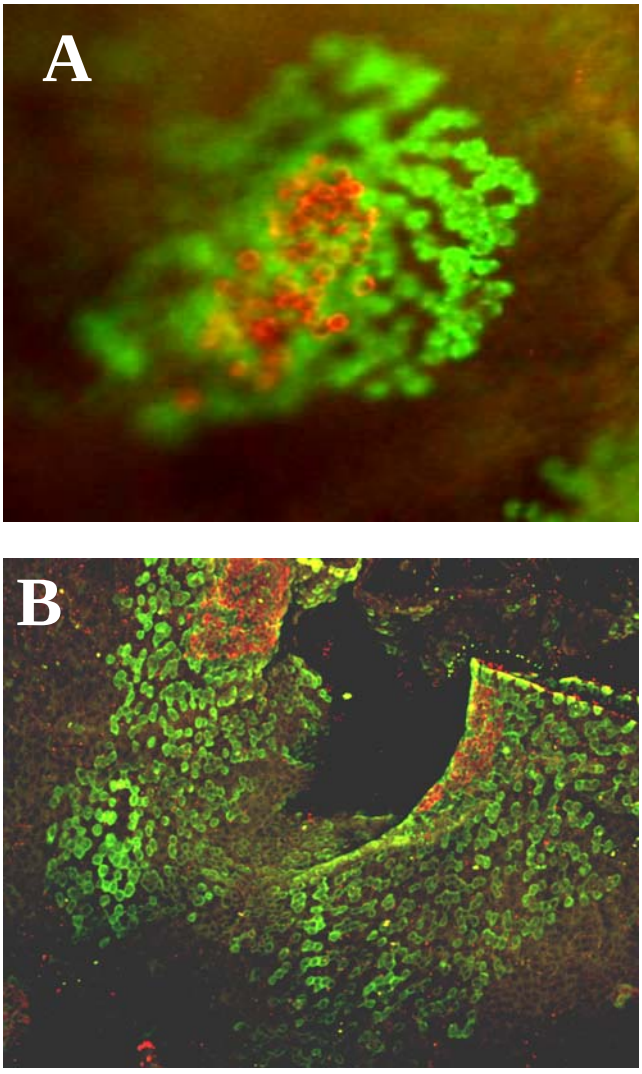

Figure 1.4 NEB microenvironment-associated expansion of a differentiated epithelium.

Microdissected airways were stained with CCSP (green) and CGRP (red) to identify regenerative NEB microenvironments 9 or 45 days after naphthalene exposure (A and B, respectively). (A) Nine days after injury, standard dual immunofluorescent detection revealed a population of nascent Clara cells immediate adjacent to NEBs. (B) After 45 days, multiphoton confocal microscopy allowed for identification of repopulated Clara cells extending for several hundred microns around branch point-associated NEB microenvironments.

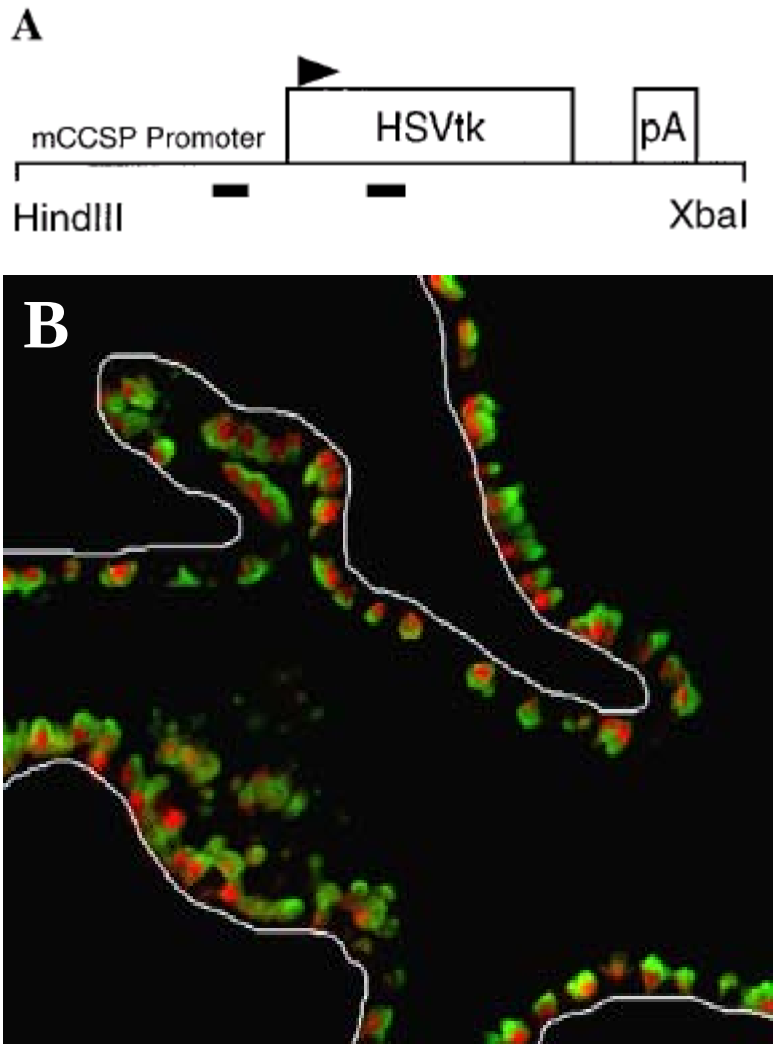

Figure 1.5 Clara cell-specific expression of herpes simplex virus thymidine kinase in CCTK transgenic mice..

(A) A schematic showing CCTK transgene construct including the murine CCSP promoter (mCCSP), bovine growth hormone polyadenylation signal (pA), and transcriptional start site (arrow). Bars indicate position of primers used to verify animal transgene status. (B) Dual color immunofluorescence of CCSP (green) and HSVtk (red) in CCTK transgenic lung tissue reveals specificity of HSVtk expression within CCSP expressing airway cells.

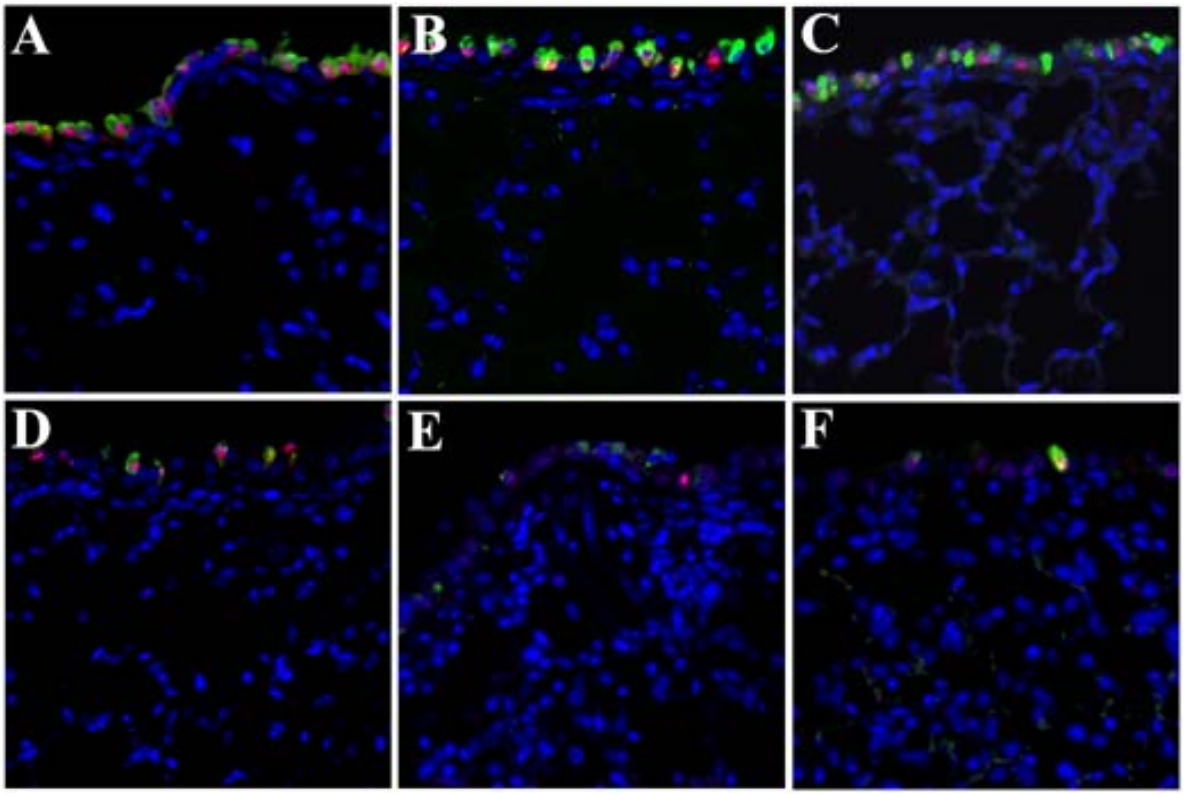

Figure 1.6 Selective and progressive loss of CCSP expressing cells following gancyclovir exposure.

The abundance and distribution of Clara cells was determined within airways of control (A) and gancyclovir exposed (B-F) CCTK mice by dual immunofluorescent detection of CCSP (green) and HSVtk (red). CCTK mice were recovered for 24 (B), 48 (C), 72 (D), 168 (E), or 264 (F) hours after initiation of gancyclovir treatment. Nuclei were counterstained using DAPI.

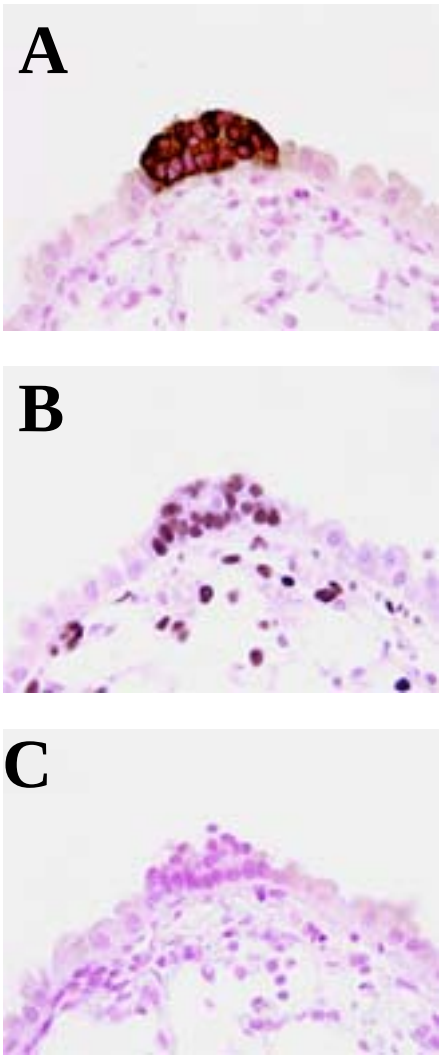

Figure 1.7 Absence of NEB-associated epithelial renewal following gancyclovir-mediated Clara cell ablation.

Gancyclovir exposed CCTK mice were continuously labeled with BrdU from days 2 to 10 of recovery. Adjacent serial sections were stained for CGRP (A), BrdU (B), and CCSP (C). BrdU labeled nuclei appear in clusters localized within NEB microenvironments. There are no CCSP immunoreactive cells associated with these foci of BrdU labeled, NEB-associated epithelial cells 10 days after gancyclovir exposure.

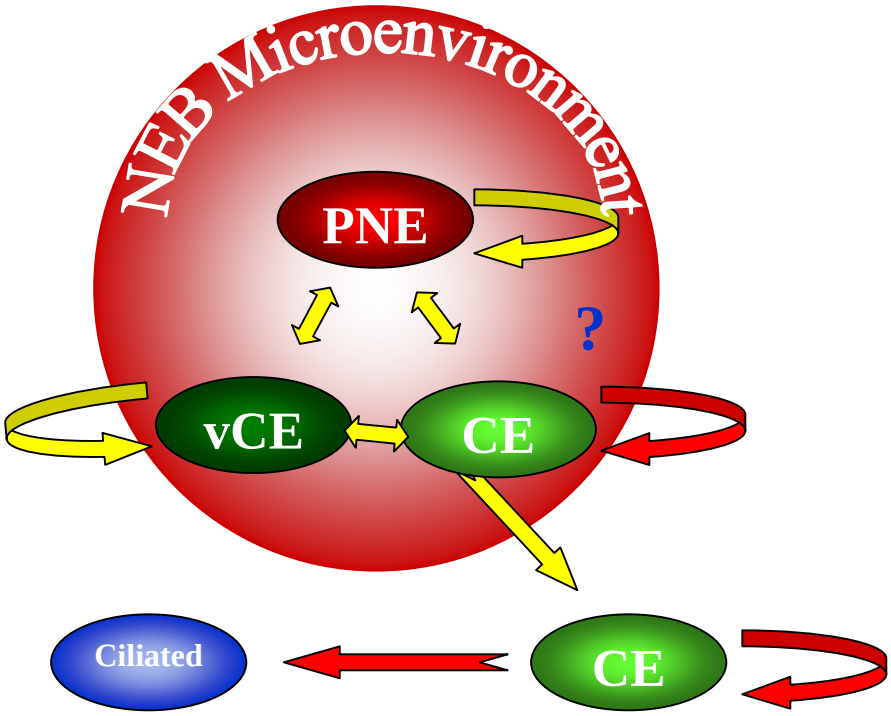

Figure 1.8 Model of cellular interactions within and adjacent to NEB microenvironment following transit amplifying cell depletion.

In the steady state and after depletion of terminally differentiated (ciliated) cells, airways are maintained through proliferation of Clara cells (CE) capable of self renewal (red arrows) and differentiation into ciliated cells (green arrow). A variant population of pollutant resistance CE cells (vCE) restricted to NEB microenvironments have robust proliferative potential (yellow arrows) and are activated following depletion of CE cell populations. Additionally, neuroendocrine cells (PNEC) are capable of robust proliferation but do not contribute directly to other airway cellular phenotypes. Neuroepithelial body microenvironments serve to maintain vCE in steady state lungs, thus preserving a critical pool of airway stem cells. Not addressed in current studies is the potential for vCE to undergo PNEC differentiation (question mark).

2. Rationale and Hypotheses

Airway injury and chronic alterations to epithelial cell diversity contribute to reductions in overall lung function. Repair is dependent on the appropriate activation and differentiation of progenitor cells resident within conducting airways. Despite significant advances in identification of airway specific progenitor cells, mechanisms regulating normal airway repair remain poorly understood. Previous studies from our laboratory determined that pulmonary neuroepithelial body (NEB) microenvironments harbor airway-specific, pollutant-resistant stem cells. Subsequent studies using transgenic ablation of all CCSP expressing (CE) cells demonstrated that NEB-associated CE cells are necessary for epithelial renewal and maintenance of lung homeostasis. These CCSP-expressing cells therefore function as intrapulmonary lung epithelial stem cells. Studies in this dissertation were undertaken to (1) determine whether alternate bronchiolar stem cell microenvironments exist, to (2) characterize potential mechanisms of airway stem cell pollutant resistance, and to (3) identify signaling mechanisms associated with stem cell-mediated repair processes.

Hypothesis One: Terminal bronchioles maintain a distinct population of airway stem cells capable of regionally appropriate epithelial renewal.

Hypothesis Two: Airway stem cells exhibit pollutant resistance due to reduced pollutant biotransformation and efficient ATP-dependent toxicant efflux.

Hypothesis Three: β-catenin signaling is associated with airway stem cell activation and epithelial renewal.

3. Terminal Bronchioles Harbor a Unique Airway Stem Cell Population that Localizes to the Bronchoalveolar Duct Junction

3.1. Abstract

Cellular mechanisms contributing to renewal of terminal bronchioles remain poorly defined. Our previous studies identified pollutant-resistant CCSP-expressing stem cells that localize to the neuroepithelial body (NEB) and contribute to renewal of the proximal bronchiolar epithelium. However, activation of NEB-associated stem cells is unlikely to contribute to renewal of terminal bronchiolar epithelium due to the paucity of NEBs at this location. Goals of this study were to determine the location and properties of cells contributing to renewal of terminal bronchioles following Clara cell depletion. Pollutant resistant CCSP expressing cells were identified that specifically localized to the broncho-alveolar duct junction (BADJ) and contribute to restoration of a phenotypically diverse epithelium. CCSP expressing cells comprise the predominant proliferative population in initial terminal bronchiolar repair and include a population of label retaining cells suggesting that they maintain characteristics of a stem cell population. Furthermore, immunohistochemical colocalization studies involving CCSP and the NEB specific marker calcitonin gene related peptide (CGRP) indicate that BADJ associated CCSP expressing stem cells function independently of NEB microenvironments. These studies identify a BADJ associated, NEB-independent CCSP expressing stem cell population in terminal bronchioles and support the notion that regio-specific stem cell niches function to maintain epithelial diversity following injury.

3.2. Introduction

Dramatic differences in the cellular composition of conducting airway epithelia exist between the trachea and terminal bronchioles; a feature that contributes to functional heterogeneity essential for normal airway homeostasis [13, 161, 205-209, 215]. While many studies have focused on regeneration of this tissue following injury, only recently have the intricacies of renewing such a complex epithelium begun to be elucidated. Injury models that target terminally differentiated cell populations identify the importance of the transit amplifying (TA) subset of progenitor cells in the regeneration process. Proliferation and differentiation of TA cells results in rapid restoration of a normal epithelium. In contrast, selective depletion of an abundant TA cell pool results in activation of rare stem cell populations [72, 148, 199, 230, 291, 292, 299]. To date, stem cells have been identified that are restricted to the trachea, submucosal gland ducts, and neuroepithelial bodies (NEBs) of the bronchiolar epithelium [29, 70, 71, 110, 224]. Even though cells that contribute to the renewal of terminal bronchioles have also been shown to exist using a model of lung progenitor cell depletion, the precise location and characteristics of putative stem cells have not been described.

The terminal bronchiole is a particularly resilient region of the airway that exhibits rapid epithelial renewal in response to depletion of either terminally differentiated (ciliated) or TA cell populations. Clara cells function as the sole TA cell that participates in maintenance of both secretory and ciliated cell types following oxidant mediated damage [76]. Importantly, depletion of this TA cell population through administration of the Clara cell specific cytotoxicant naphthalene fails to diminish the regenerative potential of terminal bronchioles [224, 274, 276]. Following Clara cell depletion, residual cells of terminal bronchioles are fully capable of epithelial renewal and restoration of differentiated cell phenotypes appropriate for this region

[274, 276]. These data support the notion that a population of pollutant resistant stem cells participate in regeneration of the surrounding terminal bronchiolar epithelium following TA cell depletion.

Even though the molecular and phenotypic characteristics of stem cell populations vary according to the tissue in which they reside, a number of unifying properties are used to distinguish this category of regenerative cells from their TA counterparts [291]. Characteristics of stem cells include a relatively undifferentiated phenotype, pluripotent differentiation potential, a low rate of steady state proliferation, an extended lifespan, and localization to a specific microenvironment commonly referred to as a stem cell niche [148, 220, 245, 291]. Using these criteria, we have previously demonstrated the existence of a CCSP-expressing (CE) cell population within NEB microenvironments of the bronchiolar epithelium that functions as an airway stem cell [224]. CE stem cells and TA cell populations within the airway epithelium have been distinguished primarily by differences in pollutant susceptibility, proliferative and differentiation potential, and spatial localization. Depletion of both of these populations via transgene mediated ablation of all CCSP positive cells results in an overall failure of bronchiolar epithelial renewal [110, 225]. These results indicate the importance of CE cells in bronchiolar regeneration and led us to hypothesize that phenotypically similar populations of stem cells may regulate epithelial renewal in both the proximal and terminal bronchioles [110, 224]. Goals of the present study were to investigate this hypothesis through defining the molecular phenotype of cells contributing to repair of terminal bronchioles, their localization, and their rate of proliferation in the steady-state and following injury. Results indicate that regeneration of the terminal bronchiole following injury is mediated by CE stem cells with characteristics similar to

those located within NEB microenvironment, but that this stem cell functions within a unique NEB-independent niche located at the broncho-alveolar duct junction.

3.3. Materials and Methods

Animal Housing

Adult male FVB/n wild type mice (2-4 months of age) were housed under specific pathogen free (SPF) conditions and tested quarterly using a 16 agent serological sentinel screening program. Animals were maintained under a 12 hour light/dark cycle, and allowed access to both food and water *ad libitum.*

Naphthalene Exposures

Naphthalene (Sigma) was dissolved in Mazola corn oil and administered to mice via intraperitoneal (i.p.) injection prior to 10:00 am. Animals were briefly anesthetized with aerosolized halothane prior to exposure to facilitate weighing and injections. Mice received 275 mg naphthalene / kg body weight; control animals received a comparable volume (10ml / kg body weight) of corn oil alone.

Pulse and Continuous Labeling

[^{3}H] thymidine (2.5 mCi / kg) was injected intraperitoneally to mice one hour prior to sacrifice for pulse labeling. For continuous labeling studies, [^{3}H] thymidine (1.0 mCi / ml) was administered over a seven day period via a subcutaneous miniosmotic pump (Alzet model #2002, 0.5ul / hour). Alzet pumps were implanted six hours after naphthalene administration and removed following the labeling period.

Immunohistochemistry and Immunofluorescence

Paraffin-embedded lung tissue was sectioned at 5μm to reveal the major axial pathway and adhered to glass slides. Slides were blocked with 0.5% Bovine Serum Albumin (BSA, Sigma) / 5% normal goat serum (NGS, Vector Laboratories) in PBS (blocking solution) for thirty minutes. Adjacent serial sections were incubated with polyclonal Rabbit-anti-CCSP ([225], 1:30,000) or Rabbit-anti-CGRP ([225], 1:16,000; Sigma) overnight at 4ºC in blocking solution. Slides were washed three times in PBS, and incubated with biotinylated-Goat-anti-Rabbit Ig (Sigma Chemical, 1:4000 dilution in blocking solution). Slides were washed, and Streptavidin-horseradish peroxidase (Sigma Chemical) added at a 1:4000 dilution in PBS. Antigen-antibody complexes were detected using a diaminobenzidine (DAB) substrate detection kit (Vector Laboratories). For detection of incorporated [^{3}H] thymidine, immunostained slides were washed overnight in PBS, dehydrated, and dried. Slides were coated with NTB-2 emulsion (Kodak), dried, stored at 4°C for two weeks, and developed according to the manufacturer's instructions. All slides are counterstained with Mayer's Hematoxylin to identify nuclei.

Standard immunofluorescence methods were used to simultaneously detect CGRP and CCSP on 5μm tissue sections [110]. Rabbit anti-CGRP (1:4,000) and Goat-anti-CCSP were diluted in 3% BSA / PBS. After a 24 hour incubation at 4 ºC, slides were incubated simultaneously with Alexa 488-conjugated Donkey-anti-goat Ig and Alexa 594-conjugated-Donkey-anti-Rabbit Ig (1:125 dilution, Molecular Probes) overnight at 4 ºC in the dark. All slides were mounted with 2 μg / ml 4,6-diamidino-2-phenylindole (DAPI, Sigma) in Fluoromount-G (Southern Biotechnology Associates) and visualized with an AX70 microscope equipped with a DAPI / Texas Red dual optical excitation filter cube and a fluorescein isothiocyanate optical excitation filter cube (Olympus).

In situ Hybridization

CCSP mRNA was detected on 5 μm paraffin sections of lung tissue using [^{35}S] antisense riboprobes. Conditions for hybridization were essentially as described [301]. Slides were washed under high stringency conditions, coated with Kodak NTB2 emulsion, exposed for 16 hours, and developed according to the manufacturer's instructions.

Morphometric Analysis and Labeling Index

Terminal bronchioles were defined by the presence of an intact broncho-alveolar duct junction (BADJ), at least 200 μm of conducting airway epithelium, and a visible alveolar duct. All cells within 200 μm of the BADJ exhibiting a nuclear profile and clear attachment to the basement membrane were included in cell density analyses. Previous studies have employed a similar methodology for analysis of neuroepithelial body (NEB) microenvironments [224]. For proliferation analysis, cells were defined as 'labeled' if they contained at least five grains localized over a visible nucleus. 'Label retaining cells' were defined as those containing greater than 15 grains / nuclei. Mean values for cellular density, percent Clara cells, and proliferative index were compared to control values using the Student's t-test. Statistical significance for all comparisons was accepted at $P < 0.05$.

3.4. Results

Pollutant resistant CCSP expressing cells occupy multiple distinct microenvironments within the conducting airway epithelium.

The terminal bronchiolar epithelium of mice is a particularly sensitive site for naphthalene toxicity, exposure to which results in rapid and extensive depletion of Clara cells [250, 274]. Although Clara cells are the principal progenitor for this region of the conducting airway [76], repair of terminal bronchioles is rapidly induced and virtually complete two weeks following administration of 200 mg / kg naphthalene [27, 250, 274, 275, 277]. Even though neuroepithelial body (NEB)-associated CCSP-expressing (CE) cells have been identified as a naphthalene-resistant stem cell pool that contributes to renewal of proximal bronchiolar epithelium, there is still debate over the identity and properties of cells contributing to renewal of terminal bronchiolar (TB) epithelium. In order to identify regions of the TB that maintained naphthalene-resistant CE cells, mice were exposed to 275 mg / kg naphthalene, recovered 24 hours, and the phenotype of pollutant resistant cells assessed by dual-color fluorescence immunostaining for the Clara cell specific marker Clara cell secretory protein (CCSP, green immunofluorescence) or the pulmonary neuroendocrine cell specific marker calcitonin gene related peptide (CGRP, red immunofluorescence). In the distal airway of untreated animals, CE cells account for 60-90% of epithelial cells while pulmonary neuroendocrine cells (PNECs) comprise only a small percentage of this population (Figure 3.1A). Naphthalene exposure resulted in extensive exfoliation of CE cells within 24 hours (Figure 3.1B). Clusters of pollutant resistant CE cells which have been previously shown to serve as regenerative foci are maintained adjacent to NEBs of bronchi ([110, 224], Figure 3.1B, asterisk). Interestingly, a second population of pollutant resistant CE cells that did not appear to colocalize with CGRP

immunoreactive PNECs was located within TB adjacent to the BADJ. (Figure 3.1B, arrow). This observation suggested that the BADJ may represent a second distinct regenerative microenvironment within bronchioles in addition to the previously characterized NEB microenvironment.

Cells within terminal bronchioles support regeneration of airways of appropriate cellular diversity.

To determine whether NEB-independent pollutant resistant cells of terminal bronchioles are capable of appropriate epithelial renewal, airways of mice were compared 45 days after administration of 275 mg / kg naphthalene or vehicle (corn oil). Efficacy of epithelial renewal within terminal bronchioles was determined by comparison of epithelial cell density and the representation of CCSP immunoreactive cells in untreated and treated animals. No qualitative differences in the abundance of CCSP within immunoreactive cells of corn oil and naphthalene-exposed groups were observed (Figure 3.2A and B, respectively). A small yet significant reduction in terminal bronchiolar cell density was observed in treated animals (Figure 3.2C). This decrease in cell density was not associated with a shift in the representation of CE cells at this location (Figure 3.2D). These data demonstrate that terminal bronchioles contain a regenerative cell population capable of restoring an airway of appropriate cellular diversity following depletion of the transit amplifying (Clara) cell population.

Pollutant resistant CCSP expressing cells represent the initial proliferative population in terminal bronchioles.

In order to investigate the kinetics of Clara cell ablation within terminal bronchioles and to identify the location and cell type responsible for initial epithelial renewal, mice were exposed to either corn oil or 275 mg / kg naphthalene, recovered for 6, 12 ,24, or 36 hours, and injected with 2.5 mCi / kg [^{3}H]-thymidine (TdR) one hour prior to sacrifice. Clara cells were identified by immunohistochemistry for CCSP and proliferating cells were identified by autoradiographic detection of incorporated [^{3}H]-TdR (Figure 3.3). Six hours post naphthalene exposure Clara cells exhibited a loss of apical projections without significant alterations in overall cell density as determined by CCSP immunoreactivity (Figure 3.3, compare A and B). Exfoliating CCSP immunoreactive cells were evident beginning at the 12 hour time point (Figure 3.3C). This change was associated with a reduction in both the overall cell density and percent of Clara cells within the epithelial population. Within 24 hours, maximal CE cell ablation was achieved as determined by the absence of exfoliating cell bodies (Figure 3.3D). The previously identified population of pollutant resistant CE cells (Figure 3.1B) was identifiable directly adjacent to the BADJ at this time point (Figure 3.3D). Although no epithelial proliferation was observed in any terminal bronchiolar cell populations at this early recovery time point, proliferating mesenchymal cells which serve as a control for appropriate [^{3}H]-TdR incorporation and detection were identified at this and all other time points analyzed (arrowheads, 3.3B-E). Proliferative epithelial cells were first observed 36 hours after naphthalene administration and exhibited a rounded morphology (Figure 3.3E). At this time point 0.6 ± 0.1 proliferative cells were detected per 100 μm (approximately one labeled cell per terminal bronchiole), of which CCSP expressing pollutant resistant cells represent 90 ± 15%. These data suggest a critical role for these cells in renewal of the distal conducting airway.

Pollutant Resistant Broncho-alveolar duct junction associated cells maintain CCSP mRNA expression.

A caveat to identification of BADJ-associated CCSP positive cells as CE cells is the relatively long half-life of CCSP which may result in immunoreactivity in cells that have undergone a de- or trans-differentiative process [165, 286]. To ascertain whether pollutant-resistant, BADJ-associated CCSP immunopositive cells actively transcribe CCSP, as well as to more fully characterize their molecular phenotype, the distribution of CCSP mRNA in TB of control and naphthalene exposed mice was determined by *in situ* hybridization (Figure 3.4A, B). CE cells present 24 hours after exposure were analyzed as these cells represent a residual, resistant population rather than nascent cells that may be the product of epithelial regeneration. Non-specific hybridization signal was minimal as determined by antisense [^{35}S]-labeled CCSP probe hybridization to tissue from CCSP -/- mice (Figure 3.4C). CCSP mRNA was detected throughout the terminal bronchiole of untreated wild-type mice (Figure 3.4A). In contrast, terminal bronchioles from naphthalene-treated mice maintained a subset of CCSP mRNA positive cells directly adjacent to the BADJ (Figure 3.4B). The levels of CCSP mRNA in this region were reduced compared with those of control, although they are significantly greater than background levels. While the cellular specificity of this transcript cannot be determined using [^{35}S]-labeled probes, the proximity of CCSP mRNA positive cells to the BADJ correlates with immunohistochemical data (Figures 3.1, 3.3). These data support the notion that pollutant-resistant cells of the BADJ are indeed a CCSP expressing population.

Regenerative CCSP expressing cells are preferentially associated with the BADJ of terminal bronchioles.

The phenotype, frequency, and spatial distribution of the initial cohort of proliferating cells within the TB were determined 36 hrs after naphthalene exposure using the BADJ as a reference point. CE cells were identified by immunohistochemical detection of CCSP and proliferating cells were identified by autoradiography. At this time point, 57% of labeled-CCSP expressing cells were located within 40 μm (approximately six cell diameters) of the BADJ and > 75% of proliferating CE cells were located within 80 μm of the BADJ (approximately 11 cells; Figure 3.5, black bars). As noted previously, CCSP expressing cells accounted for 90% ± 15% mitotic cells within the TB. A small number of labeled-CCSP negative cells were randomly distributed throughout the TB and were most likely rare CGRP immunoreactive PNECs similar to those previously identified within regenerative domains of more proximal airways (Figure 3.5, white bars). Based upon these results, we conclude that the predominant mitotic population during the initial phase of epithelial regeneration within TB are naphthalene-resistant CE cells and that these cells are spatially restricted to the BADJ microenvironment.

Two distinct microenvironments support regeneration of the terminal bronchiolar epithelium.

Previous studies have demonstrated that neuroepithelial bodies serve as microenvironments for proliferation and the maintenance of bronchial stem cells [1, 95, 110, 224, 249]. Studies by Peake and coworkers determined that the abundance of CGRP-immunoreactive cells per unit airway surface area does not change substantially along the proximal / distal axis of the airway [193]. As such, the number of CGRP immunopositive cells within an airway segment decreases in direct proportion to airway surface area, raising the possibility that not all terminal bronchioles contain a NEB microenvironment. In order to determine whether NEBs have a role in either maintenance or activation of BADJ-associated CE

cells, mice were exposed to 275 mg / kg naphthalene, recovered for 36 hours, and treated with [^{3}H]-TdR one hour prior to sacrifice to identify proliferating cells. Adjacent serial sections were stained for either CCSP or CGRP and proliferating cells visualized by autoradiography (Figure 3.6). Analysis of 23 terminal bronchioles containing at least one labeled cell (n=5 animals) demonstrated that 75% of regenerating terminal bronchioles lack CGRP immunopositive cells in an adjacent serial section, suggesting that the BADJ-microenvironment is distinct from that defined by NEBs (Figure 3.6A and B). The remaining 25% of regenerating terminal bronchioles analyzed by this method contained CGRP immunoreactive cells (Figure 3.6C, D). These data indicate that TB contain two microenvironments that harbor regenerative pollutant-resistant CE cells, the BADJ and the NEB.

The majority of terminal bronchioles lack CGRP immunoreactive pulmonary neuroendocrine cells following pollutant injury.

In order to determine whether subpopulations of TB can be distinguished by the presence or absence of a NEB microenvironment, the incidence of CGRP and CCSP immunoreactive cells in was assessed by dual color immunofluorescent analysis of twenty adjacent 5 μm serial sections through 32 TB (n=5 animals) exposed to 275 mg / kg naphthalene and recovered 24 hours. Terminal bronchioles containing a visible BADJ were scored for the presence or absence of CCSP and CGRP on at least one of the twenty adjacent serial sections. Results of this analysis indicate that all terminal bronchioles contain several CCSP immunoreactive cells closely associated with the BADJ. Thirty eight percent of terminal bronchioles do contain at least one detectable CGRP positive cell that was often located some distance from the BADJ and did not appear to colocalize with BADJ-associated CE cell populations. In contrast, sixty-two percent of

TB lacked detectable NEBs or individual CGRP immunoreactive cells (Figure 3.7). These data indicate that the majority of TB lack a NEB and support the notion that the BADJ functions as a distinct microenvironment for maintenance of pollutant-resistant regenerative cells.

Broncho-alveolar duct junction-associated CCSP expressing cells are a slow cycling (label retaining) population.

In addition to a relatively undifferentiated phenotype, a low steady-state rate of proliferation is a commonly cited property of stem cells. To assess the mitotic rate of cells in the terminal bronchiole following exposure to 275 mg / kg naphthalene, cells proliferating during the first 7 days of recovery were continuously labeled with [^{3}H]-TdR via a subcutaneous miniosmotic pump and the animals allowed to recover a total of 45 days. As the period of [^{3}H] thymidine incorporation was followed by a significant recovery time, a negative correlation between number of silver grains and the number of rounds of proliferation following initial recovery is observed [110, 148]. Numerous fibroblast-like mesenchymal cells bore a large number of silver grains 45 days after naphthalene exposure indicating the efficacy of the labeling and chase protocol utilized in this experiment (Figure 3.8, arrowheads). Two distinct populations of [^{3}H] thymidine labeled cells were distinguished by the number of grains / nucleus: 'label-retaining' cells which contained > 15 grains / nucleus (Figure 3.8, circled "1") and 'labeled' cells contained 5-10 grains / nucleus (Figure 3.8, circled "2"). Slow cycling cells ('Label-retaining') comprise 12 % of all labeled cells observed (21 cells total versus 198 total cells, n=4 animals). This finding suggests that two mitotic cell populations that differ in their cycle time are found within terminal bronchioles following acute naphthalene exposure.

In order to determine the molecular phenotype of the 'labeled' or 'label-retaining' cells and whether these populations were restricted to a particular region of the terminal bronchiole, sections were stained for CCSP and the distribution of each cell type evaluated using the BADJ as a reference point (arrow, Figure 3.8; Figure 3.9). CCSP expressing label-retaining cells exhibited a non-random distribution within TB (Figure 3.9, solid black bars). Greater than 60% of label-retaining CCSP immunopositive cells were specifically localized in the 20μm region (three cell diameters) adjacent to the BADJ. CCSP negative label-retaining, as well as CCSP positive labeled, and CCSP negative labeled cells were randomly distributed throughout the terminal bronchiole (Figure 3.9, hatched, gray and white bars, respectively). Spatial restriction of slow cycling, 'label retaining' CE cells to the BADJ microenvironment supports the notion that these cells represent a stem cell pool important for terminal bronchiolar renewal.

3.5. Discussion

Results from this study identify a novel stem cell compartment that contributes to renewal of the terminal bronchiolar epithelium following acute progenitor (Clara) cell depletion. Rare, pollutant-resistant, CCSP-expressing (CE) cells were initially identified in numerous terminal bronchioles both by immunohistochemistry and *in situ* hybridization, and were present at all time points following naphthalene administration. Interestingly, these pollutant-resistant CE cells were spatially restricted to the most distal conducting airway epithelium immediately adjacent to the broncho-alveolar duct junction (BADJ). Following depletion of naphthalene-sensitive Clara cells, BADJ-associated CE cells account for all proliferative cells within terminal bronchioles. At later time points, progeny of BADJ associated cells appear to migrate proximally and contribute to the restoration of a terminal bronchiolar epithelium of appropriate cellular composition. In addition to rapidly proliferating cells, a subset of BADJ-associated CE cells rapidly enters a quiescent state and remains spatially restricted to this region of the airway. These BADJ associated cells function independently of NEBs, and thus define a novel regenerative microenvironment. We conclude that epithelial CE cells that are enriched within the BADJ microenvironment of terminal bronchioles represent a pollutant-resistant, slow cycling population with multipotent differentiation potential. Based upon these findings we suggest that BADJ-associated CE cells represent a stem cell pool.

While this study is the first to define a specific stem cell of terminal bronchioles, the kinetics of injury and repair within the terminal bronchiolar epithelium have been extensively characterized. The time course and magnitude of Clara cell ablation noted in the present study are similar to previously published findings [210, 211, 250]. Despite differences in the dose of

naphthalene, the temporal relationship between initial injury and the subsequent onset of repair were quite similar for each model. However, the present findings are not fully consistent with previous suggestions regarding the identity of cells that actively contribute to the proliferative fraction of the renewing epithelium. Studies by Van Winkle and coworkers [274] demonstrate the existence of squamated cells, some of which possess cilia, within the residual terminal bronchiolar epithelium of naphthalene-exposed mice. The rapid pace of epithelial renewal, coupled with a lack of cells exhibiting morphologic characteristics of Clara cells, led this group to suggest that residual ciliated cells represented the most likely progenitor pool for renewal of naphthalene-injured terminal bronchioles [143, 274]. In the present study we demonstrate that residual squamated epithelial cells that resist naphthalene-induced injury include a CCSP-expressing (CE) subset and that this population of pollutant-resistant CE cells proliferate to effect renewal of terminal bronchioles. This finding is consistent with our previous studies in which systemic delivery of gancyclovir was used to achieve conditional ablation of CE cells in transgenic mice (CCSP-HSVtk) expressing the pro-toxin gene Herpes simplex virus thymidine kinase under the regulatory control of the mouse CCSP promoter [110, 225]. Ablation of all CE cell populations in those studies was accompanied by proliferation of pulmonary neuroendocrine cells of the bronchial and bronchiolar epithelium, but was not associated with renewal of the injured epithelium. Importantly, neither proliferative epithelial cells nor airway regeneration was observed within CE cell-depleted terminal bronchioles of CCSP-HSVtk transgenic mice during recovery from acute gancyclovir exposure [110], indicating the loss of a critical stem cell population. Therefore, CE cell populations within NEB and terminal bronchioles represent an essential component of epithelial renewal following injury.

Our current and previous findings identify pollutant resistance and CCSP expression as molecular criteria that are unique properties of stem cell pools within both terminal and proximal bronchiolar epithelium. Mechanisms that might contribute to resistance of the stem cell pool from pneumotoxic compounds such as naphthalene may either be intrinsic to the cell, such as differences in pollutant metabolizing enzymes, or as a result of its physical sequestration. A precedent exists for each model. A growing consensus is that stem cells exhibit a relatively undifferentiated phenotype that may confer protection from the potentially genotoxic consequences of metabolizing xenobiotic compounds [240, 291, 292]. Alternatively, the fact that stem cells of regenerative epithelia are generally sequestered within secluded microenvironments, as is the case for stem cells found in the limbus of the cornea and crypts of the small intestine [141, 265], also raises the possibility that stem cells may be physically isolated from toxic pollutants. The relative contribution of intrinsic pollutant resistance versus anatomical sequestration can not be easily discerned for stem cells of the NEB microenvironment and both mechanisms may in fact contribute to their resistance from naphthalene-induced injury. However, BADJ-associated stem cells described herein are localized to a region of the conducting airway that is most sensitive to the effects of parenterally administered naphthalene. This exposed location at the BADJ suggests that some mechanism of intrinsic resistance to xenobiotic agents is an important determinant contributing to their maintenance following naphthalene exposure.

Other insights into the molecular phenotype of regenerative cells contributing to renewal of naphthalene-injured airways have come from studies investigating expression of the growth factors epidermal growth factor (EGF) and transforming growth factor α (TGFα), and the EGF receptor (EGFR), during airway repair [276]. Elevated expression of EGFR was observed among

a population of squamated epithelial cells located within terminal bronchioles during repair from naphthalene exposure. Moreover, cells with abundant EGFR also incorporated the nucleoside analogue BrdU, suggesting a role for EGF in regulation of progenitor cell proliferation. Findings of Van Winkle and coworkers investigating the kinetics, distribution and morphology of cells expressing EGFR early in the response to naphthalene exposure show a close correlation with the distribution and proliferative kinetics of CE cells described in the present study that exhibit properties of stem cells. Clearly, microenvironmental cues are involved in both regulation of stem cell phenotype, stem cell maintenance and their activation following progenitor cell depletion.

Microenvironments that support the maintenance of adult stem cells have recently been identified within both the surface and glandular epithelium of pulmonary airways. The best characterized stem cell microenvironments include those of the submucosal gland in proximal airways [29], the neuroepithelial body (NEB) microenvironment [224], and the BADJ microenvironment identified in the present study. However, very little is known at present of the molecular and cellular mechanisms that account for stem cell maintenance within these lung microenvironments. The composition of airway epithelia at each location differs quite dramatically, a feature which raises the question of whether intrinsic or extrinsic factors influence stem cell maintenance and the fate of daughter cells. In this regard, it is interesting to note that basic features of stem cells located within BADJ and NEB microenvironments are similar despite clear differences in the cellular milieu at these locations. More thorough analysis of the molecular phenotype of stem cells located within these disparate microenvironments is needed which may, in turn, shed light on molecular mechanisms contributing to their maintenance.

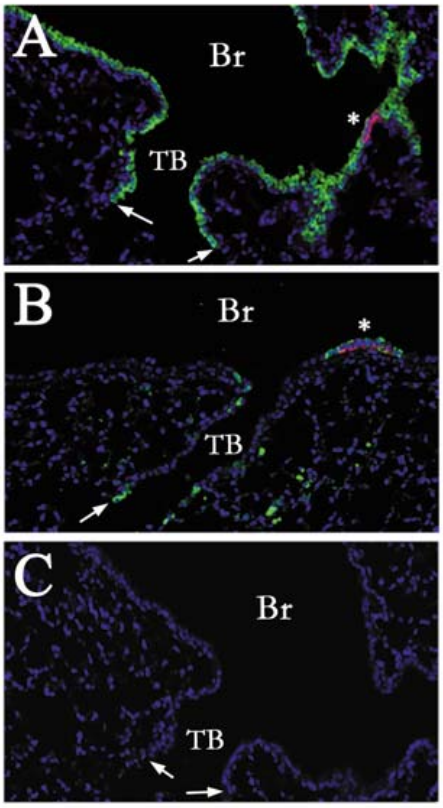

Figure 3.1 Pollutant resistant CCSP expressing cells occupy multiple distinct microenvironments within the conducting airway epithelium.

CCSP (green) and CGRP (red) immunopositive cells were detected by dual color immunofluorescent staining of lung tissue sections from either untreated control mice (A) or mice treated with 275 mg / kg naphthalene and recovered for 24 hours (B). Primary antibodies against CCSP and CGRP were omitted from untreated lung samples as a control for antibody specificity (C), and nuclei were counterstained with DAPI (blue fluorescence, A-C). Immunofluorescent cellular debris (lacking nuclei) in the alveolar space (panel B) is an artifact of inflation fixation. Analysis revealed a significant decrease in the number of CCSP positive cells in both the bronchiole (Br) and terminal bronchiolar (TB) airways of naphthalene treated mice (B). Rare populations of naphthalene-resistant CCSP-immunoreactive cells were located directly adjacent to CGRP positive neuroepithelial bodies (NEBs, asterisks in A, B), or at the broncho-alveolar duct junction (BADJ, arrows in A, B). Original magnification x100.

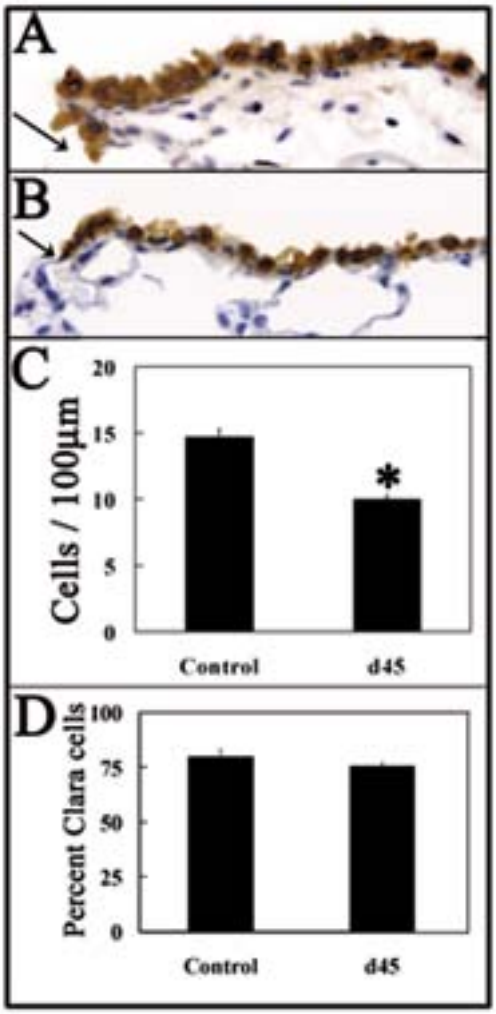

Figure 3.2 Cells within terminal bronchioles support regeneration of airways of appropriate cellular diversity.

CCSP immunopositive cells in terminal bronchioles were detected by immunohistochemistry 45 days following intraperitoneal injection of vehicle (A) or 275 mg/kg naphthalene (B). Nuclei were counterstained with hematoxylin; arrows indicate the broncho-alveolar duct junction (BADJ, A-B). Morphometric analyses of cell density (total cells / 100 μm basement membrane; panel C), and representation of Clara cells (percent Clara cells / total epithelial cells; panel D) were performed as described in Methods. Eight to sixteen terminal bronchioles were analyzed per lung (n = lungs from 3 mice). Significant changes in overall cell density (C, $P<0.005$) but not percent of Clara cells (D) indicates an appropriate differentiation potential of epithelial cells within terminal bronchioles following naphthalene induced injury. Original magnification x400.

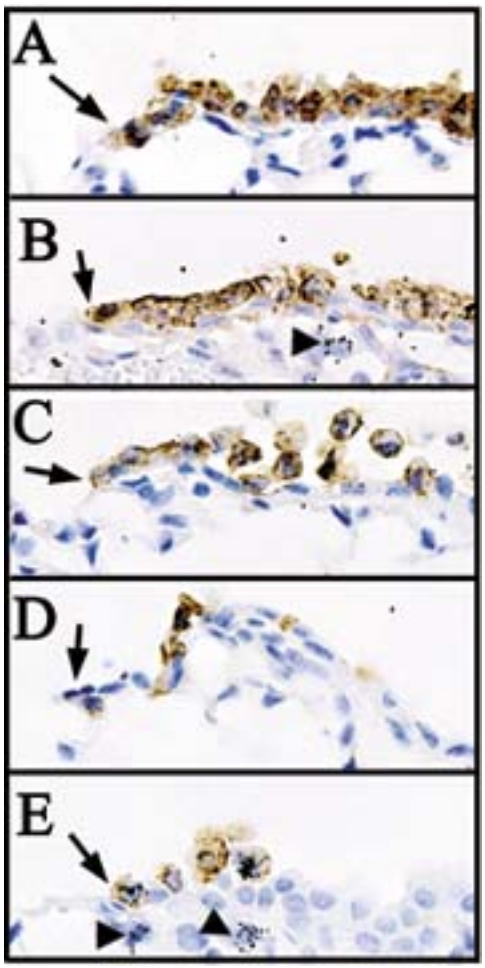

Figure 3.3 CCSP expressing cells adjacent to the broncho-alveolar duct junction are pollutant resistant and represent the initial proliferative epithelial popubation.

Mice were exposed to 275 mg/kg naphthalene and recovered for 0, 6, 12, 24 and 36 hours (panels A-E, respectively). Proliferating, mitotic cells were labeled with 2.5 mCi [^{3}H]-TdR / kg body weight 1 hour prior to sacrifice. CCSP expressing (CE) cells were detected by immunohistochemistry using DAB detection (brown) and sites of [^{3}H]-TdR incorporation identified by autoradiography (black grains). Nuclei were counterstained with hematoxylin. Naphthalene resistant CE cells are detectable adjacent to the broncho-alveolar duct junction (BADJ) at all time points (arrows in A-E), and are the initial proliferative epithelial cell type 36 hours following naphthalene administration (black grains, panel E). Arrowheads (B, E) indicate underlying proliferative mesenchymal cells. Original magnification x400.

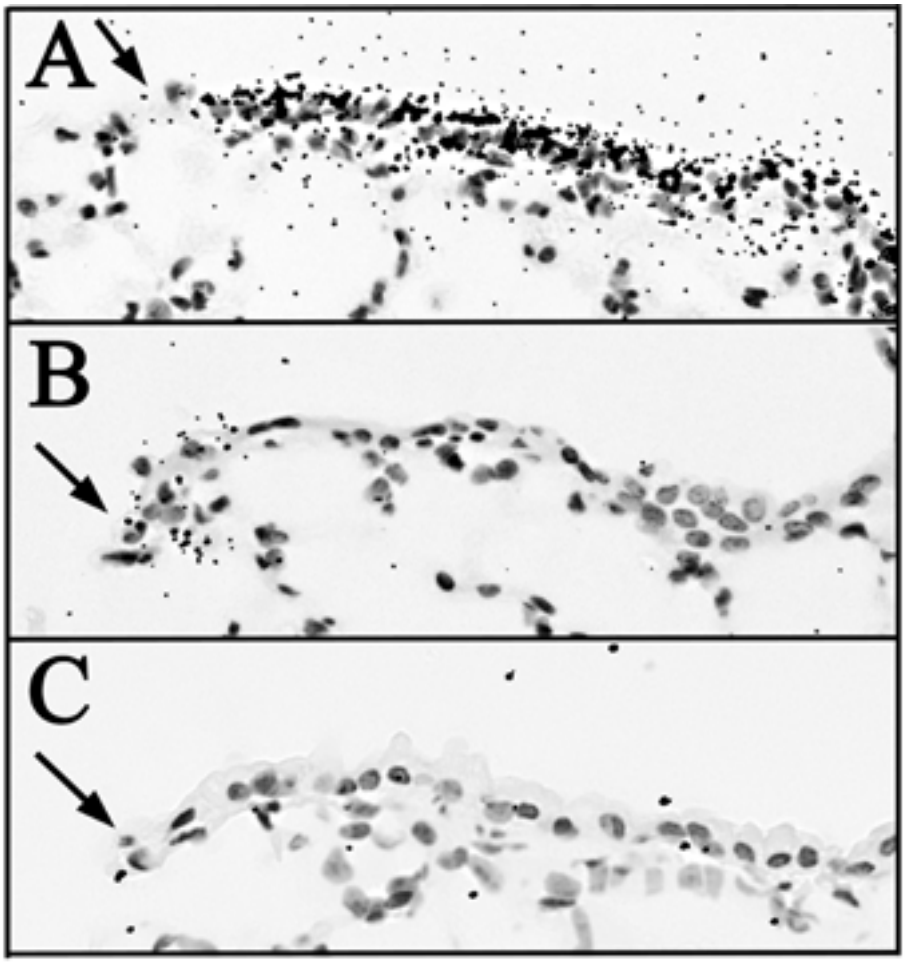

Figure 3.4 BADJ associated pollutant resistant cells maintain CCSP gene expression.

CCSP gene expression in untreated control (A) and during the period of maximum injury 24 hours following 275 mg/kg naphthalene treatment (B) was determined by in situ hybridization using an antisense [^{35}S]-labeled CCSP riboprobe. Untreated, CCSP -/- tissue was used as a negative control (C). Hybridization was detected by autoradiography (black grains), and indicates a population of pollutant resistant, CCSP mRNA positive cells immediately adjacent to the BADJ (arrows, A-C). Panels are representative of terminal bronchioles of three animals per exposure group. Original magnification x400.

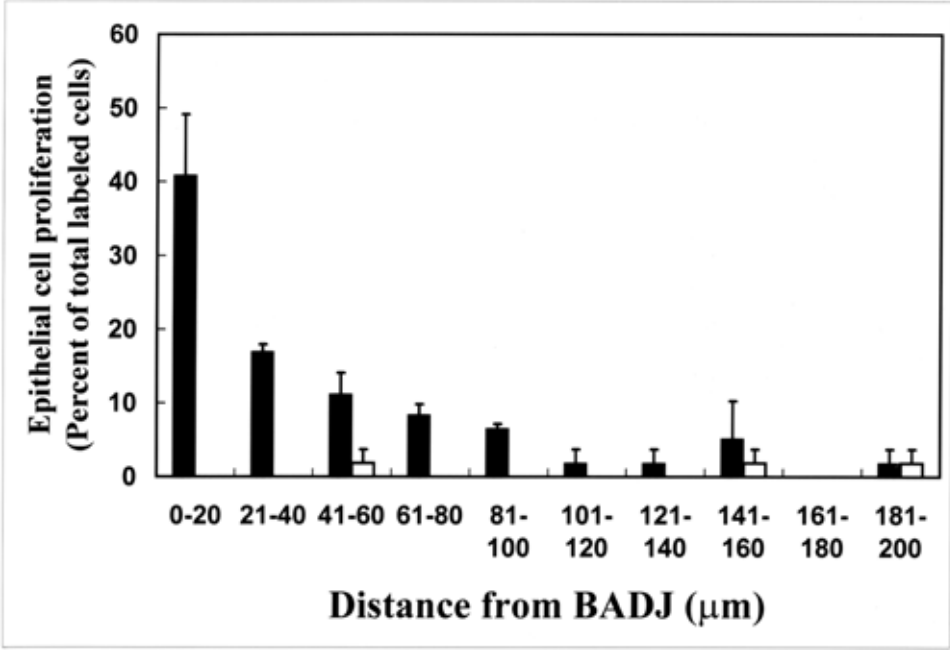

Figure 3.5 Proliferative CCSP expressing cells are preferentially associated with the broncho-alveolar duct junction.

Distribution of [^{3}H]-TdR labeled cells was determined within the terminal bronchiole 36 hours after 275mg/kg naphthalene exposure. Terminal bronchioles were divided into 20μm segments originating from the BADJ and the number of labeled CCSP expressing (CE, black bars) or CCSP negative (white bars) cells in each segment enumerated. Fifty seven percent of labeled CE cells were found within 40μm (6 cell diameters) of the BADJ. In contrast, CCSP negative cells contribute only slightly to this initial proliferative population and were not spatially restricted within the terminal bronchiole. Data represent the summation of 8-10 terminal bronchioles / section (n=3 animals) ± SEM.

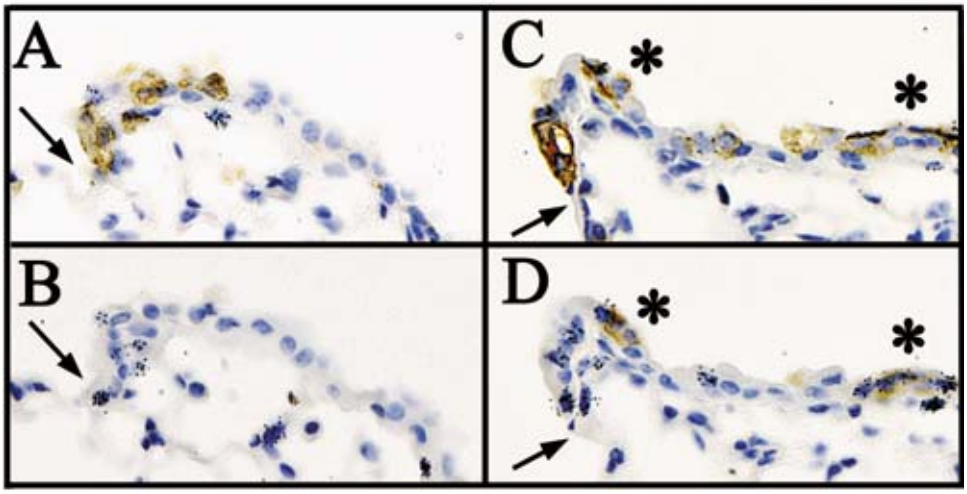

Figure 3.6 Proliferative CCSP expressing (CE) cell populations function independently of pulmonary neuroendocrine cells (PNECs) / neuroepithelial bodies (NEBs) in the terminal bronchiole.

Adjacent serial section immunostaining for CCSP (A, C) and CGRP (B, D) was coupled with autoradiography (black grains) to determine whether terminal bronchiolar proliferation was preferentially associated with CGRP immunopositive PNECs / NEBs. The majority (75%) of terminal bronchioles contain numerous mitotic CCSP expressing (CE) cells adjacent to the BADJ (A) yet lack any CGRP positive PNECs / NEBs in the adjacent serial section (B) 36 hours after 275mg / kg naphthalene. A minority of terminal bronchioles (25%) appear to contain both CCSP (C) and CGRP (D) positive mitotic cells by adjacent serial section analysis. Interestingly, the occurrence of NEBs (asterisks, C and D) appeared to relax the requirement for BADJ-association among proliferating CE cells of the terminal bronchiole (black grains; A/B versus C/D).

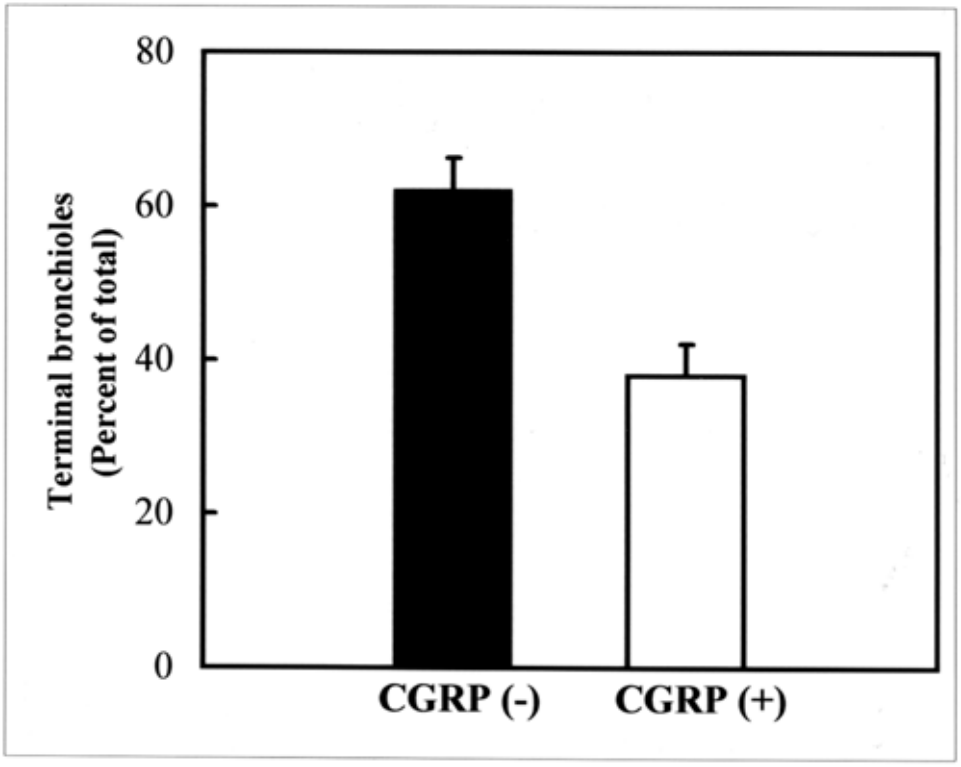

Figure 3.7 The majority of terminal bronchioles lack pulmonary neuroendocrine cells / neuroepithelial bodies following naphthalene injury.

Dual color immunofluorescent staining for CCSP and CGRP proteins was used to colocalize CCSP expressing (CE) and pulmonary neuroendocrine cell (PNEC) populations within terminal bronchioles 24 hours following exposure to 275mg/kg naphthalene. Twenty consecutive 5 μm adjacent serial lung sections were stained for the presence of CCSP and CGRP and all terminal bronchioles containing a visible broncho-alveolar duct junction were analyzed (minimum of 5 terminal bronchioles / animal; n=5 animals). While all terminal bronchioles analyzed contained detectable CCSP immunoreactive cells at or near the BADJ, greater than 60±5% lacked any CGRP positive PNECs / neuroepithelial bodies at any location within the terminal bronchiole. Error bars represent SEM.

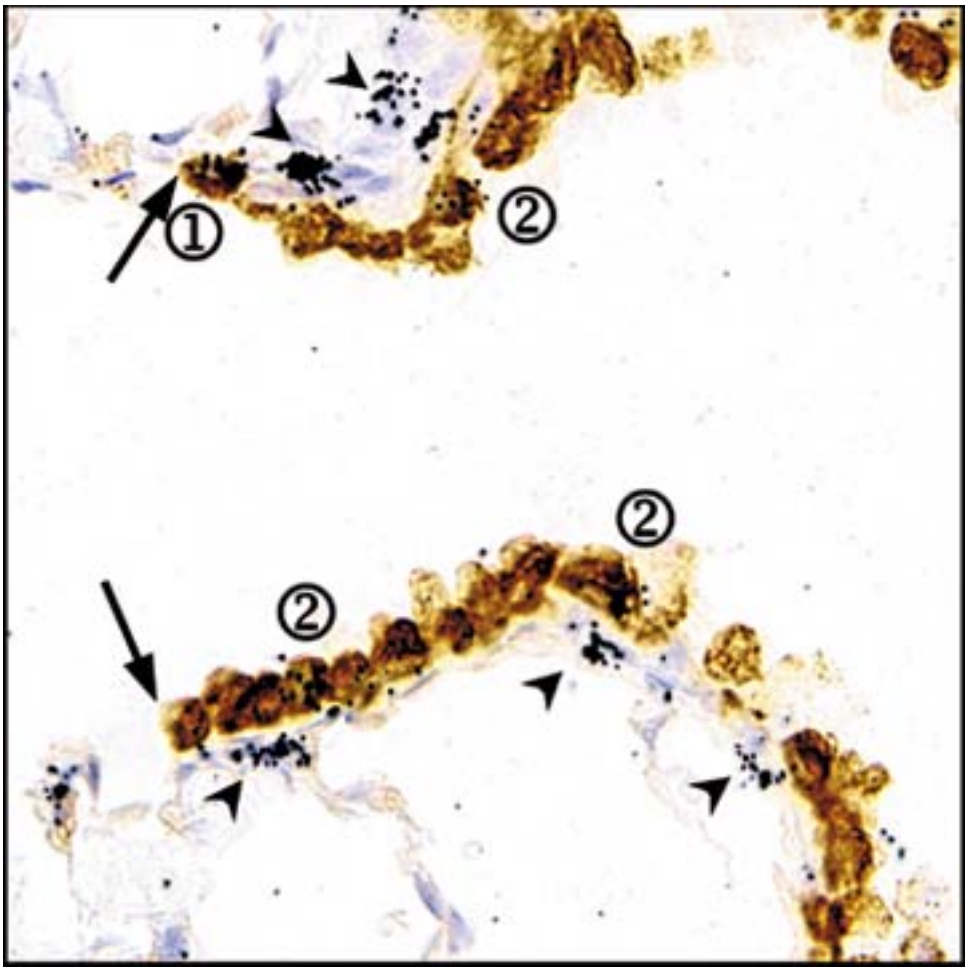

Figure 3.8 Broncho-alveolar duct junction-associated CE cells represent a slow cycling (label retaining) cell population.

Mice were exposed to 275 mg/kg naphthalene and [^{3}H]-TdR was administered continuously for the subsequent 7 day period via a miniosmotic pump. Recovering mice were sacrificed 45 days following naphthalene exposure, at which time CCSP protein expression and label retention was visualized by immunohistochemistry and autoradiography of lung tissue sections. The majority of labeled cells contained an average of 5-10 grains / nuclei, and were composed of both CCSP immunopositive (circled #2) and immunonegative cells (not evident in field). A rare population of CCSP expressing cells located near the BADJ (arrow) were more heavily labeled with an average of >15 grains / nuclei (circled #1). Fibroblasts, identified by location and nuclear morphology, also contained large numbers of grains / nuclei (arrowheads). Original magnification x1000.

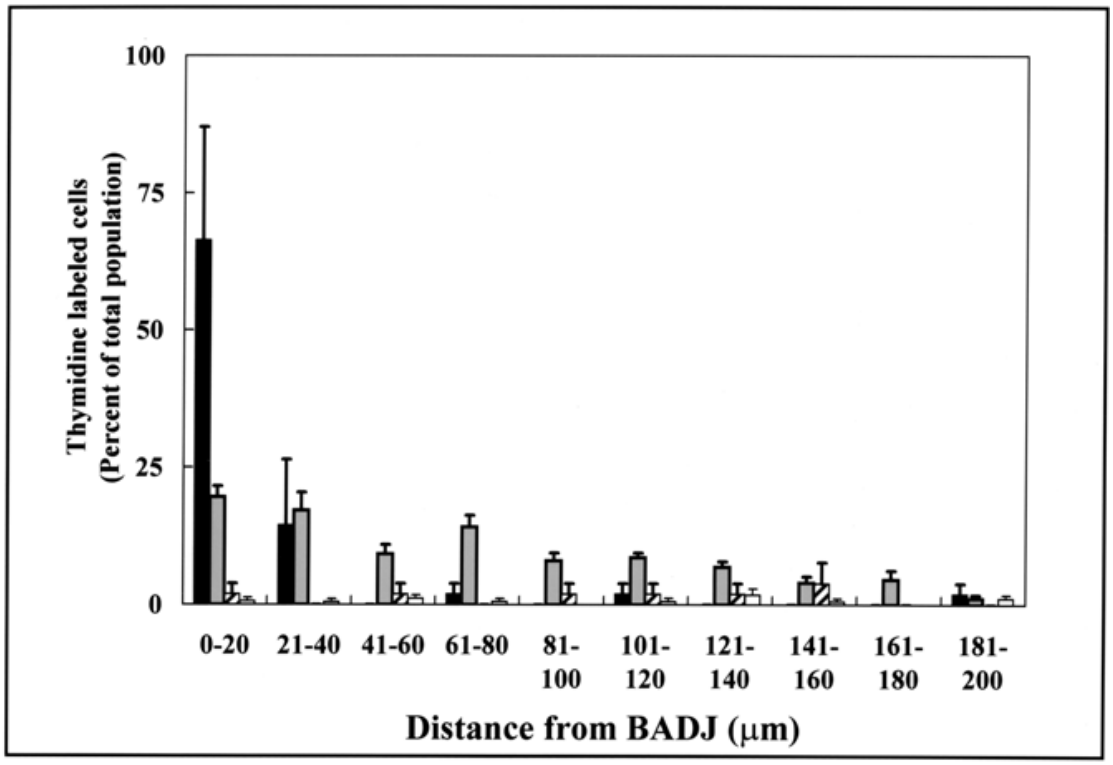

Figure 3.9 CCSP expressing label retaining cells are preferentially located at the BADJ.

The distribution of [^{3}H]-TdR labeled (5-10 grains / nuclei) and label-retaining (>15 grains / nuclei) cells in terminal bronchioles of animals exposed to 275mg/kg naphthalene and recovered for 45 days were assessed by morphometric analysis. The percent of each thymidine labeled cell population was plotted independently as a function of distance, in 20 μm increments originating from the BADJ. A correlation was observed between proximity to the BADJ and the abundance of CCSP expressing, label retaining cell populations (black bars). Very few CCSP negative cells label retaining cells (hatched white bars) were identified within terminal bronchioles, and these cells were not associated with the BADJ. Both CCSP immunopositive (gray bars) and negative (white bars) labeled (5-10 grains / nuclei) cell populations were distributed randomly throughout the terminal bronchiole. Data is the summation of 23 terminal bronchioles (n=4 mice).

4. Potential Mechanisms of Pollutant Resistance Within Airway Stem Cells

4.1. Abstract

Lung epithelial-specific stem cells have been localized to discrete microenvironments throughout the adult conducting airway. Properties of these cells include pollutant resistance, multipotent differentiation, and infrequent proliferation. Goals of the present study were to determine levels of the Phase I metabolizing enzyme CYP2F2 within airway stem cell microenvironments and to use Hoechst 33342 efflux, a property of stem cells in other tissues, to further characterize airway stem cells. NEB microenvironments were found to specifically maintain CCSP expressing cells with reduced / undetectable levels of CYP2F2, a property that likely contributes to their observed pollutant resistance. Hoechst 33342 effluxing lung cells were identified as a verapamil-sensitive side population by flow cytometry. Lung side population cells were further subdivided on the basis of hematopoietic (CD45 positive) and nonhematopoietic (CD45 negative) origin. Nonhematopoietic side population cells were enriched for stem cell antigen-1 reactivity and expressed molecular markers specific to both airway and mesenchymal lineages. Analysis of the molecular phenotype of airway-derived side population cells indicates that they are similar to identified NEB-associated, CYP2F2 low, variant Clara cells. Taken together these data suggest that the nonhematopoietic side population isolated from lung is enriched for airway stem cells. These variant CCSP expressing cell phenotypes of low CYP2F2 expression and rapid Hoechst 33342 efflux are both potential mechanisms of pollutant resistance within airway stem cell populations.

4.2. Introduction

Recent studies indicate that subsets of cells localized within discrete microenvironments of conducting airways maintain properties consistent with adult tissue-specific stem cells. Within intrapulmonary airways, stem cells are localized either to neuroepithelial bodies (NEBs) or the broncho-alveolar duct junction (BADJ) [95, 110, 224, 225, 249]. In the trachea and proximal airways, stem cells with properties of label retention and multipotent differentiation potential have been localized within both the submucosal gland duct junction and intercartilagenous zones [29, 70, 71]. Thus, regionally specific stem cell microenvironments exist at all levels of conducting airway and harbor cells with significant repopulation capacity.

Intrapulmonary stem cell pools exhibit the molecular property of Clara cell secretory protein (CCSP) expression, yet have been distinguished from Clara cells by their resistance to the Clara cell-specific toxicant naphthalene [224, 250]. Likely mechanisms of pollutant resistance among airway stem cells include a reduced level of phase I metabolizing enzymes that transform naphthalene to its reactive metabolites and maintenance of enhanced glutathione (GSH) dependent detoxification systems (phase II pollutant metabolism) [39, 83, 84, 86, 89, 145, 147, 215, 216, 274, 279, 288, 302-304]. Evidence exists supporting the presence of Clara cell subpopulations throughout airways with this second property. In steady state conditions, intracellular GSH levels varied by as much as four fold between isolated airway cells [303]. Repeated systemic low-dose naphthalene exposures result in Clara cell populations with enhanced intracellular GSH and increased naphthalene pollutant resistance [302, 304]. These data provide evidence that intracellular GSH levels do contribute to pollutant resistance within subpopulations of airway Clara cells [216, 227, 302, 303, 304]. However, there are currently no

studies investigating levels of phase I metabolizing enzymes specifically within airway stem cell microenvironment-associated Clara cells.

In addition to characteristics including infrequent proliferation and multipotent differentiation, Goodell and others have identified preferential dye / lipophilic drug efflux as a mechanism for enhanced pollutant resistance within hematopoietic stem cells [97, 98, 233]. Commonly referred to as the side population (SP) phenotype, this property was initially defined by a low Hoechst 33342 blue / red fluorescent dye signal when compared to the majority of cells within a given population (non-SP). It was subsequently shown that this SP phenotype was due to ATP-binding cassette (ABC) dependent transporter activity [138, 233, 268]. Moreover, the bone marrow SP was depleted of cells expressing either myeloid or lymphoid lineage-specific markers (Gr-1 or B220, respectively). Fractionation of CD45+ (hematopoietic) bone marrow cell populations using this approach resulted in a SP that was highly enriched for stem cells [97]. These cells exhibited HSC properties of Sca-1 and c-kit expression as well as long-term bone marrow repopulation. This finding was significant as it demonstrated that enhanced lipophilic drug transport properties confer pollutant resistance within hematopoietic stem cells.

Recently, it has been shown that populations cells bearing a characteristic SP profile (low Hoechst 33342 blue / red fluorescence) exist in a number of tissue types [8, 124, 162, 317]. Tissues included mammary gland, liver, muscle, and testicular cell populations. Tissue derived SP cells were similar to bone marrow-derived SP in their sensitivity to ABC transport inhibitors. These cells maintained both functional and molecular properties consisten with their identification as stem cells [8]. Thus, it appears that numerous tissues in addition to bone marrow harbor stem cells with HSC-like drug efflux properties. These findings suggest that ATP-

dependent, lipophilic compound transport is a common mechanism for pollutant resistance within diverse stem cell populations.

The present study tested the hypothesis that NEB- and BADJ-associated CCSP expressing stem cells exhibit their pollutant resistant phenotypes due to reductions in CYP2F2 enzyme levels and enhanced lipophilic drug efflux. Results indicated that NEB-associated CE cells exhibit reduced CYP2F2 levels compared to the majority of airway Clara cells. Results also demonstrate that freshly isolated lung cells include a rare, verapamil-sensitive (ATP-dependent) side population exhibiting molecular markers consistent with CCSP expressing stem cell populations.

4.3. Materials and Methods

Sequential Immunohistochemistry for CCSP / CGRP and CCSP / CYP450 2F2

For dual immunohistochemistry, NEBs were identified by staining the middle of three adjacent serial sections for the PNE-specific antigen CGRP. Flanking sections were stained for the Clara cell marker CYP2F2. Methods were as described in Chapter 3 and antibodies were diluted in PBS / 3% BSA and amine-ethyl carbizol was used as the chromagen. Digital images of CGRP-stained NEB and NEB-associated CYP2F2-positive cells were captured. The chromagen was removed with ethanol, and all sections were restained for the Clara cell marker CCSP as detailed above, using a goat anti-CCSP antibody (1:5000; G. Singh, University of Pittsburgh). Images of the same regions were combined using Adobe Photoshop.

CCSP / CYP450 2F2 Dual Color Immunofluorescence and Imaging

Adjacent serial sections were stained as previously described with optimal concentrations of goat-anti-CCSP (1:8,000) plus rabbit-anti-CGRP (1:15,000) or goat-anti-CCSP (1:8,000) plus a supraoptimal concentration of rabbit-anti-CYP2F2 (1:500). Supraoptimal CYP2F2 antibody concentrations were used to allow for protein abundance quantification following immunofluorescent staining. Secondary antibodies used were donkey-anti-rabbit Alexa 488 and donkey-anti-goat Alexa 594. CCSP / CGRP staining was used to identify pulmonary NEBs, defined by the presence of two or more CGRP immunoreactive pulmonary neuroendocrine cells in close proximity. Terminal bronchiolar BADJ microenvironments were identified morphologically by the presence of a visible alveolar duct. All CCSP expressing cells within 100μm of the NEB or BADJ were analyzed for relative 2F2 protein levels. Single optical images

were analyzed using Metamorph. Briefly, image masks were drawn around the borders of CCSP expressing cells with a visible nuclear profile and these image masks were transferred to CYP2F2 images. The average and integrated pixel intensities of CYP2F2 per unit surface area were calculated for all CCSP positive cells. Average cellular CYP2F2 protein levels were graphed with respect to distance from the center of NEBs or the BADJ (defined as "landmark" in text).

Animal Housing

FVB/n mice were maintained as an in-house breeding colony under specific pathogen free conditions and health status was monitored quarterly via a sentinel-screening program. Animals were maintained on a twelve hour light / dark cycle and allowed access to food and water ad libitum. All mice used in experiments were eight to twelve weeks of age.

Lung Cell Isolation

Animals were sacrificed by intraperitoneal injection of 2.5% avertin to achieve a surgical plane of anesthesia followed by exsanguination. Lungs were perfused with Hanks' Balanced Salt Solution (HBSS, Invitrogen, Grand Island, NY) and the lungs lavaged 8 times with 1 ml HBSS / 200 μM EGTA (Sigma, St. Louis, MO). Lung cells were isolated by the method of Chichester [39] with minor modifications. Briefly, the entire heart-lung unit was removed and suspended in 2 liters of 37 °C saline. One ml of elastase (3.5u / ml in HBSS; Worthington, Lakewood, NJ) was instilled into each lung via a tracheal cannula, incubated for 5 min, and the process repeated five times. Following digestion, lungs were finely minced into <1mm pieces using a razor blade, strained through a 100 μm nylon membrane (Becton Dickinson, Franklin Lakes, NJ), and

resuspended in 35 mL HBSS containing 0.2mg/ml DNase. Eight milliliters of sterile fetal bovine serum (FBS, Invitrogen) was under-layered and cells pelleted by centrifugation at 300g for 5 min at 4 °C. Cells were washed twice in HBSS containing 2% FBS / 10mM HEPES pH7.4 (HBSS+) as described above, and resuspended at $1x10^6$ live cells / milliliter in DMEM containing 2% FBS / 10mM HEPES pH7.4 [97].

Bone Marrow Cell Isolation

Animals were sacrificed as described above and the femurs recovered by blunt dissection. The epiphesial ends were removed and and the lumen of the metaphesis flushed with 5 ml HBSS. Cell aggregates were dispersed by trituration, washed twice in HBSS containing 2% FBS / 10mM HEPES pH7.4 (HBSS+) as described above, and resuspended at $1x10^6$ live cells / ml in DMEM containing 2% FBS / 10mM HEPES pH7.4 .

Hoechst 33342 Incubation

Cells were stained with 5 μg/ml Hoechst 33342 (Sigma) alone or in combination with 50 μM Verapamil (Sigma) for 90 minutes at 37°C with intermittent mixing. Immediately following staining, cells were placed on ice, pelleted, and washed twice with ice-cold HBSS+ containing 0.2 mg/ml DNase as described above. Staining for cell specific surface markers was performed at 4 °C following incubation with Hoechst 33342. Briefly, directly-conjugated mouse anti-CD45 (FITC, clone 30-F11, Becton Dickinson) and / or mouse anti-Sca-1 (PE, clone D7, Becton Dickinson) were applied at a concentration of 1 μg antibody / 10^6 cells and incubated for 30 min. at 4 °C. An isotype-matched control antibody was used to confirm the specificity of Sca-1 antibody staining. Propidium iodide (2 μg / ml, Sigma) was added to the cell suspension 5

minutes before sorting to discriminate between viable (dye impermeant) and nonviable (dye permeable) cells.

Immunostaining

After elastase digestion 10^5 cells were cytospun onto slides for immunophenotypic analysis. Cells were fixed overnight in 10% neutral buffered formalin (Fisher, Pittsburgh PA), washed three times in excess PBS, and blocked using 5%BSA / PBS. Cells were then stained using antibodies for the airway specific markers CCSP (Rabbit-anti-CCSP, 1:8000) (24) and acetylated tubulin (Mouse IgG2b-anti-ACT, 1:8000, Sigma), washed, and subsequently stained with appropriate secondary antibodies Donkey-anti-Rabbit Alexa 594 (1:500, Molecular Probes, Eugene, OR) and Goat-anti-mouse IgG2b Alexa 488 (1:500, Molecular Probes). Nuclei of cells were counterstained using 1μg/ml 4',6-Diamidino-2-phenylindole dihydrochloride (DAPI, Sigma).

Flow Cytometry

Cells were analyzed and sorted on a MoFlo (DakoCytomation, Fort Collins, CO) high-speed cell sorter equipped with 3 excitation lines (488 nm, ultraviolet, and 635nm), 8 parameters and subsystems of SortMaster Droplet Control, and CyCLONE Automated Cloner. SP cells were identified as described (in text) [97]. Bandpass filters, 670/40 nm and 450/65 nm, were used to measure the red and blue Hoechst 33342 emission, respectively. Red fluorescence due to propidium iodide staining was detected using a 613/20nm bandpass filter. Antibodies used for phenotypic analysis of SP cells were directly conjugated with FITC or PE, and emission of these fluorochromes was detected using 530/40 nm and 575/26 nm bandpass filter.

RNA Isolation and RT-PCR

Six-thousand sorted cells belonging to either total, non-side population, or side population categories (see Figure 4.7) were directly sorted into cell lysis buffer (Promega, Madison, WI) and frozen prior to RNA isolation using a glass fiber system (SV Total RNA Isolation Kit, Promega, Madison, WI). All RNA samples were eluted in 60 μl of nuclease free water. First-strand cDNA synthesis was performed on 20 μl RNA using random hexamer primers in the presence (+ RT) or absence of Superscript II reverse transcriptase (-RT, Invitrogen). RT-PCR (40 cycles) was carried out using AmpliTaq Gold DNA polymerase (Applied Biosystems, Foster City, CA) and three μl of cDNA template. Primers used in PCR were as indicated in Table 1. PCR reactions for CCSP, CYP2F2, PECAM, and Vimentin were carried out at an annealing and extension temperature of 60 °C, 1 min per cycle. PCR reactions for SP-C and β -actin were carried out at an annealing temperature of 51 °C (30 seconds / cycle) and an extension temperature of 72 °C (1 min / cycle). Products were separated on 3% agarose gels containing ethidium bromide and visualized using an Alpha Innotech video gel documentation system and digital imaging software (Alpha Innotech, San Leandro, CA).

4.4. Results

Rare populations of CCSP (high) CYP2F2 (low) cells exist within NEB microenvironments.

To determine whether differences exist in levels of phase I metabolizing enzymes present within CCSP expressing airway stem cells, adjacent serial sections were sequentially stained with CGRP + CCSP or CYP2F2 + CCSP. Antigens were visualized by sequential AEC chromagen and DAB immunohistochemistry, and images were overlaid using Adobe Photoshop (Figure 4.1). Results indicate that approximately 10% of NEB-associated cells expressed both CGRP (red, Figure 4.1A, C) and CCSP (black, Figure 4.1B, C). These cells localized to regions immediately adjacent to NEB microenvironments (Figure 4.1C, arrowheads). Adjacent serial sections were then immunostained to determine whether NEB-associated CCSP / CGRP dual expressing cells might express variant levels of the phase I metabolizing enzyme CYP2F2 (Figure 4.1, D-F). Results demonstrate that the majority of airway CCSP expressing cells coexpress significant levels of the phase I metabolizing enzyme CYP2F2 (Figure 4.1F, arrowheads). Rare, NEB-associated CCSP positive, CYP2F2 negative cells were detected in close proximity to CCSP / CGRP dual-positive cells identified on adjacent serial sections (compare arrowheads, Figure 4.1C and arrows, Figure 4.1F). Cells deficient in normal CYP2F2 protein likely exhibit enhanced pollutant resistance due to their reduced capacity to convert naphthalene to its reactive metabolite.

We next wished to determine whether CYP2F2 negative, CCSP expressing cells detected within NEB microenvironments by serial immunohistochemistry were present within airway terminal bronchioles. Dual color immunofluorescent staining was performed using optimal CCSP and supra-optimal CYP2F2 antibody dilutions (see Methods). In addition the current

study provided a semi-quantitative measurement for CYP2F2 levels in NEB-associated Clara cells. Results indicated that NEB-associated, CCSP positive cells overlying or immediately adjacent to pulmonary neuroendocrine cells contained approximately 50% less CYP2F2 than non-NEB-associated Clara cells (Figure 4.2, 4.3). BADJ-associated CCSP expressing cells did not exhibit quantitative differences in CYP2F2 levels when compared to the majority of airway Clara cells. Together these data reinforce previous findings suggesting that fundamental differences exist between identified airway stem cell microenvironments (see Chapter 3). These data also indicate that other aspects of pollutant resistance (enhanced phase II metabolism, efficient pollutant transport) must function within BADJ microenvironment-associated CCSP expressing stem cells to protect them from naphthalene toxicity.

Two distinct Hoechst 33342 effluxing populations exist within elastase digested lung.

We next determined whether efficient dye / drug efflux properties associated with stem cell populations in other tissues were present within identified airway stem cells. Briefly, lung cells were dissociated from intrapulmonary airways through instillation of porcine elastase and single cells were recovered following mincing of the digested tissue. Typical preparations yielded cells that were greater than 95% viable based upon trypan blue dye exclusion and included 32% ± 4% CCSP immunoreactive cells and 20% ± 3% acetylated tubulin immunoreactive ciliated cells (Figure 4.4). Flow cytometric analysis of CD45 expression indicated that 30% of isolated cells were of the hematopoietic lineage (Figure 4.5 and data not shown). Very few basal (less than 0.1% of total) and no immunoreactive pulmonary neuroendocrine cells were identified by immuophenotypic analysis of total cells. Thus, elastase-isolation of lung cells results in a significant enrichment for cells expressing airway-specific

markers. Isolated cells were incubated in the presence of 5 μg / ml Hoechst 33342 for 90 min, washed, and immunostained with mouse anti-CD45 for segregation of hematopoietic (CD45+) and lung (CD45-) cells. Dead cells were identified by addition of 2 μg/ml propidium iodide. For each experiment, a preliminary analysis was used to establish gates based on forward scatter (FSC) / side scatter (SSC) that eliminated erythrocytes and debris from subsequent analysis, propidium iodide fluorescence to restrict analysis to living cells, and pulse width to select for single cells. All cells were simultaneously sorted on the basis of these six parameters (Hoechst 33342 red, Hoechst 33342 blue, propidium iodide, forward scatter, side scatter, FITC-CD45 reactivity).

Cells characterized by rapid efflux of Hoechst 33342 were detected in both the CD45+ and CD45- groups (Figure 4.5A and B, respectively). Generation of each of these subpopulations was inhibited by coincubation with the ABC transport inhibitor verapamil indicating that Hoechst 33342 efflux is dependent on ATP-binding cassette (ABC) transporter function (Figure 4.5,boxes R1 in C and D). Identification of verapamil-sensitive, CD45+ and CD45- lung side population (SP) cells was independent of both gender and genetic background (FVB/n, C57/Bl6, 129/Sv, hybrid strains; data not shown). Within the FVB/n strain, the average representation of CD45+ (hematopoietic) SP cells was 0.09 ± 0.02% of CD45+ cells while the average representation of CD45- (non-hematopoietic) SP cells was 0.87 ± 0.22%. These data demonstrate that cells from elastase-digested lung tissue contain two populations of cells characterized by rapid efflux of Hoechst 33342: the CD45+ and the CD45- side populations. The overall cellular toxicity associated with 5 μg / ml Hoechst 33342 exposure for 90 min was approximately 60%. Differential susceptibility of the CD45+ and CD45- cell populations to Hoechst 33342 incubation resulted in a shift in the representation of viable cells such that ~60 %

of cells were CD45+ and ~40% were CD45-. This finding was highly consistent and did not appear to influence the representation of hematopoietic or non-hematopoietic SP cells identified in the present study. This lineage dependent toxicity observed following Hoechst 33342 incubation was not entirely unexpected as previous studies confirm that there is significant time, species, and cell type-specific dependence associated with Hoechst 33342 exposure [61, 92, 135, 281]. To address whether the Hoechst 33342 stained, PI negative, sorted cell population remains viable following the initial FACS analysis, CD45- cells were subjected to re-sorting in the presence of PI 30 min after their initial isolation. Approximately 5% of cells were PI permeable after this time interval indicating that the vast majority of initially sorted cells retain viability. Similar findings were obtained by evaluating trypan blue dye exclusion up to 90 minutes after initial sorting (data not shown).

Stem cell antigen-1 (Sca-1) is enriched within lung SP cells.

In order to further characterize SP cells released by elastase digestion of lung tissue, expression of stem cell antigen-1 (Sca-1), an antigen highly enriched in SP cells of the hematopoietic lineage, was assessed [97]. Lung or bone marrow-derived cells were stained with Hoechst 33342, a FITC-conjugated mouse anti-CD45, and a PE-conjugated mouse anti-Sca-1 antibody. The minimum fluorescence intensity required for classification of cells as Sca-1 positive (brackets, Figure 4.6A-C) was established by staining cells with an isotype-matched control antibody (see Methods). As has been reported previously, Sca-1 expressing cells were significantly enriched within bone marrow-derived SP (78% positive) and were infrequent within the non-SP fraction (3% positive, Figure 4A, gray and black, respectively). In contrast, Sca-1 immunoreactivity was not significantly observed among CD45+ SP or non-SP cells (Figure

4.6C, grey and black respectively). The majority of lung CD45- SP cells expressed Sca-1 (80%, Figure 4.6B, grey); however this antigen was also expressed by 30% of cells within the non-SP fraction (Figure 4.6B, black tracing). While these results demonstrate molecular similarity between SP cells of the bone marrow and CD45- SP cells of the lung, expression of Sca-1 by CD45- non-SP cells limits the utility of this antigen as a positive selectable marker for putative lung stem cells.

Non-hematopoietic lung side population cells exhibit a unique molecular phenotype.

In order to characterize the molecular phenotype of CD45- lung SP, RNA was purified from pools of 6000 unfractionated CD45- cells (Figure 4.7A, R3), 6000 CD45- non-SP (Figure 4.7A, R2), and 6000 CD45-SP cells (Figure 4.7A, R1) and gene expression was assayed by reverse transcription-polymerase chain reaction (RT-PCR). Expression of gene products detailed in Table 1 was analyzed. A no reverse transcriptase negative control reaction was performed for all samples and total lung RNA served as the positive control.

The cell-specific genes CCSP and CYP2F2 (Clara cells), SP-C (Type II cells), and vimentin (Fibroblasts) were expressed in the unfractionated CD45- cell population (Figure 4.7B, Total). Platelet-endothelial cell adhesion molecule (PECAM) was not detected in this population suggesting minimal endothelial cell isolation within the elastase preparation. All genes expressed within the unfractionated CD45- population were also detected in RNA isolated from non-SP cells, indicating that this gate provides an adequate representation of the total CD45- population (Figure 4.7B, Non-SP). In contrast, only CCSP and vimentin were detected in the CD45- SP cells. Based upon these findings it is likely that the CD45- lung SP fraction includes at least two populations of cells, one with molecular characteristics of mesenchymal cells (vimentin

positive) and the other with characteristics of airway epithelial cells (CCSP positive). The finding that CYP2F2 mRNA is undetectable within the CD45- SP cells suggests that lung epithelial cells represented within this fraction do not exhibit a molecular phenotype typical of Clara cells. This finding is consistent with our previous identification of a NEB-associated CCSP expressing cell population that lacks immunoreactive CYP2F2 protein [224].

4.5. Discussion

The current study demonstrates that neuroepithelial body-associated CCSP-expressing stem cells contain reduced levels of CYP2F2 enzyme [110, 224, 225]. These cells, which are specifically NEB microenvironment-associated and contain approximately 50% less CYP2F2 than other CCSP expressing cells, should not efficiently metabolize naphthalene to its reactive metabolites. These cells would therefore be resistant to the direct cytotoxicity of parenterally administered naphthalene. A similar deficiency in phase I metabolism has been proposed to confer protection to hepatic oval cells following pollutant exposure [88, 197, 283]. Studies of in vivo 1,1-Dichloroethylene (DCE) exposures provide direct evidence that Clara cell-specific phase I metabolizing enzyme levels directly influence cellular pollutant sensitivity [56, 86, 87, 89, 147]. In these studies, A/J and C57/Bl6 strain mice were injected with [^{14}C]-DCE and their relative reactive metabolite levels and Clara cell damage were assessed. Bronchiolar damage and metabolite formation were significantly greater in A/J strain mice that exhibit increased levels of baseline CYP450 enzymes. Subsequent studies revealed that inhibition of CYP450 activity using isotype-specific inhibitors reduced intracellular metabolite formation and Clara cell toxicity. Therefore, a precedent exists for differences in CYP2F2 enzyme levels regulating relative pollutant sensitivity / resistance within Clara cell subsets.

Results of this study also demonstrate the existence of a population of lung cells capable of effluxing Hoechst 33342 through a verapamil-sensitive ABC-transporter. These side population (SP) cells were further segregated into hematopoietic and non-hematopoietic lineages according to the presence or absence of cell surface CD45, respectively. Expression of stem cell antigen (Sca-1), a cell surface antigen enriched within the bone marrow SP [97], was enriched

among CD45 negative lung SP. However, unlike bone marrow SP cells, expression of Sca-1 was not unique to the SP cells of lung. Nonhematopoietic lung SP cells expressed the molecular markers vimentin and Clara cell secretory protein (CCSP) but not the type 2 cell marker surfactant protein-C (SP-C) or the endothelial cell marker PECAM. Thus, the gene expression profile of CD45 negative lung SP indicates the presence of only mesenchymal and conducting airway-derived cells. The finding that CCSP-positive, CYP2F2 –negative cells are enriched within the SP further supports the contention that these cells exhibit properties of previously characterized stem cell populations. The relative paucity of nonhematopoietic SP (less than 0.9% of viable, CD45 negative cells) is consistent with the frequency of airway stem cells.

It is hypothesized that the genetic integrity of stem cells is critical for maintenance of normal differentiation within a given organ system. Due to their long life and robust differentiation potential mutations within stem cells could have significant effects on the health status of the entire organism. While infrequent proliferation and sequestration within a microenvironment are mechanisms for maintenance of this genetic integrity, the expression of ABC transporters (resulting in the SP phenotype) may provide a further level of protection. Targeted deletion of the ABC transporter BCRP1 resulted not only in loss of all SP cells but also increased susceptibility of hematopoietic stem cells to the chemotherapeutic agent mitoxantrone [318]. Thus, factors directly related to identification of hematopoietic SP cells also serve to protect this cell from toxicant injury. Studies are ongoing to determine the role of ABC transporter activity in maintenance and observed pollutant resistance of lung stem cell populations.

In addition to identification of nonhematopoietic SP, we also confirmed the presence of a subset of CD45(+) cells with an SP phenotype in lung. One interpretation of this finding in other

organs has been that CD45(+) SP cells represent a population of tissue-resident stem cells [124]. This hypothesis is contradicted by the recent work of Weissman and colleagues in which parabiotic sex- or CD45 isotype-mismatched mice are used to identify circulating partner-derived HSC within multiple tissues [285, 309]. This has led to a new theory which states that circulating / transiently resident HSC are common throughout multiple tissues and that these cells are distinct from indigenous tissue-specific stem cells. Further support for this hypothesis comes from a recent study by McKinney-Freeman et. al. detailing the differentiation potential of muscle-derived SP cells [162]. In this work, the authors demonstrate that heterogeneity in CD45 expression can be used to segregate cells harboring either hematopoietic or myogenic potential within the muscle-derived SP. While each of these types of muscle SP show enhanced differentiation potential relative to its corresponding non-SP, it was clear that only CD45(+) SP cells were capable of colonizing the hematopoietic lineage *in vitro* [162]. Moreover, studies by Asakura and Rudnicki demonstrate that a large number of tissues contain SP with hematopoietic colony forming potential [8]. As was the case in muscle, only the CD45(+) fraction of these cells demonstrate the ability to undergo any hematopoietic differentiation. Therefore, it is most likely that the CD45(+) lung SP cells identified in this study are only capable of hematopoietic differentiation.

A recent paper by Summer, et al. also describes the identification of lung-derived SP cells with properties similar to bone marrow SP [253]. Side population cells identified in this corresponding study are predominately CD45 positive, expresses high levels of platelet-endothelial cell adhesion molecule (PECAM, CD31), and are uniformly Sca-1 positive. In addition to these distinct findings, the SP they identify was significantly less abundant than SP identified in our study (0.05% versus 0.87% of total cells). This discrepancy likely results from

differences in the methods used for lung cell isolation, particularly methods used for enzymatic dissociation of lung tissue. Whereas the SP identified by Summer et al. is predominately positive for PECAM / CD31 [253], endothelial cell-specific mRNA species were not detected in any isolated cell populations (total, non-SP, nor SP) within the current study. This data suggests that these isolation protocols and the SP subsequently purified from them are composed of distinct subsets of cells, further supporting the hypothesis that multiple distinct populations of stem cells likely exist within different lung compartments [29, 71, 95, 110]. Future studies are needed to determine whether SP subsets exist within other cellular compartments of the lung that were not adequately sampled with the isolation methods employed in this study.

In summary, studies presented herein demonstrate the existence of variant Clara cell populations characterized by low CYP2F2 protein levels and rapid Hoechst efflux. Included within the SP identified in elastase digests of lung tissue is a CD45-negative fraction that includes cells expressing marker genes indicative of fibroblast (vimentin) and nonciliated airway epithelial (CCSP) lineages. Expression of CCSP by CD45-negative SP cells was not associated with expression of the mature Clara cell marker CYP2F2, a property that is consistent with the molecular phenotype of a subpopulation of cells residing within NEB microenvironments.

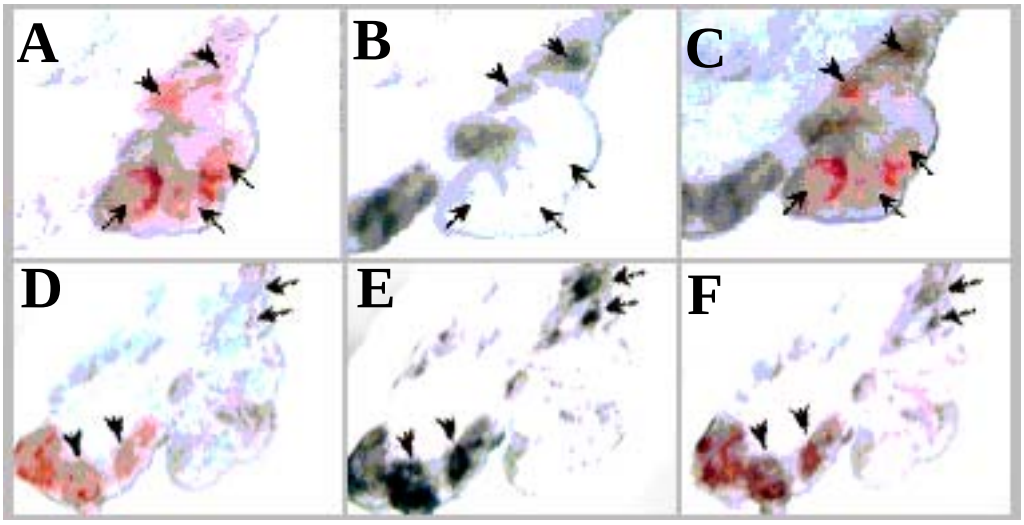

Figure 4.1 Two variant Clara cell subpopulations are associated with NEBs in the normal lung.

Sequential immunohistochemistry was used to detect CGRP (A) and CCSP (B) on the same section. Amine-ethyl carbizol (pink-red) was used to detect CGRP, and DAB (black / gray) was used to detect CCSP immunocomplexes. C: Image generated by overlaying A and B. Long arrows in A–C indicate CGRP-IP/CCSP-immunonegative cells, whereas short arrows indicate cells expressing both CGRP and CCSP. Similar methods were used to detect the Clara cell markers P450–2F2 (D, amine-ethyl carbizol detection) and CCSP (E, DAB detection) on an adjacent serial section of (A-C). F: Image generated by overlaying D and E. Short arrows in D–F indicate P450–2F2-IP/CCSP-IP cells, and long arrows mark P450–2F2 immunonegative / CCSP-IP cells. Original magnification, x1000. .

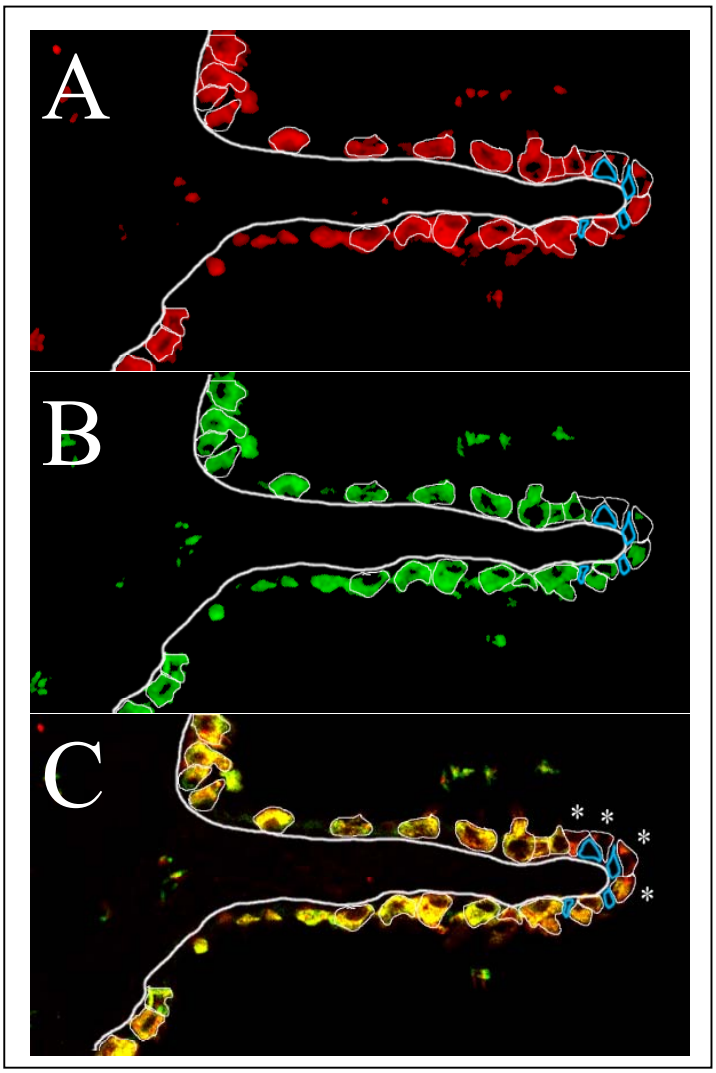

Figure 4.2 Dual color confocal immunofluorescence detection of CCSP and CYP2F2 within NEBs.

Dual color immunofluorescence and confocal microscopy were used to simultaneously detect CCSP (A, red) and CYP2F2 (B, green) in single optical sections. CCSP expressing cells with a visible nuclear profile were compared based on relative CYP2F2 fluorescence intensity. (C) An overlay of the images in (A) and (B) reveals a subpopulation of CCSP expressing cells with reduced CYP2F2 immediately adjacent to NEB microenvironments (asterisks: CYP2F2 low cells; blue tracings: PNEC).

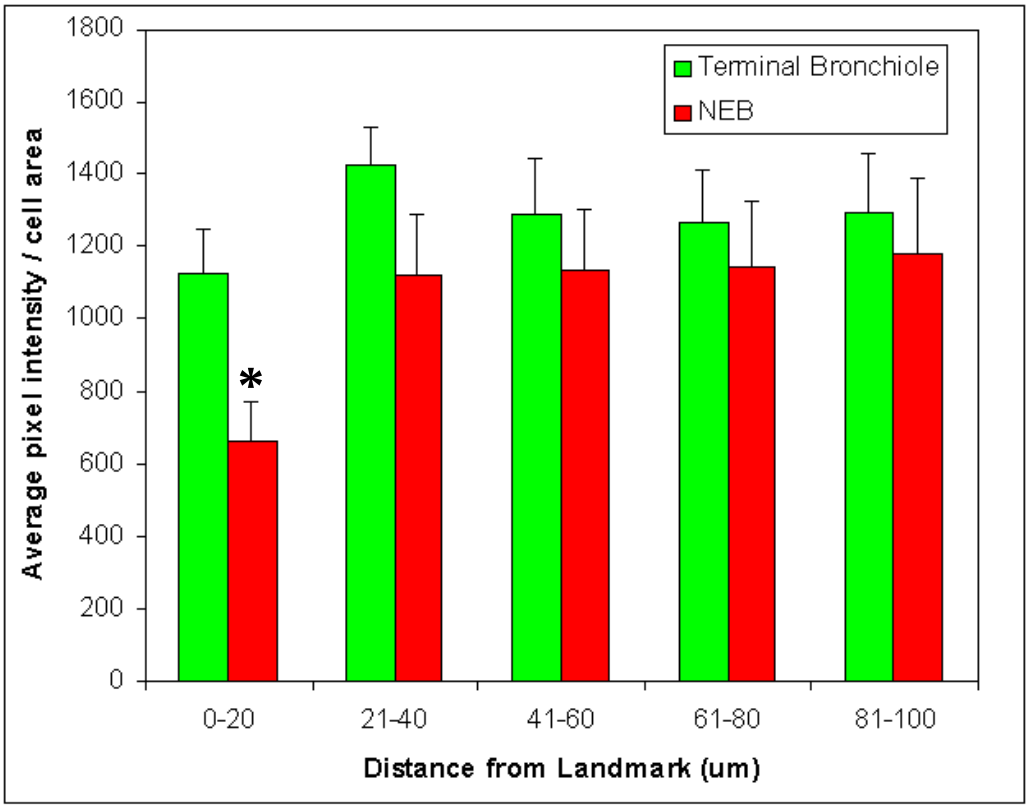

Figure 4.3 Quantitation of CYP2F2 protein levels within NEB- and BADJ-associated Clara cells.

Quantificiation of CYP2F2 protein levels was performed using images comparable to those obtained in Figure 4.2, and analyzed in Metamorph with respect to their average fluorescence intensity / cell area. These values were then graphed with respect to distance from either the center of NEB microenvironments (green) or the BADJ (red). Results indicate that NEB- but not BADJ-associated CCSP expressing stem cells exhibit reduced CYP2F2 protein levels.

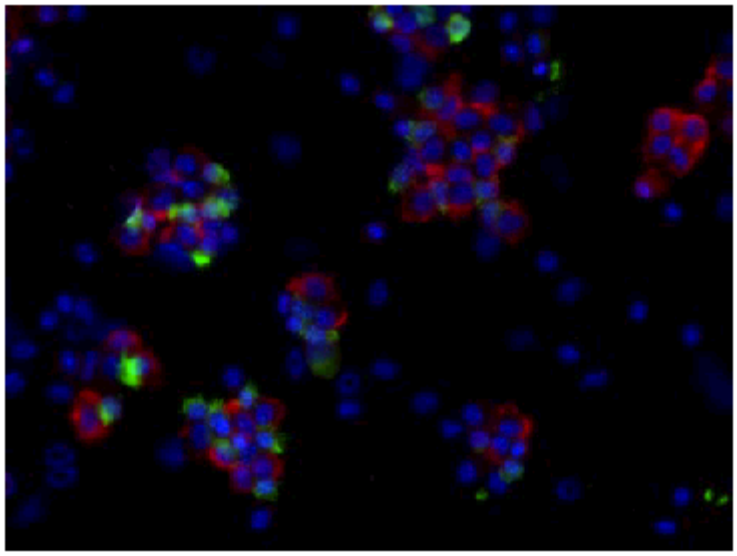

Figure 4.4 Phenotypic characterization of isolated lung cells.

Lung cells were isolated by elastase digestion, fixed, cytospun onto glass slides, and immunostained for airway-specific markers. Controls for antibody specificity included an omission of primary antibody and analysis of CCSP knockout-mouse derived cells. Analysis of eight cell preps indicated that 32±4% of nucleated cells express the Clara cell marker CCSP (red) and that 20±3% of cells express the ciliated cell marker ACT (green). The basal cell marker cytokeratin 14 was extremely rare (<0.1% of total cells) and the neuroendocrine cell marker calcitonin gene related peptide was not detected following immunostaining of the total cell isolate (data not shown). Fluorescence activated cell sorter analysis (Figure 2) indicated that approximately 30% of the total cells expressed the hematopoietic lineage marker CD45 and 20% of all cells lacked both the aforementioned airway markers as well as CD45. Results are representative of eight experiments.

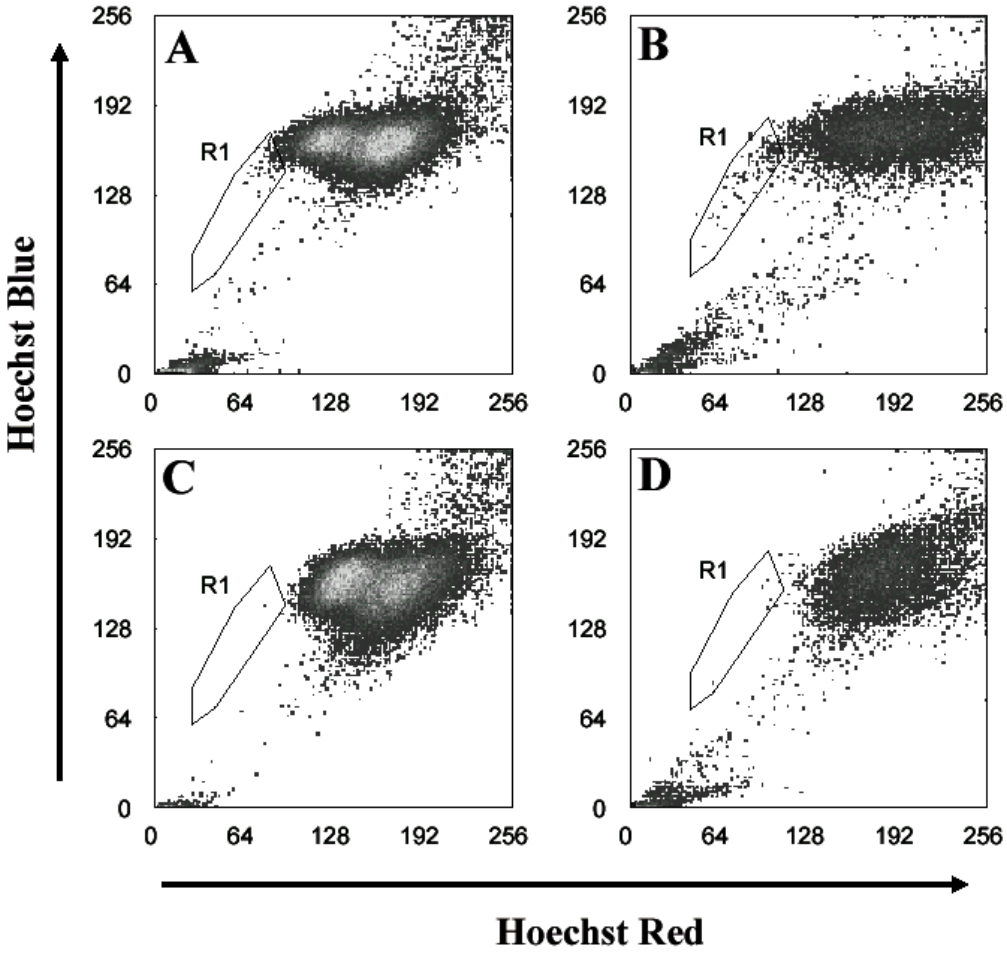

Figure 4.5 Identification of lung side populations.

Isolated lung cells were stained with 5ug/ml Hoechst 33342 alone (A and B) or in combination with 50uM Verapamil (C and D) followed by segregation into hematopoietic (A, C) or non-hematopoietic lineages (B, D) on the basis of CD45 immunoreactivity. Results indicate that a distinct side population of cells exists in both hematopoietic (A, box R1) and non-hematopoietic cell lineages (B, box R1), and that detection of these side populations was inhibited by the ABC transport inhibitor Verapamil (C and D box R1, respectively). Data shown in panels A-D are representative of three experiments.

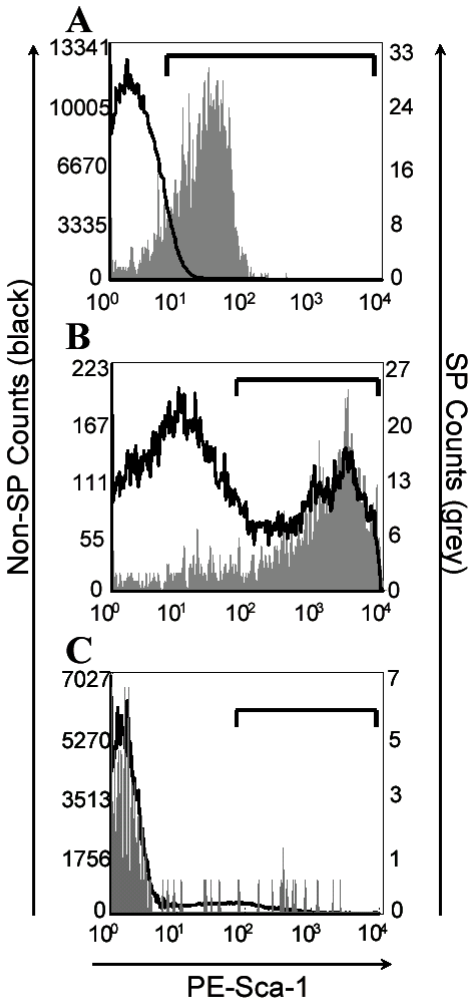

Figure 4.6 Sca-1 Expression in Lung SP.

Bone marrow (A) or lung cells (B,C) were stained with Hoechst 33342 and the lung cells fractionated into non-hematopoietic (B) or hematopoietic (C) populations on the basis of CD45 expression. Surface expression of stem cell antigen-1 (sca-1) was assessed simultaneously in the side population (gray) and the non-side population (black tracing). The sca-1 positive gate is indicated by the bar in each panel and was set using an isotype specific control antibody. As previously shown, sca-1 is expressed exclusively on SP cells of the bone marrow (78% positive SP; 3% positive non-SP, panel A). Sca-1 was expressed on 80% of CD45- lung SP (B, grey) and on a minority of CD45(-) non-SP (30 %, B, black). In contrast, the majority of CD45(+) lung SP and non-SP cells are negative for this marker (C, grey and black). Representative results of two experiments are presented.

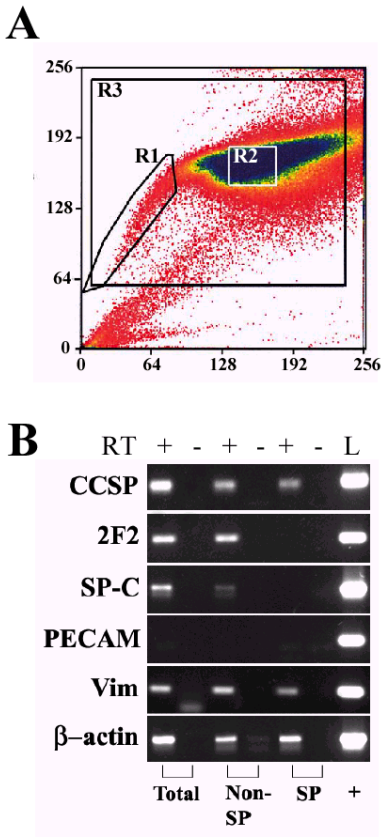

Figure 4.7 Molecular phenotype of CD45(-) lung SP cells

The molecular phenotype of lung-derived SP and non-SP cells was determined by reverse transcription-polymerase chain reaction (RT-PCR) analysis. Equal numbers (6000) of total (4.7A box R3), non-side population (non-SP, 4.7bA box R2), or side population (SP, 4A box R1) cells were sorted directly into RNA lysis buffer. RNA was purified and reverse transcribed in the presence (+) or absence (-) of reverse transcriptase (RT). Candidate gene products were amplified using primers detailed in Table 1 and conditions detailed in methods. Total lung RNA (4.7B, total, 0.5 ug) was reverse transcribed and used as a positive control. The Clara-cell specific gene products CCSP and CYP2F2 (2F2), the type 2 pneumocyte gene product SP-C, the fibroblast-specific gene Vimentin, and β-actin (used as a load control) were detected in control, total, and non-side population cells (Figure 4.7B). In contrast, side-population cells expressed only CCSP and Vimentin. These results indicate that the CD45(-) SP contains two subpopulations that may be derived from the epithelial and mesenchymal lineages. Representative results of two experiments are presented.

Table 1 Primers Used in RT-PCR of Lineage Specific Gene Products

CCSP Forward: CCAGCTGAAGAGACTGGTGGAT
CCSP Reverse: TTACACAGAGGACTTGTTAGGATTTTCT
2F2 Forward: TCATCGACTGCTTCCTCACAAA
2F2 Reverse: CATCAGCAGGGTATCCATATTGAA
SP-C Forward: TTTCCTAGGCCTTGCTGT
SP-C Reverse: TTTGTGATAGGATCCCCC
PECAM Forward: AACAGAAACCCGTGGAGATGTC
PECAM Reverse: CATCATAACCGTAATGGCTGTTG
Vimentin Forward: GCACCCTGCAGTCATTCAGA
Vimentin Reverse: GATTCCACTTTCCGTTCAAGGT
β-actin Forward: TTCTTTGCAGCTCCTTCG
β-actin Reverse: GGGTCATCTTTTC ACGGT

5. β – Catenin Signaling is a Component of Airway Stem Cell Mediated Renewal

5.1. Abstract

Previous studies have determined that epithelial remodeling and loss of airway heterogeneity are risk factors for the development of airway diseases including cancer. Additionally, recent evidence indicates that aberrant stem cell activity contributes to the development of numerous tissue-specific cancers. Data from our laboratory previously identified neuroepithelial body (NEB) and bronchoalveolar duct junction (BADJ) associated Clara cell secretory protein expressing cells as unique intrapulmonary stem cells. Stem cells were primarily responsible for restoration of epithelial diversity following selective depletion of transit amplifying populations. Currently mechanisms regulating airway stem cell activation, migration, and differentiation remain incompletely understood. Studies in other tissue types have identified the β-catenin signaling pathway as a central regulator of stem cell fate. The current study was undertaken to test the hypothesis that β-catenin signaling is a component of airway stem cell activation and epithelial renewal. Immunofluorescent localization of β-catenin protein within control and naphthalene-injured airways indicated that stabilization of intracellular β-catenin protein indicative of signaling occurs predominately within neuroepithelial body and bronchoalveolar duct junction microenvironments. Using TOPgal transgenic β-catenin signaling pathway reporter mice, we determined that β-catenin downstream target genes are activated within airway NEB and BADJ microenvironments following acute lung injury. Furthermore, our results indicate that β-catenin signaling is apparent immediately after initial stem cell activation and is inactivated upon restoration of normal epithelial diversity. These results suggest that β-catenin signaling is a component of airway regeneration and may be an important regulator of processes including airway remodeling and disease predisposition.

5.2. Introduction

The conducting airway epithelium is lined by numerous distinct epithelial cell types that differ in frequency and function along the proximal-distal axis [10, 34, 46, 104, 115, 121, 129, 209, 229, 286]. Homeostatic mechanisms triggered through acute injury or cell senescence involve increases in the proliferation of either transit amplifying (TA) or stem cell pools for restoration of a normal epithelium [74-76]. In contrast, chronic lung injury or disease is associated with epithelial remodeling, loss of heterozygosity, and increased cancer predisposition [54, 91, 108, 130, 151, 152, 202, 203, 212, 278, 310]. Recent studies have revealed that the conducting airway is maintained through the coordinated action of a stem cell hierarchy of tissue-specific stem cells and their transit-amplifying progeny. Stem cells are localized within intrapulmonary neuroepithelial body (NEB) and bronchoalveolar duct junction (BADJ) microenvironments and are activated following injury that depletes TA pools [95, 110, 186, 187, 224, 225, 249, 250].

A number of recent studies indicate that β-catenin signaling is an important mediator of stem cell fate within numerous distinct tissues [63, 113, 141, 157, 169, 223, 269, 308]. Nuclear translocation of β-catenin and downstream target gene activation enhances hematopoietic stem cell growth and survival [223]. Tcf4-mediated β-catenin signaling regulates intestinal crypt associated stem cell proliferation and daughter cell migration [141, 269, 308]. Nuclear β-catenin signaling regulates cell fate and promotes survival of mammary gland progenitors [102]. Wnt / β-catenin signaling within skin epidermal stem cells regulates appropriate follicle-associated proliferation and TA cell migration [49, 94, 113, 176, 293]. Additionally, inappropriate activation of β-catenin signaling contributes to the development of several types of cancer

including numerous epidermal carcinomas and the majority of colon cancers [102, 170, 176, 178, 269, 284]. Taken together, these data highlight the widespread involvement of β-catenin signaling in regulating aspects of stem cell-associated proliferation, differentiation, and migration in injury / repair. Evidence is also emerging that supports a role for b-catenin signaling activation within several airway epithelial hyperproliferative diseases, including idiopathic pulmonary fibrosis (IPF).

Normally, β-catenin is a component of polarized epithelial surfaces and an important intracellular signaling molecule. Membrane-associated β-catenin interacts with E-cadherin, α-catenin, and γ-catenin (plakoglobin) to form cellular junctions that facilitate cell-cell communication [99, 102, 218]. Free cytoplasmic β-catenin is phosphorylated by GSK3β resulting in Axin / APC complex recruitment and ubiquitin-mediated protein degradation. Inhibition of GSK3β prevents phosphorylation-mediated β-catenin breakdown and enables nuclear β-catenin translocation. Inhibition of β-catenin degradation occurs through a number of direct and indirect mechanisms, including Wnt signaling through Frizzled receptors, PI3K-dependent activation of Akt, and direct inhibition of GSK3β byFgf-2 [62, 102, 170, 218, 234]. Nuclear β-catenin interacts with Tcf / Lef family members and functions as a transcription cofactor.

There is growing evidence supporting the importance of β-catenin signaling in airway development and disease. Tcf / Lef gene family members and intracellular β-catenin are present within developing mouse and human intrapulmonary airways [64, 173, 228, 244, 260]. Studies have determined that Lef1 expression within proximal airway submucosal glands is necessary for appropriate submucosal gland morphogenesis [57, 58, 228]. Surfactant protein-C promoter dependent β-catenin gene deletion disrupts normal alveolar epithelial maturation [173]. Wnt

proteins associated with inhibition of GSK3β / activation of β-catenin signaling are expressed during distal airway maturation [64, 105, 106, 171, 237, 296, 298]. Nuclear β-catenin localization and downstream target gene activation are associated with human idiopathic pulmonary fibrosis [41, 171]. Together, these findings led us to hypothesize that β-catenin signaling is a component of airway epithelial renewal and differentiation. The purpose of this study was to characterize the spatio-temporal pattern of β-catenin signaling activation within naphthalene-injured and repairing conducting airways. Immunofluorescent localization of β-catenin and TOPgal transgenic β-catenin signaling reporter mice was utilized to define the pattern of β-catenin signaling activation. Our results indicate that β-catenin signaling is associated with the transition between mitotic and differentiated epithelial phenotypes during airway stem cell microenvironment-associated renewal.

5.3. Materials and Methods

Animal Housing.

Colonies of either wild-type FVB/n or TOPgal transgenic mice in the CD-1 background were maintained as in house breeding colonies under specific pathogen free conditions. Health status was monitored quarterly by performing a comprehensive serology screen on co-housed sentinel mice. All experimental and breeding animals were maintained on a twelve hour light / dark cycle and given access to food and water *ad libitum*. Mice used in naphthalene experiments were between eight and twelve weeks of age, and weighed between 25-35 grams. Animals were sacrificed by injection of 2.5% avertin (50% *tert*-amyl-alcohol / 50% tribromoethanol) to achieve a surgical plane of anesthesia followed by exsanguination.

Naphthalene Administration.

Naphthalene administration was carried out as previously described [250]. Experimental animals were injected with 275 or 375 mg naphthalene / kg body weight prior to 10:00am. Animals were checked daily to ensure health status following high-dose naphthalene injection. All experimental animals received Bromodeoxyuridine (50 mg / kg body weight; BrdU, Sigma) two hours prior to sacrifice.

Tissue Preparation.

Following exsanguination, tracheas were cannulated and their lungs gently lavaged six times with sterile PBS to remove residual dead cells. Left lobes were removed and homogenized in 2.5mL 4M guanidinium isothiocyanate containing 0.7% 2-mercaptoethanol for RNA analysis

by S1 nuclease protection as previously described [110, 250]. The right rostral (upper) lobe was removed and ground in 1mL RIPA buffer (50mM Tris-Cl pH7.4, 1% Nonidet P-40, 0.5% Sodium deoxycholate, 5mM EDTA pH8.0, 150mM NaCl) containing 1mM PMSF protease inhibitors. The remaining cardiac, caudal, and accessory lobes were inflation fixed in situ for 10 minutes with 10% neutral buffered formalin (NBF), removed, and immersion fixed in 10% NBF for an additional 10 minutes. Formalin-fixed tissue was extensively washed in excess PBS and blotted on paper towels prior to X-gal staining solution for 12 hours.

LacZ Histochemical Detection.

The X-gal staining solution used for TOPgal transgenic animals contained 5 mM $K_3Fe(CN)_3$, 5 mM $K_4Fe(CN)_6$, 2mM $MgCl_2$, 0.02% Nonidet P-40, 0.01% sodium deoxycholate, 1x PBS, and 1 mg / ml X-gal. LacZ histochemical detection by X-gal staining was performed in the dark at 37°C. Tissues were gently rocked for the duration of X-gal staining to ensure stain penetration. Following X-gal staining tissues were washed in PBS to remove residual X-gal staining solution and post-fixed for an additional 12 hours in 10% NBF at 4°C. X-gal stained accessory lobes were microdissected to expose the lumen of intrapulmonary conducting airways. The surface of the airway epithelium was examined for the presence of X-gal stained (blue) cells using a dissecting microscope and representative images were obtained. X-gal stained cardiac lobes were cryoprotected / OCT embedded as previously described [111, 112].

Immunohistochemistry.

Optimal cutting temperature (OCT)-embedded frozen tissue was sectioned at 6μm to reveal the major axial pathway as well as numerous airway terminal bronchioles. Sections were post-fixed in 10% neutral buffered formalin, washed in PBS, and blocked with 5% bovine serum albumin (Roche) / 5% normal goat serum (Vector Laboratories) in PBS. Adjacent serial sections were incubated with rabbit-anti-CCSP (1:30,000) or rabbit-anti-CGRP (1:15,000, Sigma) overnight at 4°C. Slides were then washed extensively in PBS and incubated with biotinylated goat-anti-rabbit Ig (1:4000 in blocking solution) for one hour at room temperature. Slides were washed and further incubated with streptavidin-horseradish peroxidase (1:4000) in PBS alone. Antigen-antibody complexes were detected using a diaminobenzidine substrate detection kit (DAB, Vector Laboratories), and counterstained with Nuclear Fast Red (Vector Laboratories). Images were obtained using an Olympus Provis AX70 microscope equipped with a Spot RT digital camera and processed using Image-Pro Plus and Adobe Photoshop.

Immunofluorescence

Immunofluorescence techniques coupled with confocal microscopy were used to detect the following antigens simultaneously: β-catenin and CCSP or CGRP, BrdU and CCSP or CGRP, and Ki67 with CCSP. Slides were post-fixed and cleared (as detailed above), microwaved for 20 minutes in 10mM citrate buffer (pH 6.0) and cooled for one hour at 4°C prior to immunostaining. All sections were blocked with 5% BSA / PBS prior to application of primary antibodies. Primary antibodies were used at the following concentrations: rabbit-anti-CCSP (1:15,000) or rabbit-anti-CGRP (1:10,000) + monoclonal mouse IgG_1-anti-β-catenin (1:400, Transduction Laboratories clone 14), rabbit-anti-CCSP or rabbit-anti-CGRP plus

polyclonal sheep-anti-BrdU (1:4000, Bethyl), monoclonal mouse IgG_1-anti-Ki67 (1:1,000, Upstate Biotechnology) plus polyclonal rabbit-anti-CCSP (1:15,000). Slides were incubated overnight at 4°C, washed, and secondary antibodies applied for 3 hours at room temperature. Secondary antibodies combinations were donkey-anti-sheep Alexa488 (1:500, Molecular Probes) + donkey-anti-rabbit Alexa 594 (1:500) or donkey-anti-mouse IgG_1 Alexa594 (1:500) + donkey-anti-rabbit Alexa 488(1:500). After washing, slides were coverslipped using Fluoromount-G containing 2μg/mL 4,6, diamidino-2-phenylindole (DAPI, Sigma). Antigen-antibody complexes were visualized as single optical planes using an Olympus Fluoview confocal microscope equipped with Nomarski optics for simultaneous brightfield detection. Images were acquired and processed using Metamorph imaging software.

Western Blotting and Quantification

Right rostral (upper) lung lobes lysed in 1mL RIPA buffer / 10% PMSF were centrifuged for 10 minutes at 1500 rpm to remove cellular debris, and protein concentrations were determined by Coomassie protein assay. Twenty micrograms of protein was loaded on 12% NuPage-Tris precast protein gels (Invitrogen) and separated under denaturing and reducing conditions. Protein was transferred to PVDF membranes overnight and nonspecific binding sites subsequently blocked in 5% non-fat dry milk / 0.05%Tween-20 / 1x PBS (PBST). Primary antibodies were used at the following concentrations in 1% non-fat dry milk / PBST: mouse monoclonal IgG_1-anti-β-catenin 1:1000, mouse monoclonal IgG_1-anti-E-cadherin 1:200 (santa cruz biotechnology), mouse monoclonal IgG_1-anti-cyclin D1 1:200 (Pharmingen), polyclonal rabbit-anti-CCSP 1:15,000, and mouse monoclonal IgG_1-anti-β-actin 1:4000 (Sigma). Following incubation, primary antibodies were washed extensively with PBST, and HRP-conjugated

secondary antibodies goat-anti-rabbit (1:4000, Southern Biotechnology Associates) or goat-anti-mouse IgG_1 (1:5000, Southern Biotechnology Associates) diluted in 1% milk / PBST were placed on blots for one hour at room temperature. Protein-antibody complexes were detected using a chemiluminescent substrate. Relative antibody abundance was determined by digital densitometry. Immunoreactivity was normalized to β-actin protein standards.

Morphometric Analysis.

Terminal bronchioles used in morphometric analysis were defined by the presence of an intact broncho-alveolar duct junction (BADJ), at least 150μm of conducting airway epithelium immediately proximal to the BADJ (defined as airway epithelium that directly transitions into an alveolar duct). Neuroepithelial bodies (NEBs) used in morphometric analysis were defined by the presence of two or more CGRP-immunoreactive pulmonary neuroendocrine cells. LacZ expressing cells were identified by the presence of X-gal histochemical staining. Cells were defined as "mitotic" if they contained a detectable BrdU immunoreactive nucleus and were present within 150μm of a defined stem cell microenvironment. Cells outside these regions were not considered in this analysis. Neuroepithelial bodies contained within terminal bronchioles matching these criteria were excluded from all analysis. The distribution of LacZ expressing cells with respect to defined microenvironments was measured using calibrated measurement tools in Image Pro Plus. The frequency of LacZ expressing cells within the NEB or BADJ was determined using this method.

5.4. Results

Changes in the Abundance and Distribution of β-catenin Following Clara Cell Depletion

β-catenin has been shown to regulate stem cell mediated epithelial renewal in multiple organs including intestine, skin, and the hematopoietic system where it appears to influence both stem cell proliferation and differentiation states [14, 49, 50, 94, 141, 204, 218, 223, 252, 269, 308, 312]. Stabilization of β-catenin that results from inhibition of GSK3β allows for its cytoplasmic and nuclear accumulation, heterodimerization with transcription cofactors belonging to the Tcf / Lef family, and activation of downstream gene expression. We used a model of airway injury involving extensive progenitor cell depletion to determine whether there was any evidence for β-catenin stabilization indicative of potential signaling activity following stem cell activation. FVB/n strain mice were injected with 275 mg/ kg naphthalene, recovered, and whole lung homogenate characterized by Western immunoblot analysis. We first determined levels of immunoreactive CCSP protein to confirm the extent of naphthalene-induced Clara cell ablation. Results show significant depletion of CCSP within 48 hours of injury and evidence of airway renewal by 120 - 240 hours of recovery. An antiserum specific for β-catenin recognized a single protein species with an apparent molecular weight of ~92 kDa, the abundance of which remained unchanged or are slightly elevated at 48, 72, 120, and 240 hours after naphthalene exposure when compared to untreated controls (Figure 5.1).

In order to determine the cellular localization of stabilized β-catenin proteins observed in Figure 5.1, adjacent frozen tissue sections of naphthalene injured and recovered lungs were immunostained for β-catenin and CCSP or CGRP. In the steady state mouse lung all β-catenin immunoreactivity was localized to basolateral plasma membranes of epithelial cells lining the

conducting airway, with minimal if any staining within subepithelial mesenchymal cell populations (Figure 5.2, A). This localization of b-catenin to the basolateral membrane of epithelia that were largely restricted to intrapulmonary conducting airways was similar to that previously described for the epithelia of tracheobronchial airways [228]. The broad distribution of epithelial β-catenin immunoreactivity was largely lost after naphthalene-induced airway injury, a finding that was apparent 12 hours after exposure and most prominent by the 24 hours recovery time point (Figure 5.2, B-E). This dramatic decrease in β–catenin staining with epithelial cells of conducting airways correlated with morphological alterations and exfoliation of CCSP-expressing epithelial cells. Residual CCSP and CGRP expressing cells that maintained well-defined baslateral β-catenin staining at these recovery time points were restricted to NEB microenvironments. Nuclear / cytoplasmic β-catenin signaling was detectable within NEB microenvironment-associated cells 48 hours after injury (yellow dual color staining, Figure 5.2, F+G). There was continued NEB-associated nuclear / cytoplasmic β-catenin expression at 72 hours, as well as some restoration of membrane-associated β-catenin within nascent Clara cells (Figure 5.2, H+I). Five days after injury, most epithelial cells adjacent to NEBs displayed only membrane-associated β-catenin (Figure 5.2, J+K). These data demonstrate that naphthalene-induced airway injury results in the loss of most airway membrane-associated β-catenin and a change in β-catenin subcellular distribution within residual epithelial cells of the repairing lung. The observation that β-catenin protein abundance is unchanged as visualized by Western blot analysis whereas immunofluorescent data indicates a significant depletion of plasma membrane-associated β-cateinin throughout conducting airways can be reconciled by the finding that β-catenin proteins are likely present throughout the subepithelial and alveolar epithelial lung compartments. These data suggest that increased cytoplasmic β-catenin staining is a

characteristic of pollutant resistant cells within previously identified stem cell microenvironments.

Injury-Repair Kinetics are Comparable Between FVB/n and TOPgal β-catenin Reporter Mice

Despite clear evidence for β-catenin protein stabilization and cytoplasmic translocation within identified airway stem cell microenvironments following progenitor cell depletion, our results do not allow for the definitive identification of downstream β-catenin / TCF target gene activation. To identify whether microenvironment associated cytoplasmic β-catenin localization results in downstream target gene activation, we investigated the kinetics of epithelial renewal using previously characterized β-catenin reporter mice [4, 36, 49, 50, 164]. These mice contain three β-catenin / TCF transcription factor optimal cis (TOP-) elements upstream of the LacZ / β-galactosidase reporter gene (-gal; TOPgal). However, these transgenic mice are in the CD-1 outbred genetic background. To appropriately determine whether airway-specific progenitor cell depletion results in β-catenin signaling induction, we first needed to compare the injury / repair kinetics of TOPgal transgenic mice with our previous assessment of injury within FVB/n strain animals. Empirical analysis of Clara cell specific RNA abundance by S1 nuclease protection assay revealed that a dose of 375 mg/kg naphthalene was necessary to elicit consistent >95% reduction in the abundance of Clara cell specific marker genes in TOPgal transgenic mice (Figure 5.3 and data not shown). While this dose was significantly greater than that used for previous studies TOPgal animals did not exhibit greater mortality than FVB/n strain animals. Moreover, evidence for recovery of the airway epithelium of CD-1 mice following naphthalene exposure was evident within 120 and 240 hours post-exposure (Figure 5.3). Additionally, as was the case following FVB/n strain naphthalene exposures, total β-catenin protein levels in

TOPgal lungs remained unchanged between control and naphthalene recovery time points (data not shown). Thus, it appears that TOPgal transgenic and FVB/n strain mice exhibit similar kinetics of epithelial injury and repair, albeit with variability between strains in overall naphthalene sensitivity.

Activation of a β-catenin / TCF -Responsive Reporter Transgene in Repairing Airways of Naphthalene Exposed Mice

We next sought to determine whether changes in β-catenin localization that accompany airway repair are associated with active expression of downstream targets of the β-catenin / TCF transcription factor complex. TOPgal mice were exposed to naphthalene and recovered for 48, 72, 120, or 240 hours for analysis of the temporal and spatial pattern of LacZ reporter gene expression. LacZ expression was identified by X-gal histochemical staining of naphthalene injured lungs (Figure 5.4). No X-gal positive cells were observed in 5 out of 6 uninjured lungs (Figure 5.4A and B). Approximately 20 randomly distributed LacZ expressing cells were present in distal airways of one uninjured animal (data not shown). No changes in X-gal histochemical staining were observed at the 48 hour recovery time point (Figure 5.4C+D). The first indication of TOPgal transgene activation was observed within the epithelium and subepithelial mesenchyme of airway from some but not all mice recovered for 72 hours. Two of seven lungs recovered for 72 hours were similar to 48-hour recovered specimens and contained no detectable X-gal stained cells. Three lungs contained infrequent X-gal stained cells in the epithelium and underlying mesenchyme (Figure 5.4E and 5.4F, asterisks and arrowheads, respectively). The remaining two 72 hour recovered lungs contained numerous LacZ positive cells within the epithelium and underlying mesenchyme. These lungs closely resembled 120

hour recovered lungs (data not shown; see Figure 5.4G for comparison). Among mice showing signs of TOPgal transgene activation at this time, X-gal stained epithelial cells were typically localized to airway branch points and terminal bronchioles. Lungs of all mice from the 120 hour recovery time point contained numerous X-gal stained cells within both the epithelium and sub-epithelial mesenchyme indicative of robust β-catenin / TCF transcription factor activation. X-gal stained epithelial cells were localized to airway branch points and terminal bronchioles in 5-20 cell clusters (Figure 5.4H, asterisks). X-gal stained, fibroblast-like mesenchymal cells were not associated with LacZ expressing epithelial clusters, but were randomly distributed throughout the largest caliber intrapulmonary airways (Figure 5.4H, arrowheads). Individual X-gal stained cells were also observed in peripheral lungs adjacent to airway terminal bronchioles. Ten days (240 hours) after naphthalene injury all lungs harbored numerous cell that exhibited evidence of β-catenin signaling including cells within the airway epithelium, mesenchyme, and interstitium (Figure 5.4I and J). Clusters of β-catenin signaling, X-gal stained cells at airway branch points and terminal bronchioles appeared larger and less cohesive suggesting that these populations had undergone some degree of migration (Figure 5.4J, asterisks). The number of X-gal stained fibroblast-like cells was lower than those observed 5 days after injury (compare 5.4H and 5.4J, arrowheads). Together these results indicated that prolonged activation of β-catenin signaling occurs following progenitor cell depletion and is restricted within the epithelium predominately at airway branch points and terminal bronchioles.

Expression of the TOPgal β-catenin-Responsive Transgene Occurs in Both CGRP and CCSP Expressing Cells of NEB and BADJ Microenvironments

To identify the molecular phenotype of X-gal stained, β-catenin signaling cells in airways depleted of Clara cell populations, tissues were frozen and adjacent serial sections were stained for CCSP and CGRP (Figure 5.5 and 5.6). NEB microenvironments identified by the presence of CGRP expressing cells and morphologically identified BADJ microenvironments were analyzed. There was no detectable X-gal staining indicative of active β-catenin signaling within uninjured or 48 hour recovered terminal bronchioles (Figure 5.5A+B). Seventy-two hours after injury a small number of CCSP / X-gal dual stained cells were localized preferentially at the BADJ (Figure 7C, asterisks and Table One). Several X-gal positive, CCSP negative cells were also visible in terminal bronchioles at this time (Figure 5.5C, arrowheads). X-gal stained, β-catenin signaling cells expanded in a distal-to-proximal fashion outward from the BADJ at 120 and 240 hours recovery concomitant with restoration of normal epithelial cellular phenotypes (figure 5.5D+E and table 2). These results indicate that β-catenin signaling is associated with terminal bronchiolar repair and is most common within CCSP expressing cell types.

To determine whether β-catenin signaling is activated within NEB stem cell microenvironments, frozen tissue sections were processed as described above. There were no X-gal stained, β-catenin signaling cells within NEB-associated neuroendocrine or Clara cell populations prior to injury (Figure 5.6A and B, respectively). X-gal stained cells were first detected 72 hours after naphthalene administration immediately adjacent to NEB microenvironments, and represented a subset of total NEB-associated CCSP expressing cells (Figure 5.6 E and F, asterisks). X-gal staining was also infrequently detected within subepithelial fibroblasts throughout large airways (Figure 5.6). X-gal stained, β-catenin signaling epithelial and mesenchymal cells increased in abundance 120 hours after injury. Additionally, a small number of CGRP / X-gal dual stained cells were detectable at this time. X-

gal stained patches indicative of β-catenin signaling were significantly larger than NEB microenvironments at 240 hours recovery and were predominantly composed of nascent CCSP expressing cells. This temporal and spatial induction of β-catenin signaling suggested a correlation between β-catenin signaling induction and NEB microenvironment-associated repair (Table Two).

Stem Cell Proliferation Precedes β-catenin Signaling During Airway Repair

Numerous studies have identified the involvement of β-catenin signaling in regulating cellular proliferation [49, 94, 217, 269, 308, 315]. To determine if β-catenin signaling in airway microenvironments is associated with stem cell proliferation 50 mg/kg BrdU was administered to mice two hours prior to sacrifice. Dual immunofluorescent staining of BrdU and CCSP or CGRP on X-gal stained tissues was used to determine the molecular phenotype of mitotic airway cells (Figure 5.7). Results indicate that uninjured terminal bronchioles and NEBs did not contain proliferating cells after a two hour labeling period (Figure 5.7A). Forty-eight hours after injury the mitotic index of terminal bronchioles was 0.3 cells / 100 μm basement membrane (10 cell diameters). The majority (>85%) of these BrdU positive cells are immediately adjacent to the BADJ. Neuroepithelial bodies have a mitotic index of 0.5 cells / 100μm (Figure 5.7A). A large percentage of TB and NEB-associated mitotic cells 48 hours after naphthalene injury express CCSP and likely represent previously identified airway stem cells (Figure 5.7B and C). Mitotic, phenotypically indistinguishable cells in terminal bronchioles (41%) and NEBs (40%) at 48 hours recovery are pollutant resistant Clara cells with extremely low CCSP protein expression (data not shown). These results indicate that the initial NEB and TB associated, stem cell mediated renewal processes precede detectable LacZ expression / β-catenin signaling.

Terminal bronchiolar proliferation increased 72 hours after injury and reached a maximum of 1.3 cells / 100μm 120 hours after naphthalene administration (Figure 5.7A). While CCSP expressing cells accounted for the majority of proliferating cells during initial terminal bronchiolar regeneration, CCSP / LacZ dual positive mitotic cells increase in abundance 72 to 240 hours after injury (Figure 5.7B). This finding suggests that β-catenin signaling is associated with later stages of terminal bronchiole-associated repair. Proliferation peaked among cells within the NEB microenvironment at 72 hours after injury, with a mitotic index of 1.3 cells / 100μm (Figure 5.7A). At this time there were very few LacZ expressing cells within NEBs (see Table Two), none of which contributed directly to epithelial proliferation. The mitotic index of cells within the NEB microenvironment dropped to 0.6 cells / 100μm 120 hours after injury and was declined to control levels by 10 days (Figure 5.7A). NEB associated CCSP positive cells were the predominant mitotic populations seventy-two and 120 hours after injury (78 and 81%, respectively; Figure 5.7C). Very few mitotic LacZ positive or CCSP / LacZ dual positive cells were detected in NEBs at any time after injury (Figure 5.7C). These data suggest that NEB-associated β-catenin signaling cells were not integral components of stem or progenitor cell-associated proliferation. Altogether, these results indicate that intrapulmonary β-catenin signaling is detectable immediately after microenvironment associated stem cell activation and suggests that this signaling pathway likely mediates aspects of stem cell differentiation potential and daughter cell migration.

Inappropriate Epithelial Renewal Results in Chronic β-catenin Signaling Activation

To identify whether lung β-catenin signaling is chronically activated following acute progenitor cell injury, naphthalene injured TOPgal mice were recovered for 45 days. Results

identified significant inter-individual variability in X-gal staining (Figure 5.8A-F). Most lungs (5 of 7) were devoid of X-gal staining or contained rare, individual X-gal stained cells randomly distributed throughout airways (Figure 5.8A,B,E,F). These lungs contained no detectable X-gal stained sub-epithelial fibroblasts or interstitial cells. Immunohistochemical staining for CCSP revealed that this majority of 45 day recovered lungs displayed regions of extensive epithelial renewal separated by small patches of abnormal epithelial morphology (Figure 5.8G, H, arrows). Randomly distributed, individual LacZ positive cells coexpressed CCSP and were restricted to regions of extensive epithelial renewal (Figure 5.8H, asterisks). These results suggested that β-catenin signaling is down regulated following restoration of normal epithelial diversity.

Interestingly, the two additional lungs that contained extensive X-gal staining within epithelial patches and subepithelial fibroblasts (Figure 5.8C, F) displayed large regions of unrepaired, CCSP negative epithelia (Figure 5.8I, arrows). Regions of appropriate epithelial cellular diversity were restricted to airway terminal bronchioles and patches within midlevel conducting airways, and were the sole source of airway LacZ expressing cells (Figure 5.8I, asterisks). These results indicated that chronic β-catenin signaling activation is associated with inappropriate epithelial renewal.

5.5. Discussion

Results of the present study represent the first identification of links between β-catenin signaling and airway microenvironment-associated epithelial renewal. Using TOPgal transgenic mice and immunohistochemical staining we defined the spatial and temporal pattern of β-catenin signaling during microenvironment-associated stem cell activation. Importantly, the current study identified conducting airways as a primary source of β-catenin signaling during airway repair. Nuclear / cytoplasmic β-catenin localization indicative of signaling was detected in both NEB and BADJ stem cell microenvironments shortly after TA cell depletion. Downstream targets of β-catenin signaling were activated concomitant with airway re-epithelialization and cellular differentiation, but not stem cell proliferation. These findings revealed that after airway injury β-catenin signaling occurs most frequently in postmitotic airway cells, and suggested multiple roles for lung β-catenin signaling as a regulator of cellular maturation, migration, and differentiation. Additionally, chronic activation of β-catenin signaling was associated with incomplete epithelial renewal. Taken together, these data support a model in which airway-specific β-catenin signaling functions to regulate cellular migration and maturation during repair (Figure 5.9).

In TOPgal mice, expression of β-galactosidase is restricted to cells undergoing active β-catenin signaling. Numerous in vitro reporter assays have used this TOP promoter construct linked to a luciferase reporter to confirm β-catenin signaling induction [94, 142, 176, 217, 231, 269, 270]. These studies demonstrate that expression of genes by the TOP promoter specifically reflects β-catenin signaling activation and not induction via other signaling pathways. In vivo,

the specificity of TOPgal transgene reporter activation was determined by crossing TOPgal mice with transgenic mice expressing a constitutively active form of β-catenin in epidermal basal cells (K14-ΔNβ-catenin) [49, 94]. Results of these studies demonstrated increases in TOPgal activity that localized to regions of β-catenin transgene expression. TOPgal reporter mice have also been bred with transgenic mice expressing a dominant negative form of β-catenin (K14-ΔNΔCβ-catenin) [50]. In these experiments, TOPgal activation was inhibited within cells specifically expressing the dominant negative β-catenin protein construct. Based on these *in vitro* and *in vivo* studies, it is highly unlikely that LacZ expression in TOPgal mice could be due to nonspecific promoter activation.

These results also indicate that the degree of X-gal histochemical staining / β-catenin signaling activation is more broadly distributed than was previously observed via staining for nuclear / cytoplasmic β-catenin protein localization. This is most likely due to the fact that nuclear β-catenin levels necessary for signaling and TOPgal transgene activation are below the levels necessary for detection of nuclear β-catenin by immunostaining [49]. For this reason, it appears that X-gal histochemical staining is a more sensitive method for detecting β-catenin / TCF downstream target gene activation. A second possible explanation for this observed difference is that the TOPgal transgene reporter used in these studies can be activated independently from β-catenin / TCF transcription factor complex assembly. This is unlikely due to the high specificity of TOPgal LacZ expression observed in numerous previous *in vitro* and *in vivo* studies [36, 49, 50, 94, 125, 142, 164, 176, 217, 231, 269, 270]. Altogether, these results strongly implicate a role for β-catenin signaling activation concomitant with epithelial renewal processes.

The current study's identification of associations between microenvironment-associated β-catenin signaling and cell migration or differentiation is not without precedent. The importance of intestinal Wnt / β-catenin signaling in differentiation and migration has been revealed using various transgenic and knockout approaches [14, 141, 150, 204, 308]. Numerous studies involving skin follicular bulge stem cells have highlighted the importance of β-catenin signaling in cell fate regulation [49, 50, 94, 113, 176, 290]. The importance of β-catenin signaling to intestinal stem cell fate was first discovered in Tcf4 knockout mice that lack their normal crypt-villus architecture [12, 141, 204]. Intestinal Wnt / β-catenin signaling influences EphB / ephrin-B levels resulting in differential segregation between stem and daughter cells [14, 269]. In skin, TOPgal reporter studies confirm activation of β-catenin signaling in stem cell microenvironments at discrete times during epidermal development and follicular growth [50, 94, 125]. Skin-specific alterations to β-catenin regulatory domains results in altered epidermal daughter cell phenotypes and eventual tumorigenesis [50, 94, 176, 178]. Specifically, these transgenic mice exhibit *de novo* follicular growth in normally (interfollicular) epidermal regions [49, 94]. Additionally, disruption of both N- and C-terminal domains of β-catenin protein induces a fate choice reversal between follicular and interfollicular stem cell [50]. Together these findings confirm that β-catenin signaling serves important roles in regulating stem and daughter (TA) cell fate choice within numerous tissue types.

Results of the current study also provide evidence that airway injury results in abnormal cell signaling within other lung compartments. Specifically, β-catenin signaling induction occurs within the mesenchyme and alveolus following airway TA cell depletion. Since naphthalene-mediated injury is Clara cell specific, activation of mesenchymal and alveolar β-catenin signaling must occur independent of direct cellular injury. There are a number of

possible explanations for this phenomenon. First, it is conceivable that airway Clara cell secretory products directly affect mesenchymal and alveolar cell phenotypes. This hypothesis is supported by the discovery of Clara cell secretory product receptors on several alveolar cell types [22]. Second, naphthalene-mediated Clara cell ablation may result in indirect mesenchymal / alveolar toxicant susceptibility through loss of differentiated airway functions. Third, airway basement membrane exposure following Clara cell ablation may induce altered signaling adjacent cell types. Whatever the case, it is clear that further studies are needed to identify the specific mechanisms inducing mesenchymal / alveolar signaling after airway-specific injury.

While the current study definitively identifies activation of β-catenin signaling within airways during renewal, numerous aspects of lung β-catenin signaling remain elusive. First, it will be important to determine the necessity of β-catenin signaling in airway microenvironment-associated cellular migration and differentiation. Second, identification of airway-specific β-catenin target genes will aid in determining how β-catenin signaling mediates airway renewal. Finally, defining the mechanisms of activating β-catenin signaling will provide significant advances in understanding airway repair processes. Studies are ongoing to determine the necessity of β-catenin signaling in epithelial maturation and renewal as well as identify lung-specific β-catenin downstream target genes and activators.

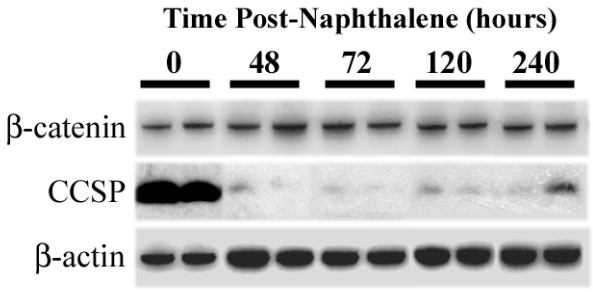

Figure 5.1. β-catenin cofactor and target gene protein expression following progenitor cell depletion.

Representative immunoblots from FVB/n animals recovered for 0, 48, 72, 120, or 240 hours. Total lung protein was recovered and western blot analysis performed with antibodies to β-catenin (92kD), CCSP (10kD), and β-actin (42kD). Total β-catenin protein levels remain stable or show a moderate increase following injury and repair. CCSP levels are dramatically reduced within 48 hours of naphthalene exposure and reflect depletion of airway Clara cells. CCSP levels increase at 120 and 240 hours concomitant with continuing epithelial renewal.

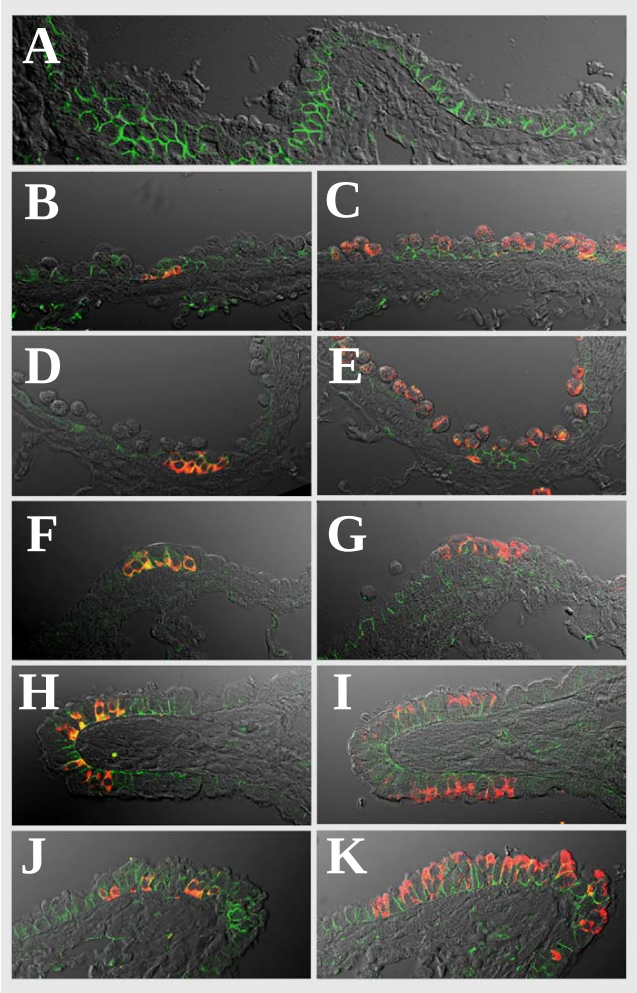

Figure 5.2 Dual immunofluorescent detection of β-catenin within NEBs following naphthalene mediated injury.

(A) β-catenin (green) is normally expressed at the basolateral surface of epithelial cells throughout the adult conducting airway. (B-E) Basolateral β-catenin (green) is rapidly lost from the majority of epithelial cells at 12 (B,C) and 24 (D,E) hours post-naphthalene injury as a result of CCSP expressing Clara cell depletion (red, C,E). β-catenin expression is retained in and immediately adjacent to CGRP expressing NEBs (red, B,D). (F-I) Nuclear / cytoplasmic b-catenin is detected at 48 (F,G) and 72 hours (H,I) after Clara cell ablation within NEB-associated CGRP expressing neuroendocrine (yellow dual staining, F,H) and Clara cell subsets (yellow, G, I). Basolateral membrane-associated b-catenin is also detected in nascent Clara cells at 72 hours (red, I). (J,K) Levels of nuclear / cytoplasmic b-catenin are reduced and normal basolateral β-catenin expression is restored within both neuroendocrine (J) and Clara cells (K) five days after injury.

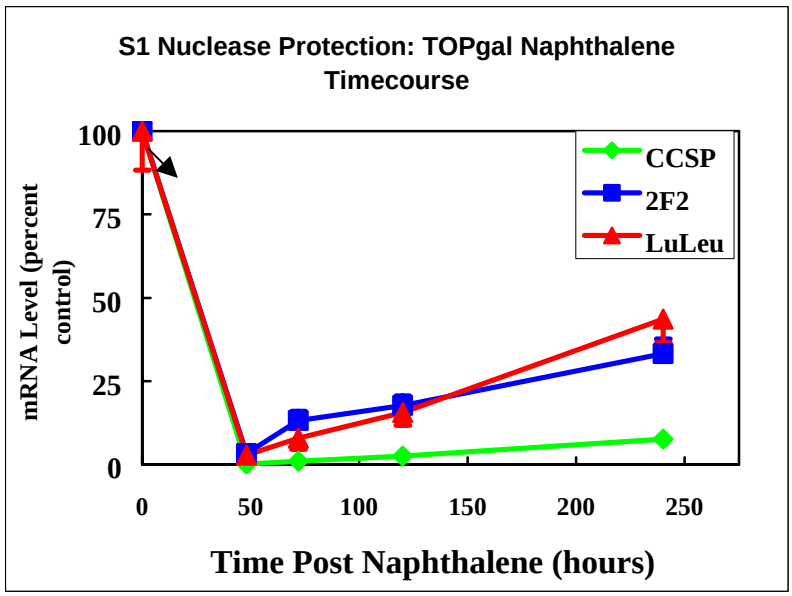

Figure 5.3 Significant CCSP expressing cell depletion following TOPgal naphthalene exposures.

Total lung RNA samples isolated from untreated control and naphthalene treated TOPgal transgenic mice were analyzed by S1 nuclease protection assay to measure changes in abundance of Clara cell-specific markers (CCSP, CYP2F2, and Uteroglobin gene related protein / LuLeu). Phosphorimager data was normalized to L32 ribosomal mRNA abundance as an internal control. The Y-axis shows relative mRNA abundance as a percent of untreated control levels; the X-axis shows the number of hours recovery post-exposure. Data represents the means of n=4-6 animals / time point ± SEM.

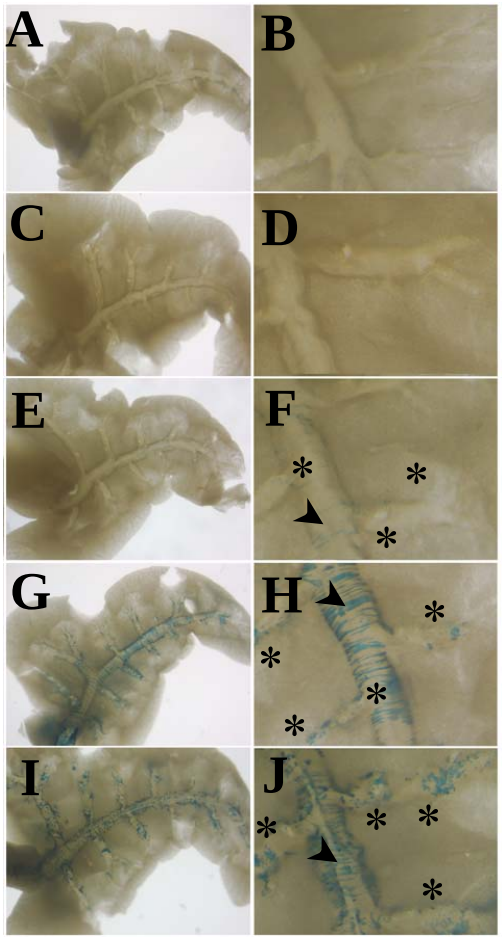

Figure 5.4 Spatio-temporal induction of β-catenin signaling / LacZ expression after naphthalene injury.

Naphthalene recovered lungs were fixed, X-gal stained and microdissected to identify LacZ expressing cells. Representative low (A,C,E,G,I) and high magnification (B,D,F,H,J) images of airways are presented. (A-B) Control, untreated lungs do not contain detectable b-catenin signaling cells. (C-D) Forty-eight hours after naphthalene injury, there is no induction of LacZ expression when compared to controls. (E-F) At seventy-two hours recovery infrequent LacZ expressing cells are visible at airway epithelial branchpoints and terminal bronchioles (asterisks, F), as well as within underlying fibroblast-like mesenchymal cells (arrowheads, F). (G-H) The number of LacZ expressing epithelial cells is dramatically increased 120 hours after injury yet cells remain associated with airway branchpoints and terminal bronchioles (asterisks, H). LacZ positive fibroblast-like cells also increase in frequency within large intrapulmonary conducting airways (arrowheads, H). (I-J) Ten days after naphthalene injury LacZ expressing cells remain abundant but are more broadly distributed throughout conducting airways (asterisks, J). There are fewer LacZ expressing fibroblast-like cells at this time point (arrowheads, J).

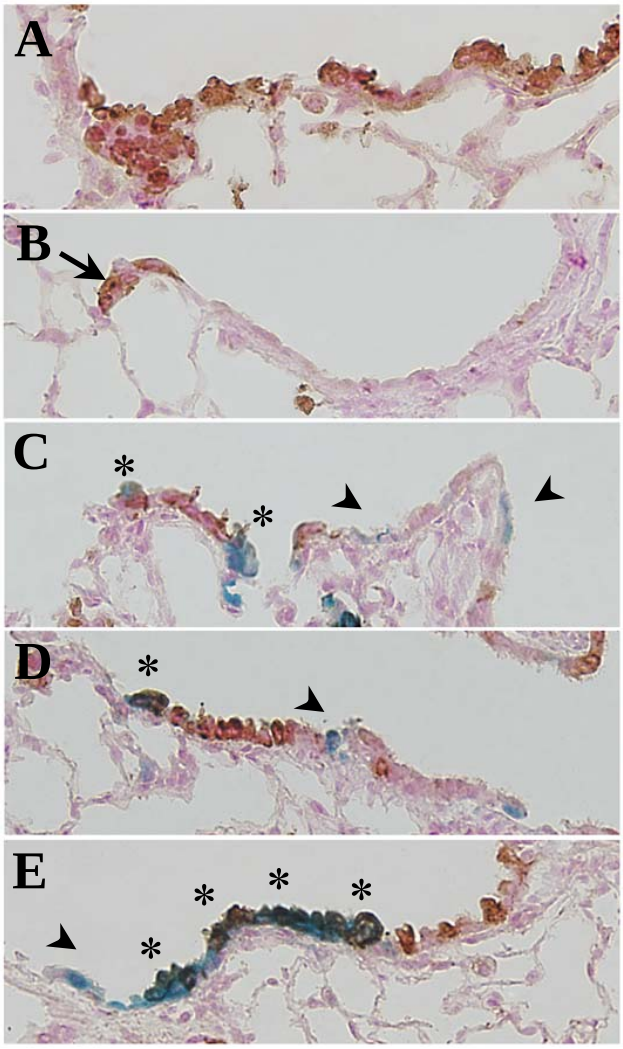

Figure 5.5 β-catenin signaling is activated within terminal bronchiole associated CCSP expressing cells.

(A-E) X-gal stained TOPgal tissue sections were immunostained for the presence of CCSP at 0, 48, 72, 120, and 240 hours post-naphthalene injury. (A) Uninjured airways contain numerous CCSP expressing Clara cells but no detectable β-catenin signaling. (B) Forty-eight hours after naphthalene exposure CCSP expressing cells are restricted to the BADJ (arrow) but do not express detectable LacZ protein. (C) At 72 hours post injury, LacZ expressing CCSP(+) cells are detectable immediately adjacent to the BADJ (arrow; dual expressing cells indicated by asterisks). Additionally, infrequent LacZ single-positive cells exist adjacent to BADJ-associated Clara cells (arrowhead). (D-E) LacZ / CCSP dual positive cells expand proximally from the BADJ at five (D) and ten days (E) after injury concomitant with BADJ-associated epithelial renewal.

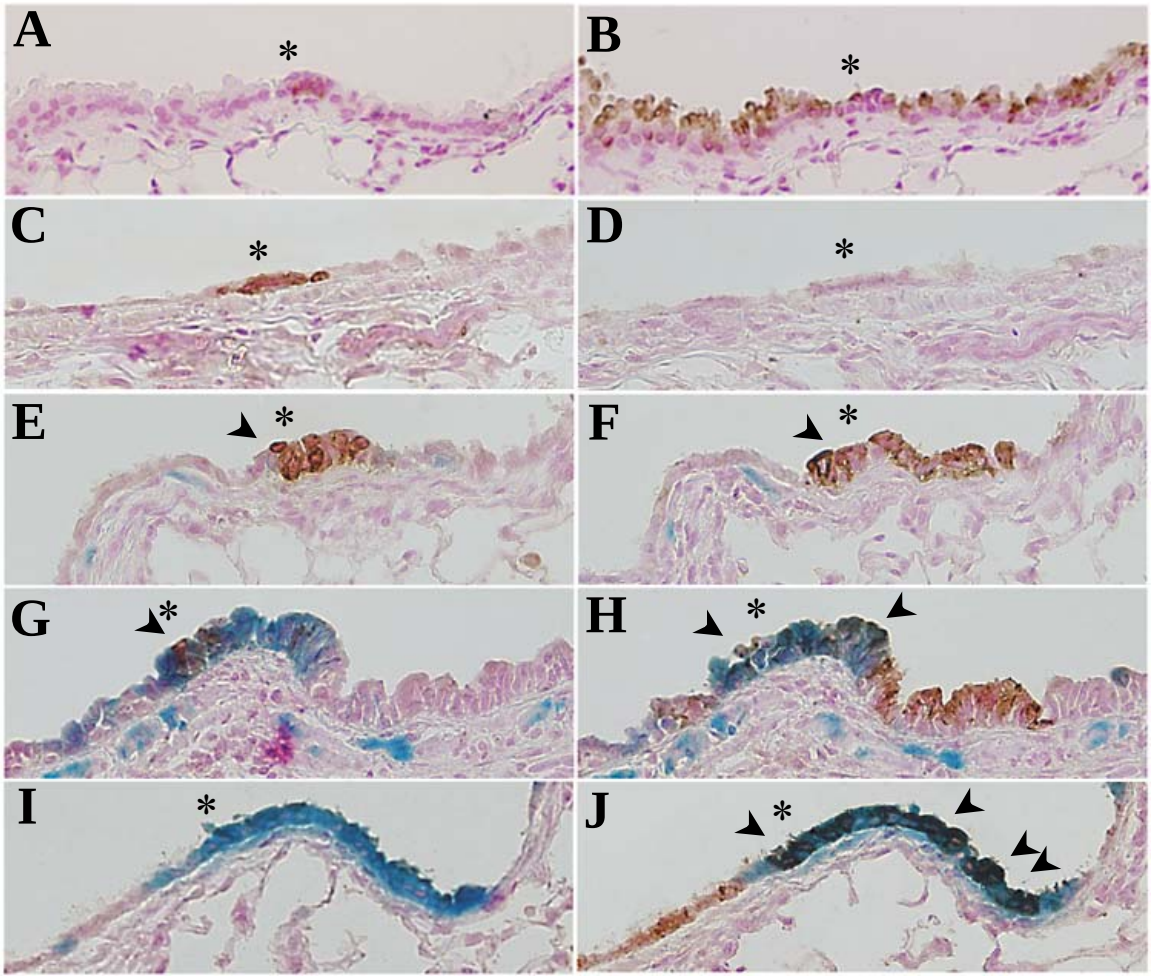

Figure 5.6 β-catenin signaling is induced within NEB microenvironments following naphthalene injury.

Adjacent serial sections of naphthalene injured, X-gal stained lungs were stained for CGRP (A,C,E,G,I) or CCSP (B,D,F,H,J) to identify NEB microenvironment-associated regeneration (asterisks, A-J). (A-B) Normal distribution of CCSP / CGRP cell phenotypes but no LacZ expressing cells are detected within NEB microenvironments in the absence of injury. (C-D) Forty eight hours after naphthalene injury there is extensive depletion of airway Clara cells (D) but no detectable NEB-associated LacZ expression. (E-F) At 72 hours recovery there is an expansion of NEB-associated CCSP expressing cells (F) independent of detectable LacZ expression in either neuroendocrine (E) or Clara cells (F). (G-H) Five days after injury b-catenin signaling, LacZ positive cells are present within a population of NEB-associated neuroendocrine (arrowheads, G) and nascent Clara cells (arrowheads, H). (I-J) Numerous LacZ / CCSP dual positive cells are present throughout NEB microenvironments ten days after naphthalene-mediated progenitor cell depletion (arrowheads, J).

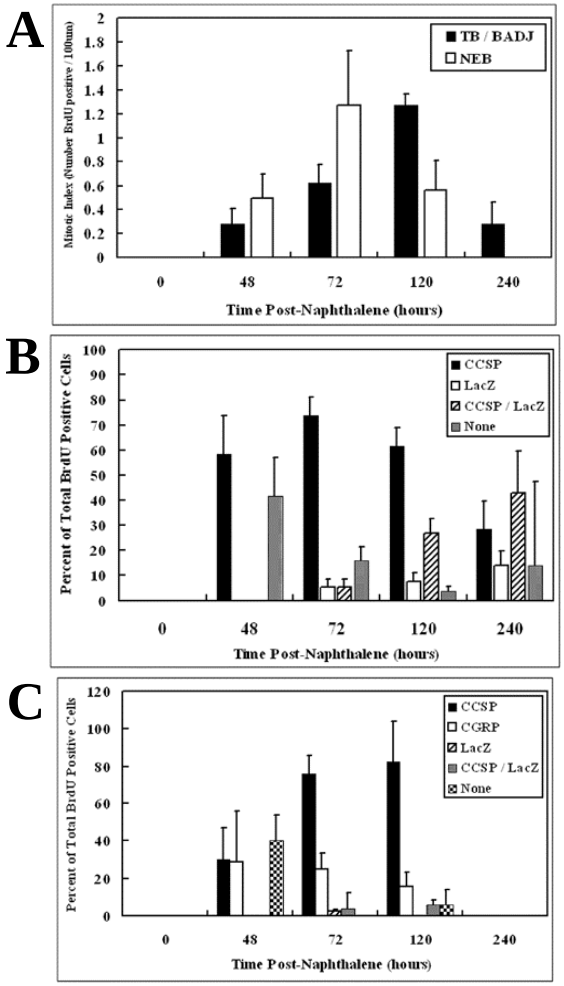

Figure 5.7 Initiation of epithelial regeneration / proliferation precedes detectable β-catenin signaling.

(A) Analysis of mitotic index (# BrdU positive cells / 100μm basement membrane) within BADJ and NEB microenvironments indicates that stem cell-mediated renewal is initiated within 48 hours of injury. Proliferation peaks 72 hours after injury within NEB microenvironments and 120 hours after injury within terminal bronchioles, and is reduced in each region to near steady-state levels within 10 days. (B) CCSP expressing cells comprise the majority of BrdU positive cells in terminal bronchioles 48, 72, and 120 hours after naphthalene injury (solid bars). By 240 hours recovery CCSP / LacZ dual positive cells represent most TB-associated proliferation (hashed bars). (C) In NEB microenvironments there is equal representation of CCSP, CGRP, and phenotypically indeterminate cells 48 hours after naphthalene injury (black, white, and checkered bars, respectively) By 72 hours nearly 80% of mitotic cells express CCSP but not LacZ (black bars). No significant single or dual LacZ expressing cells contribute to NEB-associated epithelial renewal at any time point studied after injury (hashed and gray bars, C).

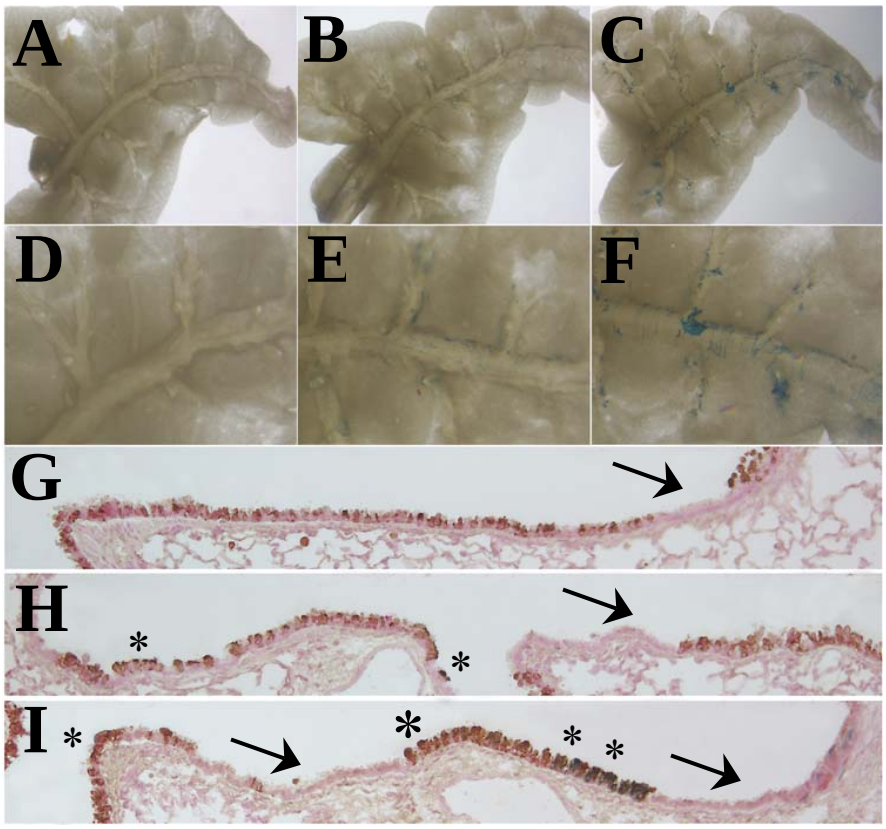

Figure 5.8 Variability in chronic activation of β-catenin signaling reflects the degree of overall epithelial renewal.

(A-F) Microdissection of 45 day recovered, X-gal stained lungs revealed heterogeneity in LacZ protein expression. One lung displayed a complete absence of X-gal staining (A, D) while the majority of 45 day recovered lungs displayed infrequent, individual LacZ positive cells (B, E). These were distributed randomly throughout airways. The remaining two lungs contained significant patches of branch point / terminal bronchiole associated LacZ expressing epithelial cells as well as numerous LacZ positive fibroblasts (C,F). (G) CCSP staining of lung sections lacking X-gal staining revealed near-complete airway regeneration with infrequent abnormal epithelial patches (arrow). (H) Lung sections containing infrequent LacZ expression display regions of extensive epithelial renewal containing individual LacZ expressing, CCSP positive cells (asterisks) bordered by abnormal epithelial zones (arrows). (I) Lungs with significant X-gal staining exhibit only partial epithelial renewal with large areas of highly abnormal epithelia (arrows, I). These patches of LacZ expressing epithelial cells demarcate border regions between normal and abnormal epithelia (asterisks, I).

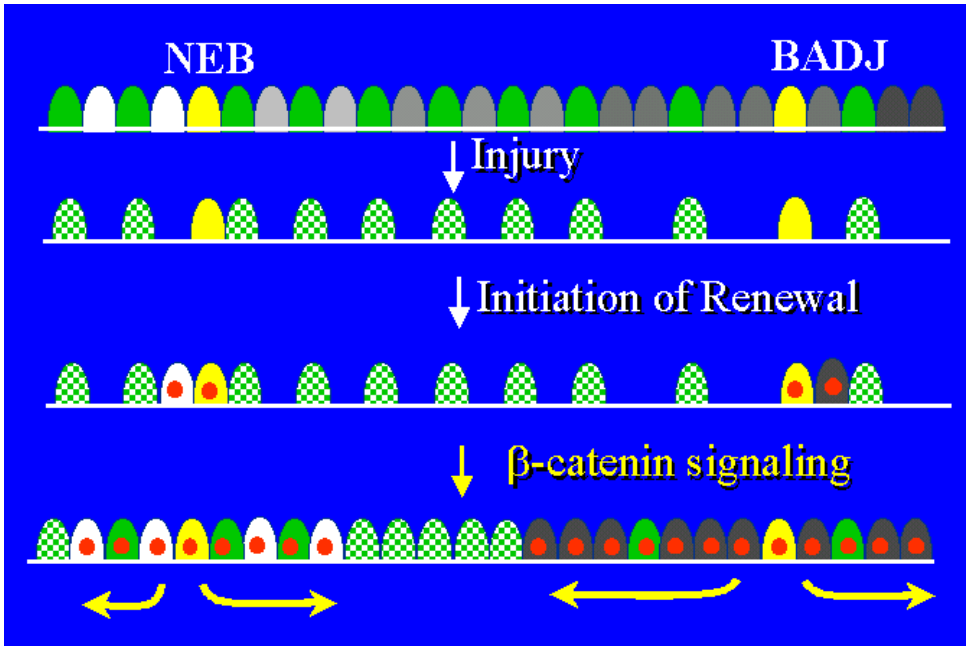

Figure 5.9. Model illustrating activation of β-catenin signaling during airway injury and repair.

In the steady state epithelium, CCSP expressing and ciliated cells are present throughout airways (white-grey and green cells, respectively) and there is no detectable β-catenin signaling. Naphthalene administration results in rapid depletion of Clara cells throughout airways with the exception of NEB and BADJ-associated CCSP expressing stem cells (CE, yellow cells). Microenvironment associated CE cells proliferate to faciliate epithelial renewal within 48 hours of Clara cell depletion (red nuclei). After initial stem cell activation, β-catenin signaling is detected within NEB and BADJ microenvironments and is associated with migration and differentiation of nascent cell populations (red nuclei; migration indicated by arrows). Restoration of a phenotypically diverse epithelium is accompanied by downregulation of β-catenin signaling.

Table 2. Incidence of LacZ-Positive Cells per 100μm Basement Membrane (Percent of Total LacZ Positive Cells)

Incidence of LacZ-Positive Cells per 100 μm Basement Membrane *(Percent of Total LacZ-Positive Cells)*										
	Hours Post-Naphthalene Exposure									
Distance From Landmark (μm)	0		48		72		120		240	
	NEB	BADJ	NEB	BADJ	NEB	BADJ	NEB	BADJ	NEB	BADJ
0-50	0(0)	0(0)	1.3 (33.3)	1.2 (22.6)	2.1 (54.5)	2.8 (40)	10 (37.0)	9.8 (31.0)	7.3 (36.3)	6.2 (30.1)
51-100	0(0)	0(0)	0.9 (22.2)	1.2 (22.6)	0.5 (13.6)	0.9 (13.3)	6.5 (24.1)	6.6 (21.0)	5.0 (25.0)	4.8 (23.3)
101-150	0(0)	0(0)	0.4 (11.1)	0.8 (16.1)	0 (0.0)	1.4 (20)	2.5 (9.3)	6.1 (19.4)	2.5 (12.5)	3.1 (15.0)
151-300	0(0)	0(0)	0.4 (33.3)	0.7 (38.7)	0.4 (31.8)	0.6 (26.7)	2.7 (29.6)	3.0 (28.6)	1.8 (26.3)	2.2 (31.6)

6. Synopsis

6.1. Summary and Conclusions

6.1.1. Overview

The elucidation of mechanisms for epithelial maintenance and renewal after injury are central to understanding aspects of normal airway diversity and the pathobiology of lung diseases including asthma, chronic obstructive pulmonary disease (COPD), idiopathic pulmonary fibrosis (IPF), and cancer. Towards this end, previous studies from our laboratory and others have attempted to identify and characterize adult conducting airway-specific stem cell populations [29, 70, 71, 95, 110, 111, 224, 225, 253]. Studies of lung maintenance and regeneration revealed that most airways exhibit extremely low rates of cellular turnover, and that most proliferation is accomplished by airway transit amplifying (TA) cell populations [74, 76, 77, 81]. Using an injury model that specifically targeted airway TA cell populations allowed for the identification of normally obscure airway stem cells [250]. Results indicated that latent stem cell populations localized to neuroepithelial body (NEB) microenvironments were activated specifically in response to Clara / TA cell loss [224]. These cells exhibited a slow cycling, label retaining phenotype [110]. They also maintained a molecular phenotype of CCSP expression yet were phenotypically distinct from most airway Clara cells [110, 224]. Subsequent studies revealed that NEB-associated CCSP expressing cells were both necessary and sufficient to restore a phenotypically diverse epithelium within intrapulmonary airways [110, 225]. In addition to identification of stem cells localized within NEB microenvironments, recent studies have identified a subset of tracheal basal cells with characteristics of proximal airway stem cells. Lineage tagging studies revealed that some tracheal basal cells maintained robust mitotic and differentiation potential and could repopulate proximal airways following TA cell depletion

[111, 112]. Independent studies of Borthwick et. al. reached a similar conclusion, identifying label retaining basal cells adjacent to submucosal glands and cartilaginous rings [29].

Studies presented in this dissertation add significantly to current understanding of airway stem cell molecular and functional phenotypes. Together, these findings constitute important advancements in our knowledge of the spatial and temporal kinetics of epithelial renewal, identify cell-intrinsic properties that contribute to airway stem cell pollutant resistance, and provide evidence that β-catenin signaling contributes to airway epithelial renewal.

6.1.2. Terminal Bronchioles Harbor a Unique Airway Stem Cell Population that Localizes to the Bronchoalveolar Duct Junction

The goal of this study was to determine whether NEB-independent stem cell microenvironments exist within intrapulmonary conducting airways. Specifically, previous observations indicate that NEB-associated stem cells are unlikely to contribute to renewal of the terminal bronchiolar epithelium due to the paucity of NEB microenvironments at this location [10, 193]. Additionally, terminal bronchioles are a frequent source of neoplastic transformations following repeated, chronic injury or pollutant exposure [54, 123, 127, 168, 175, 201, 202, 213, 214, 267]. For these reasons, we hypothesized that terminal bronchioles maintain a distinct population of airway stem cells capable of regionally appropriate epithelial renewal. Results presented in Chapter 3 describe the identification of novel, bronchoalveolar duct junction associated cells capable of regionally appropriate epithelial renewal following progenitor / Clara cell depletion. These cells were CCSP expressing (CE) and comprise the predominant proliferative population in initial terminal bronchiolar repair. BADJ-associated, pollutant-resistant CE cells also exhibit properties of label retention suggesting that they maintain

characteristics ascribed to stem cells. Furthermore, these studies confirmed that BADJ-associated CE cells function independently of NEBs, and therefore define a novel regenerative microenvironment. Based on each of these observations we concluded that the terminal bronchiolar BADJ represents a novel microenvironment for CE stem cells. These findings support a model proposed by Engelhardt and others in which multiple stem cell microenvironments maintain appropriate cellular diversity throughout airways [71]. It is also interesting to speculate that inappropriately activated BADJ-associated stem cells may be a source for TB-associated neoplastic transformations.

6.1.3. Potential Mechanisms of Pollutant Resistance Within Airway Stem Cells

The purpose of these studies was to identify mechanisms to explain the observed pollutant resistance within airway stem cell populations and provide a means for further airway stem cell characterization. Previous studies in other organs have shown that stem cells frequently exhibit properties of reduced CYP450-mediated bioactivation and efficient clearance of potential toxicants [88, 138, 197, 222, 233, 268, 299]. These properties have been shown to confer significant resistance to injury both within stem cells and many stem cell-derived cancers [170, 188, 191]. Based on these observations we hypothesized that airway stem cells would exhibit reduced CYP450 activity as well as efficient toxicant clearance. Results of these experiments identified a population of CCSP expressing cells within NEB microenvironments that exhibited reduced CYP2F2 protein abundance. Additionally, a subpopulation of CCSP expressing cells with efficient lipophilic molecule efflux was identified by Hoechst 33342 staining and fluorescence associated cell sorting. Efficient Hoechst 33342 efflux resulting in a 'side population' phenotype is an identified property of stem cells from numerous tissues [5, 8, 9,

144, 233, 300, 311]. In lungs, purified airway side population cells were enriched for stem cell antigen 1 expression and expressed reduced levels of CYP2F2. Together, these data provide evidence for specific mechanisms of pollutant resistance within identified CCSP expressing airway stem cells. These findings also provide potential methods for the isolation and molecular characterization of quiescent versus activated lung stem cells.

6.1.4. β – Catenin Signaling is a Component of Airway Stem Cell Mediated Renewal

Goals of this study included the identification of signaling pathways associated with stem cell microenvironment activation and a determination of their downstream effects. Studies in other tissues have identified the β-catenin signaling pathway as a central regulator of stem cell fate [113, 141, 164, 178, 223, 252, 308, 315]. β-catenin signaling has been shown to regulate aspects of stem cell activation, migration, and daughter cell differentiation through regulation of downstream target genes [14, 93]. We hypothesized that β-catenin signaling is a component of airway stem cell-mediated renewal, and that expression of β-catenin downstream target genes would be induced following airway TA cell injury. Studies presented in Chapter 5 definitively identified β-catenin signaling and downstream target gene induction following airway injury. Moreover, β-catenin signaling cells were predominately NEB and BADJ microenvironment-associated nascent Clara cells. β-catenin signaling cells increased in number during airway renewal and spread from stem cell microenvironments during epithelial renewal. Signaling was subsequently down-regulated upon restoration of normal airway phenotypes. Despite a lack of association with initial stem cell proliferation, these results indicated that airway stem cell microenvironment-associated β-catenin signaling is associated with cellular migration and differentiation during restoration of airway TA / Clara cell populations. The recent observations

indicating activation of β-catenin signaling in human airway remodeling and disease raise the possibility that this signaling pathway is an important regulator of overall epithelial homeostasis.

6.2. Future Directions

6.2.1. Functional Consequences of β-catenin Signaling

Chapter 5 of this thesis demonstrates changes in the subcellular distribution of β-catenin protein and the activation of β-catenin signaling targets within NEB and BADJ microenvironments following naphthalene-mediated Clara cell injury. Despite these findings, it remains unclear what specific endogenous target genes are induced following β-catenin signaling activation. The functional consequences of β-catenin signaling pathway activation also remain elusive.

In numerous tissues, β-catenin signaling has been shown to regulate cellular proliferation, migration, and differentiation in stem cell populations from numerous tissues. Traditional downstream target genes activated by β-catenin include cyclin D1, c-myc, matrilysin (MMP7), and various signaling pathway genes including BMP4, Lef1, and Axin2 [49, 102, 125, 128, 137, 150]. In skin, activation of β-catenin target genes induces bulge-associated stem cell migration and initation of follicular growth [49, 50, 94, 113]. Also in skin, conditional basal cell-specific c-myc activation results in loss of cell-microenvironment adhesive interactions and promotes stem cell migration [93]. Intestinal β-catenin signaling appears to principally regulate stem cell maintenance, TA cell fate, and cellular differentiation [14, 141, 308]. Transgenic disruption of intestinal β-catenin signaling through ablation of Tcf4 or Dkk1 overexpression results in loss of intestinal crypts due to terminal differentiation of local stem cell populations. In recent studies by Batlle et. al. EphB / ephrin levels regulated by β-catenin signaling were shown to principally important in restricting progenitor cells towards either a mitotic or differentiated cellular fate [14]. Recent studies indicate that aberrant activation of β-catenin signaling may also influence

tissue remodeling and is associated with numerous types of cancers [191, 222]. Constitutive epidermal β-catenin signaling results in perturbations to normal skin stem cell fate, hypertrophic follicular morphogenesis, and eventual formation of pilomatricomatous tumors [94]. Intestinal APC mutations resulting in unregulated β-catenin signaling lead to hyperproliferation and tumorigenesis [159, 308]. In airways, aberrant signaling is associated with chronic lung diseases as well as both NSCLC and SCLC formation [41, 175, 183, 198, 244].

To explore the functional consequences of β-catenin signaling, experiments must first be carried out to determine the components of this pathway that are active in steady state versus repairing airways. Wnt / β-catenin pathway specific microarrays are currently available and should allow for the characterization of all known β-catenin signaling targets simultaneously. Following identification of the β-catenin target genes induced during epithelial renewal, it will be equally important to determine their functional significance. Future *in vitro* and *in vivo* studies will determine the necessity of β-catenin signaling and specific target gene activation in epithelial stem cell-mediated renewal.

6.2.2. Mechanisms of β-catenin Signaling Induction

It is currently known that aberrant activation of β-catenin signaling is associated with remodeling of airways, hyperproliferative disorders such as IPF, and lung cancers. Results of studies presented in this dissertation indicate that defined airway stem cell populations initiate β-catenin signaling during epithelial renewal. Despite these observations, mechanisms responsible for initiating β-catenin signaling are not well defined. Pinto and others recently determined that Wnt signaling through Frizzled receptors was the dominant mechanism of β-catenin signaling activation in intestine [204]. Here, ectopic expression of the Wnt inhibitor Dickkopf1 (Dkk1)

resulted in a failure to maintain normal crypt-villus architecture [142, 204]. Subsequent studies revealed that this phenotype was primarily due to Wnt's inability to stimulate β-catenin signaling [141, 269, 308]. Additionally, the role of Wnt in β-catenin signaling was demonstrated in epidermis using skin-specific Dkk1 expressing mice [6]. These mice displayed progressive hair loss coupled with preferential sebaceous and interfollicular cell differentiation, and phenotypically resembled mice expressing dominant negative Lef1 transcriptional cofactors. While stabilization of β-catenin proteins and activation of the TOPgal transgene reporter have most frequently been attributed to Wnt signaling, there are other alternative mechanisms for β-catenin signaling activation. Fibroblast growth factor 2 (FGF-2) has been shown to directly inhibit Gsk3β resulting in β-catenin stabilization / nuclear transcription factor activity [102, 109, 118]. Similarly, insulin like growth factor and epidermal growth factor have both been shown to inhibit GSK3β through either the PI3K or MAPK pathways, respectively [153, 280].

It is apparent that future studies are needed to define the mechanisms of β-catenin signaling activation and the specific role of Wnt proteins in airway epithelial renewal. It is anticipated that a greater understanding of β-catenin signaling activation during airway injury / repair may reveal potential therapeutic strategies for manipulating β-catenin signaling in the context of disease. Results from microarray experiments outlined in the previous section will provide preliminary evidence as to whether Wnt proteins are expressed in steady state and injured adult lungs. To determine the role of Wnt signaling in β-catenin signaling activation, *in vitro* and *in vivo* experiments will be performed in which ectopic expression of Dkk1 is induced during airway injury and repair. Cultures and mice will then be evaluated for cellular proliferation, migration, and β-catenin signaling activation.

6.2.3. Molecular Phenotype of Airway Stem Cells

In addition to the immediate future goals presented above, defining the molecular phenotype of airway stem cells remains a long-term goal within our laboratory. As stem cells are widely considered progenitors for cancer, a more complete understanding of an airway stem cell's phenotype could allow for the rational design of anticancer treatments [191, 222]. Additionally, tissue-specific stem cells (such as those isolated from skin) remain the only effective, clinically relevant stem cell-based therapeutics [4, 266]. Characterization of airway stem cell-specific markers could allow for the prospective isolation of airway stem cells and enable their eventual use as therapeutic agents. Furthermore, the identification of stem cell and microenvironment-specific genes would be valuable tools for investigating airway stem cell mitotic differentiation potentials.

Some of the unique molecular and functional properties of airway stem cells uncovered during the course of these studies may provide methods to uncover an airway stem cell's molecular phenotype. Specifically, the identification of airway stem cells bearing a characteristic Hoechst 33342 effluxing, side population phenotype now allows for purification and characterization of side population (SP) versus non-SP cells. While SP cells have not functionally demonstrated airway stem cell activity, they do exhibit phenotypic properties similar to NEB-associated CE cells [96]. Additionally, similar approaches can be used to fractionate isolated airway epithelial cells on the basis of their expression of a fluorescent β-catenin / TCF responsive reporter transgene. These transgenic mice, designed by Costantini and colleagues, express a destabilized form of GFP under regulation of the Axin2 promoter (Axin2-de-GFP) and exhibit a fluorescent pattern identical to X-gal staining patterns observed in developing TOPgal transgenic lungs [128]. Using these Axin2-de-GFP mice it should be possible to prospectively

isolate actively β-catenin signaling airway cells following naphthalene injury and initation of repair. Together, these strategies could provide new understanding of a prospectively isolated airway stem cell's molecular phenotype.

Laser capture microdissection (LCM) may provide a second method for the isolation and characterization of airway stem cells. This method has been used is mouse lung tissues to successfully isolate and characterize the molecular phenotype of morphologically distinct regions [19]. Similar approaches coupled with gene expression profiling could be used to compare active versus quiescent airway stem cell microenvironments. These approaches are especially appealing due to their isolation of both individual stem cells and their surrounding microenvironment. This data may provide additional data regarding airway stem cell regulation within their endogenous microenvironments. While current LCM technologies are labor intensive and do require morphologically distinct cell populations, new technologies are emerging that may facilitate a high-throughput, fluorescence based LCM-derived cell isolation. Altogether, a comparison of data from LCM-isolated stem cells, airway SP cells, and β-catenin signaling (GFP or LacZ expressing) cells should greatly improve our current knowledge of airway stem cells.

6.3. Closing Remarks

Lung diseases, and especially lung cancers remain among the most deleterious human illnesses in terms of morbidity and mortality. Despite recent successes in the identification of airway stem cell associated functional propterties and signaling pathways, numerous questions remain unanswered. Therefore, continued studies regarding the role of airway stem cells as putative lung cancer progenitors and investigations into their usefulness as potential therapeutic agents remain of paramount importance.

APPENDIX A

Evidence for β-catenin Signaling During Airway Development and Maturation

Results

β-catenin Signaling is a Component of Airway Development

Activation of the β-catenin / TCF signaling pathway in the developing lung has been implicated through analysis of the spatial expression of a GFP reporter under control of the Axin2 promoter and through conditional ablation of β-catenin within the developing lung epithelium [64, 128, 173, 228, 260]. Regulation of downstream signaling by β-catenin requires its cytoplasmic accumulation and formation of nuclear β-catenin / TCF heterodimers [62, 99, 102, 170, 218, 234]. To gain a more complete understanding of roles for β-catenin signaling in epithelial cell proliferation and differentiation in developing lungs we initially determined the spatial context of β-catenin localization during embryonic and post-natal lung development. At embryonic day 16.5, β-catenin was present on all airway epithelial cell basolateral plasma membranes. Additionally, nuclear / cytoplasmic β-catenin was observed throughout the conducting airways and less frequently in peripheral lungs (Figure 1A, arrowheads). By embryonic day 18.5 most airway cells expressed only membrane-associated β-catenin, with nuclear / cytoplasmic staining restricted to distal airways and the periphery (Figure 1B, arrowheads). This staining pattern persists through postnatal day 5, and by postnatal day 7 all epithelial β-catenin is membrane associated (data not shown). Nuclear / cytoplasmic β-catenin was not observed in underlying mesenchymal cells at any time during lung development. Immunostaining was also performed on embryonic skin containing developing hair follicles as a positive control for nuclear / cytoplasmic β-catenin (Figure 1D, arrowheads). These data

demonstrate cytoplasmic accumulation of β-catenin in a defined spatial-temporal pattern during lung development suggesting the potential for formation of β-catenin signaling complexes and activation of downstream target genes.

Activation of a β-catenin / TCF signaling reporter transgene during mouse lung development.

To determine whether cytoplasmic accumulation of β-catenin led to functional signaling and activation of downstream target genes we characterized the temporal-spatial expression of a transgenic LacZ reporter under control of an optimal TCF reporter (TOPgal transgenic mice) [4, 49, 50]. Embryonic and postnatal TOPgal mouse lungs were fixed and whole-mount stained with X-gal to identify sites of LacZ expression (Figure 2). Conditions used for X-gal histochemistry resulted in complete absence of staining within lungs of transgene negative mice. Positive histochemical staining of epithelial cells with X-gal was present at embryonic days 14.5, 16.5, and 18.5, in addition to postnatal days 1 and 5. (Figure 2A and data not shown). X-gal histochemical staining was present throughout conducting airways and to a lesser extent in peripheral epithelial buds at embryonic days 14.5 and 16.5 (Figure 2B and C, asterisks), and was restricted to distal airway bronchioles and alveoli by postnatal day one (Figure 2D, asterisks and arrowheads, respectively). No LacZ expressing cells were present in postnatal day seven lungs (Figure 2A and 2E). Thus, it appears that X-gal histochemical staining patterns do not always correlate with patterns of detectable nuclear β-catenin protein expression. As stated previously, this is most likely due to the fact that nuclear β-catenin levels necessary for signaling and TOPgal transgene activation are below the level of detection by β-catenin immunostaining. For this reason, it appears that X-gal histochemical staining is a significantly more sensitive / accurate method for detecting activation of b-catenin / TCF downstream targets genes. Based on

previous studies, it is unlikely that differences between β-catenin immunostaining and TOPgal reporter activation are due to non-β-catenin signaling-dependent activation of the LacZ transgenic reporter.

Developmental β-catenin Signaling is Associated With Cellular Differentiation but not Proliferation

Wnt / β-catenin signaling has been implicated in the regulation of cell proliferation and differentiation in intestinal, follicular, hepatic, and hematopoietic tissues during development [36, 50, 102, 113, 125, 164, 176, 177, 185, 218, 231, 312, 315]. In order to determine the role β-catenin signaling plays in the regulation of epithelial cell proliferation and differentiation in developing lungs we determined the spatial context of TOPgal activation relative to the proliferation marker Ki67 and the airway differentiation marker CCSP. Colocalization of X-gal, CCSP, and Ki67 was determined at embryonic days 14.5, 16.5, 18.5 and postnatal day 1 (Figure 3). Results indicate that most proliferation is restricted to peripheral lungs at embryonic days 14.5 and 16.5 (Figure 3A and 3B, arrowheads). Very few LacZ expressing airway or peripheral lung cells expressed detectable Ki67 antigen. In addition, there was no detectable CCSP immunoreactivity in airways at embryonic days 14.5 and 16.5. By embryonic day 18.5 and postnatal day one there were very few mitotic, Ki67 immunoreactive cells (Figure 3C and D, red) although CCSP was readily detected throughout conducting airways (Figure 3C and D, green). Only terminal bronchiole-associated CCSP expressing cells coexpressed LacZ (Figure 3C and 3D, asterisks). The ciliated cell-specific marker acetylated tubulin was also detected throughout airways at embryonic day 18.5 and colocalized with X-gal staining in terminal bronchioles (data not shown). These results raised the possibility that lung developmental β-

catenin signaling regulates the transition between airway / alveolar proliferation and differentiation.

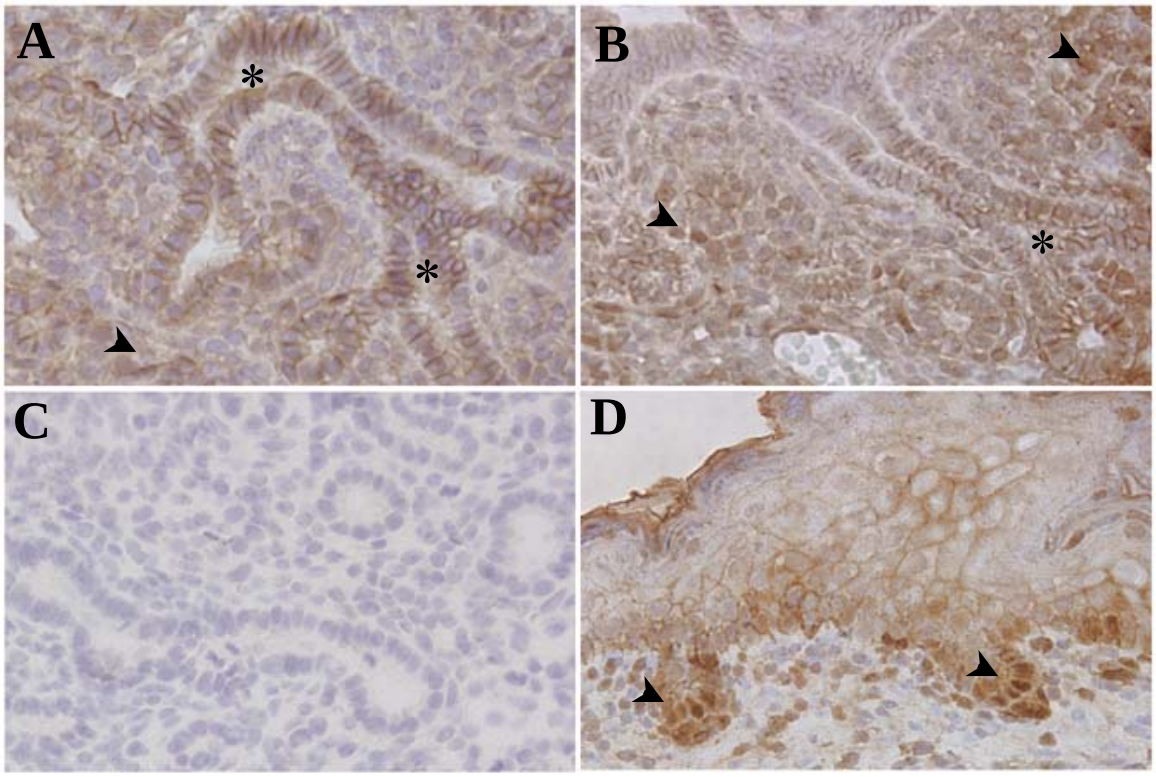

Appendix A Figure 1 Immunohistochemical localization of β-catenin during lung development.

(A) Nuclear / cytoplasmic β-catenin is sporadically detected throughout conducting airways (asterisks) and to a lesser extent within peripheral lungs (arrowheads) of embryonic stage 16.5 lungs. (B) Embryonic day 18.5 proximal airways exhibit primarily membrane-associated β-catenin with nuclear staining restricted to distal airways (asterisks) and the surrounding periphery (arrowheads). (C) Omission of β-catenin primary antibody reveals specificity of staining in A-B. (D) Developing hair follicles serve as a positive control for nuclear β-catenin (arrowheads).

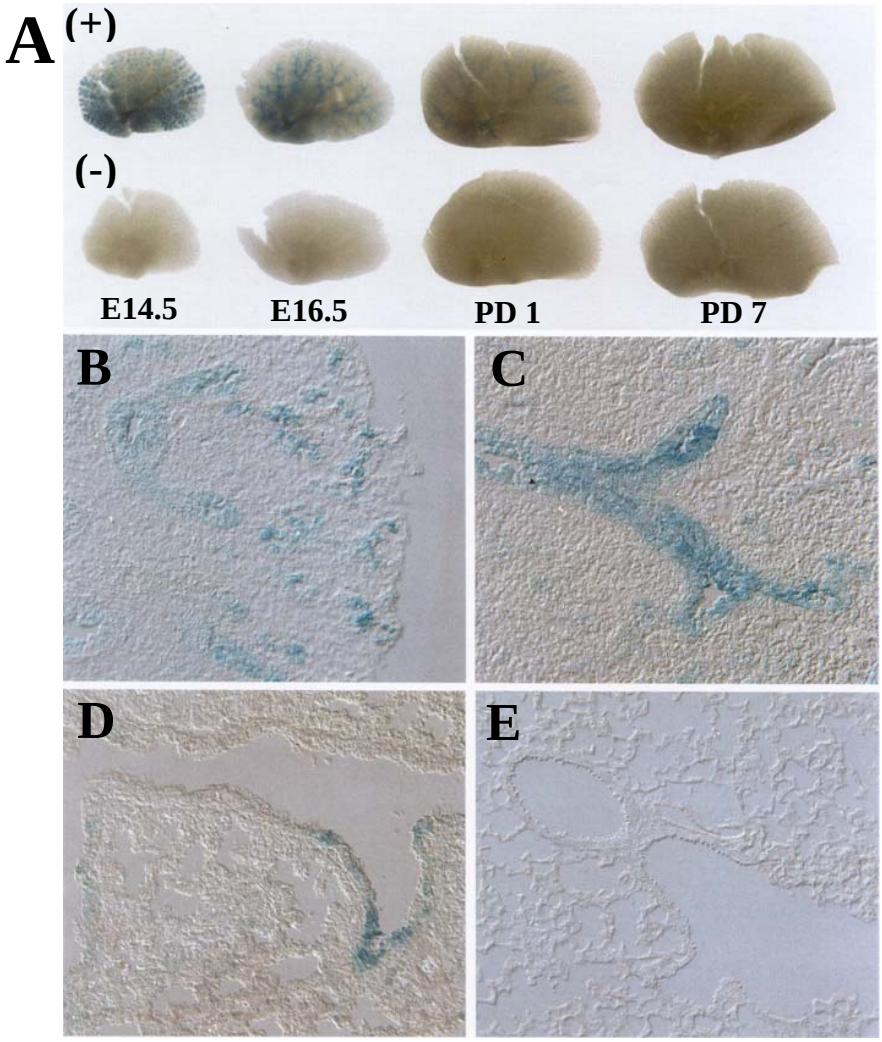

Appendix A Figure 2 . Developmental TOPgal transgene activation definitively identifies β-catenin signaling lung epithelial cells

(A) TOPgal activation / LacZ expression is detected throughout airways of stage 14.5 and 16.5 embryos by X-gal histochemistry (B,C). Expression is restricted to distal conducting airways by embryonic stage 18.5 – postnatal day 1 (D), and is not detected by postnatal day seven (E). Frozen tissue sections of 14.5 (B), 16.5 (C), postnatal day 1 (D), and postnatal day 7 (E) X-gal-stained TOPgal transgenic lungs show expression within developing airway and alveolar epithelia but not mesenchyme.

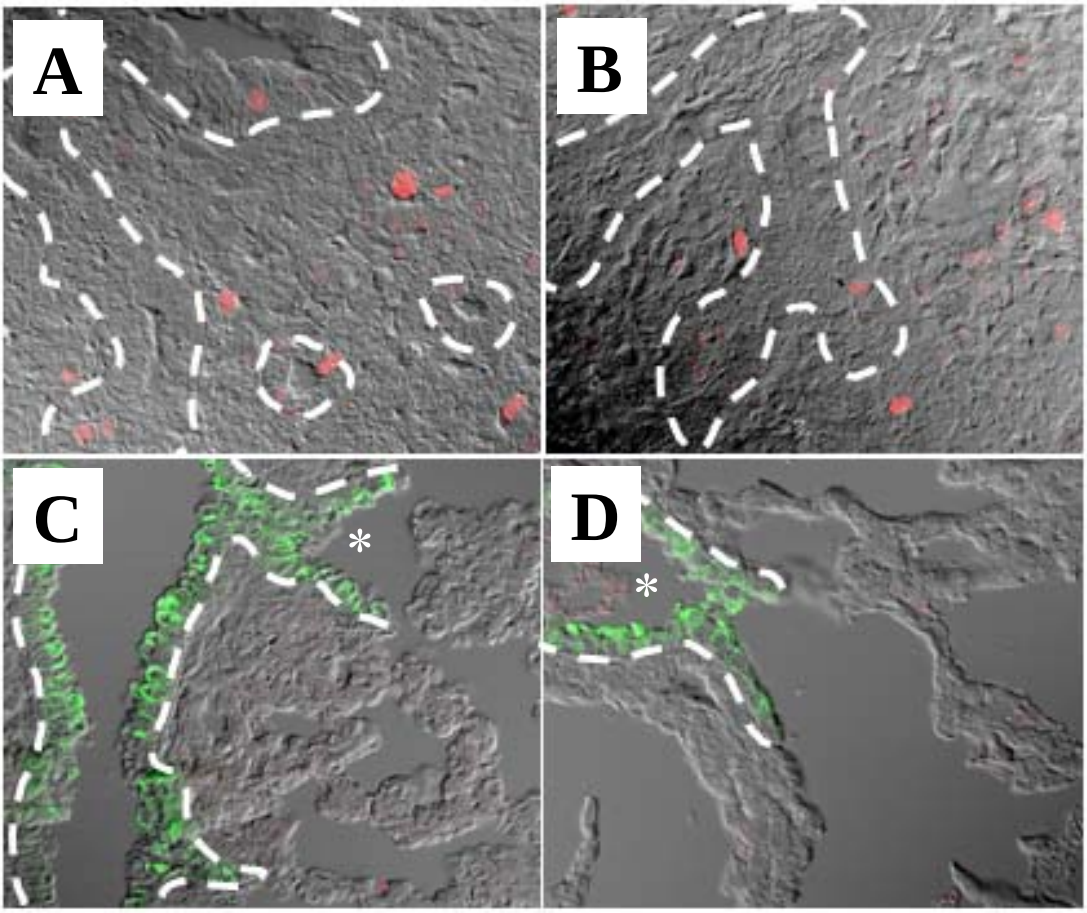

Appendix A Figure 3 Ki67 and Clara cell secretory protein expression do not colocalize with TOPgal activation in developing airways.

(A-B) Embryonic stage 14.5 – 16.5 lungs with airway-specific TOPgal activation lack CCSP expression (green) but contain numerous mitotic, Ki67 positive cells in the lung periphery (red). (C-D) Embryonic stage 18.5 and postnatal day 1 lungs express CCSP throughout conducting airways (green) but lack frequent Ki67 reactive cells (red). LacZ expression is coincident with CCSP immunoreactivity only in terminal bronchiole-associated epithelial cells (asterisks, C and D). Dashed lines in (A-D) denote the airway epithelial basement membrane.

APPENDIX B

List of Publications

Reynolds SD, **Giangreco A,** Power JH, Stripp BR. Neuroepithelial bodies of pulmonary airways serve as a reservoir of progenitor cells capable of epithelial regeneration. *Am J Pathol.* 2000 Jan; 156(1):269-278

Reynolds SD, Hong KU, **Giangreco A,** Mango GW, Guron C, Morimoto Y, Stripp BR. Conditional Clara cell ablation reveals a self-renewing progenitor function of pulmonary neuroendocrine cells. *Am J Physiol Lung Cell Mol Physiol.* 2000 Jun; 278(6): L1256-1263

Hong KU, Reynolds SD, **Giangreco A,** Hurley CM, Stripp BR. Clara cell secretory protein-expressing cells of the airway neuroepithelial body microenvironment include a label-retaining subset and are critical for epithelial renewal after progenitor cell depletion. *Am J Respir Cell Mol Biol.* 2001 Jun; 24 (6): 671-681

Pombrio JM, **Giangreco A,** Li L, Wempe MF, Anders MW, Sweet DH, Pritchard JB, Ballatori N. Mercapturic acids (N-acetylcysteine S-conjugates) as endogenous substrates for the renal organic anion transporter-1. *Mol Pharmacol.* 2001 Nov; 60 (5):1091-1099

Giangreco A, Sowden MP, Mikityansky I, Smith HC. Ethanol stimulates apolipoprotein B mRNA editing in the absence of de novo RNA or protein synthesis. *Biochem Biophys Res Commun.* 2001 Dec; 289(5):1162-1167

Giangreco A, Reynolds SD, Stripp BR. Terminal bronchioles harbor a unique airway stem cell population that localizes to the bronchoalveolar duct junction. *Am J Pathol.* 2002 Jul; 161(1) 173-182

Giangreco A, Shen H, Reynolds SD, Stripp BR. Molecular phenotype of airway side population cells. *Am J Physiol Lung Cell Mol Physiol.* 2004 Apr; 286(4) L624-630.

Reynolds SD, **Giangreco A**, Stripp BR. Transgenic mouse models of airway injury and repair. In *Lung Biology in Health and Disease.* 2004. *In press.*

Giangreco, A, Watkins, SC, Reynolds, SD, Stripp BR. Beta-catenin signaling is a component of airway renewal. *Submitted.*

Reynolds SD, **Giangreco A**, Stripp BR. Pulmonary alveolar inflammation following Clara cell ablation. *In preparation.*

Giangreco A., Teisanu, R, Reynolds, SD, Watkins, SC, and Stripp BR. Evidence for beta-catenin signaling during airway development and maturation. *In preparation.*

BIBLIOGRAPHY

1. Adriaensen, D. and D.W. Scheuermann, Neuroendocrine cells and nerves of the lung. *Anat Rec*. **236**(1): p. 70-85; discussion 85-6 1993.

2. Aita, K., M. Doi, K. Tanno, H. Oikawa, O. Myo Thaik, N. Ohashi, and S. Misawa, Quantitative analysis of pulmonary neuroendocrine cell distribution of the fetal small airways using double-labeled immunohistochemistry. *Forensic Sci Int*. **113**(1-3): p. 183-7 2000.

3. Alavanja, M.C., R.C. Brownson, J.D. Boice, Jr., and E. Hock, Preexisting lung disease and lung cancer among nonsmoking women. *Am J Epidemiol*. **136**(6): p. 623-32 1992.

4. Alonso, L. and E. Fuchs, Stem cells in the skin: waste not, Wnt not. *Genes Dev*. **17**(10): p. 1189-200 2003.

5. Alvi, A.J., H. Clayton, C. Joshi, T. Enver, A. Ashworth, M.M. Vivanco Md, T.C. Dale, and M.J. Smalley, Functional and molecular characterisation of mammary side population cells. *Breast Cancer Res*. **5**(1): p. E1 2002.

6. Andl, T., S.T. Reddy, T. Gaddapara, and S.E. Millar, WNT signals are required for the initiation of hair follicle development. *Dev Cell*. **2**(5): p. 643-53 2002.

7. Arias, A.M., New alleles of Notch draw a blueprint for multifunctionality. *Trends Genet*. **18**(4): p. 168-70 2002.

8. Asakura, A. and M.A. Rudnicki, Side population cells from diverse adult tissues are capable of in vitro hematopoietic differentiation. *Exp Hematol*. **30**(11): p. 1339-45 2002.

9. Asakura, A., P. Seale, A. Girgis-Gabardo, and M.A. Rudnicki, Myogenic specification of side population cells in skeletal muscle. *J Cell Biol*. **159**(1): p. 123-34 2002.

10. Avadhanam, K.P., C.G. Plopper, and K.E. Pinkerton, Mapping the distribution of neuroepithelial bodies of the rat lung. A whole-mount immunohistochemical approach. *Am J Pathol*. **150**(3): p. 851-9 1997.

11. Ayers, M.M. and P.K. Jeffery, Proliferation and differentiation in mammalian airway epithelium. *Eur Respir J*. **1**(1): p. 58-80 1988.

12. Barker, N., G. Huls, V. Korinek, and H. Clevers, Restricted high level expression of Tcf-4 protein in intestinal and mammary gland epithelium. *Am J Pathol*. **154**(1): p. 29-35 1999.

13. Barth, P.J., M. Wolf, and A. Ramaswamy, Distribution and number of Clara cells in the normal and disturbed development of the human fetal lung. *Pediatr Pathol*. **14**(4): p. 637-51 1994.

14. Batlle, E., J.T. Henderson, H. Beghtel, M.M. van den Born, E. Sancho, G. Huls, J. Meeldijk, J. Robertson, M. van de Wetering, T. Pawson, and H. Clevers, Beta-catenin and TCF mediate cell positioning in the intestinal epithelium by controlling the expression of EphB/ephrinB. *Cell*. **111**(2): p. 251-63 2002.

15. Bellusci, S., R. Henderson, G. Winnier, T. Oikawa, and B.L. Hogan, Evidence from normal expression and targeted misexpression that bone morphogenetic protein (Bmp-4) plays a role in mouse embryonic lung morphogenesis. *Development*. **122**(6): p. 1693-702 1996.

16. Bellusci, S., Y. Furuta, M.G. Rush, R. Henderson, G. Winnier, and B.L. Hogan, Involvement of Sonic hedgehog (Shh) in mouse embryonic lung growth and morphogenesis. *Development*. **124**(1): p. 53-63 1997.

17. Bellusci, S., J. Grindley, H. Emoto, N. Itoh, and B.L. Hogan, Fibroblast growth factor 10 (FGF10) and branching morphogenesis in the embryonic mouse lung. *Development*. **124**(23): p. 4867-78 1997.

18. Betsuyaku, T., Y. Fukuda, W.C. Parks, J.M. Shipley, and R.M. Senior, Gelatinase B is required for alveolar bronchiolization after intratracheal bleomycin. *Am J Pathol*. **157**(2): p. 525-35 2000.

19. Betsuyaku, T., G.L. Griffin, M.A. Watson, and R.M. Senior, Laser capture microdissection and real-time reverse transcriptase/ polymerase chain reaction of bronchiolar epithelium after bleomycin. *Am J Respir Cell Mol Biol*. **25**(3): p. 278-84 2001.

20. Bettenhausen, B., M. Hrabe de Angelis, D. Simon, J.L. Guenet, and A. Gossler, Transient and restricted expression during mouse embryogenesis of Dll1, a murine gene closely related to Drosophila Delta. *Development*. **121**(8): p. 2407-18 1995.

21. Bianco, P. and P.G. Robey, Stem cells in tissue engineering. *Nature*. **414**(6859): p. 118-21 2001.

22. Bin, L.H., L.D. Nielson, X. Liu, R.J. Mason, and H.B. Shu, Identification of uteroglobin-related protein 1 and macrophage scavenger receptor with collagenous structure as a lung-specific ligand-receptor pair. *J Immunol*. **171**(2): p. 924-30 2003.

23. Bonner, A.E., W.J. Lemon, and M. You, Gene expression signatures identify novel regulatory pathways during murine lung development: implications for lung tumorigenesis. *J Med Genet*. **40**(6): p. 408-17 2003.

24. Bonner, A.E., W.J. Lemon, T.R. Devereux, R.A. Lubet, and M. You, Molecular profiling of mouse lung tumors: association with tumor progression, lung development, and human lung adenocarcinomas. *Oncogene*. **23**(5): p. 1166-76 2004.

25. Borczuk, A.C., L. Gorenstein, K.L. Walter, A.A. Assaad, L. Wang, and C.A. Powell, Non-small-cell lung cancer molecular signatures recapitulate lung developmental pathways. *Am J Pathol*. **163**(5): p. 1949-60 2003.

26. Borges, M., R.I. Linnoila, H.J. van de Velde, H. Chen, B.D. Nelkin, M. Mabry, S.B. Baylin, and D.W. Ball, An achaete-scute homologue essential for neuroendocrine differentiation in the lung. *Nature*. **386**(6627): p. 852-5 1997.

27. Born, S.L., A.S. Fix, D. Caudill, and L.D. Lehman-McKeeman, Selective Clara cell injury in mouse lung following acute administration of coumarin. *Toxicol Appl Pharmacol*. **151**(1): p. 45-56 1998.

28. Borthwick, D.W., J.D. West, M.A. Keighren, J.H. Flockhart, B.A. Innes, and J.R. Dorin, Murine submucosal glands are clonally derived and show a cystic fibrosis gene-dependent distribution pattern. *Am J Respir Cell Mol Biol*. **20**(6): p. 1181-9 1999.

29. Borthwick, D.W., M. Shahbazian, Q.T. Krantz, J.R. Dorin, and S.H. Randell, Evidence for stem-cell niches in the tracheal epithelium. *Am J Respir Cell Mol Biol*. **24**(6): p. 662-70 2001.

30. Braun, K.M., C. Niemann, U.B. Jensen, J.P. Sundberg, V. Silva-Vargas, and F.M. Watt, Manipulation of stem cell proliferation and lineage commitment: visualisation of label-retaining cells in wholemounts of mouse epidermis. *Development*. **130**(21): p. 5241-55 2003.

31. Breuer, R., G. Zajicek, T.G. Christensen, E.C. Lucey, and G.L. Snider, Cell kinetics of normal adult hamster bronchial epithelium in the steady state. *Am J Respir Cell Mol Biol*. **2**(1): p. 51-8 1990.

32. Bunting, K.D., ABC transporters as phenotypic markers and functional regulators of stem cells. *Stem Cells*. **20**(1): p. 11-20 2002.

33. Busse, W., J. Elias, D. Sheppard, and S. Banks-Schlegel, Airway remodeling and repair. *Am J Respir Crit Care Med*. **160**(3): p. 1035-42 1999.

34. Cardoso, W.V., L.G. Stewart, K.E. Pinkerton, C. Ji, G.E. Hook, G. Singh, S.L. Katyal, W.M. Thurlbeck, and C.G. Plopper, Secretory product expression during Clara cell differentiation in the rabbit and rat. *Am J Physiol*. **264**(6 Pt 1): p. L543-52 1993.

35. Cassel, T.N., G. Suske, and M. Nord, C/EBP alpha and TTF-1 synergistically transactivate the Clara cell secretory protein gene. *Ann N Y Acad Sci*. **923**: p. 300-2 2000.

36. Castelo-Branco, G., J. Wagner, F.J. Rodriguez, J. Kele, K. Sousa, N. Rawal, H.A. Pasolli, E. Fuchs, J. Kitajewski, and E. Arenas, Differential regulation of midbrain dopaminergic neuron development by Wnt-1, Wnt-3a, and Wnt-5a. *Proc Natl Acad Sci U S A*. **100**(22): p. 12747-52 2003.

37. Chen, H., M.A. Biel, M.W. Borges, A. Thiagalingam, B.D. Nelkin, S.B. Baylin, and D.W. Ball, Tissue-specific expression of human achaete-scute homologue-1 in neuroendocrine tumors: transcriptional regulation by dual inhibitory regions. *Cell Growth Differ*. **8**(6): p. 677-86 1997.

38. Chen, J., H.J. Knowles, J.L. Hebert, and B.P. Hackett, Mutation of the mouse hepatocyte nuclear factor/forkhead homologue 4 gene results in an absence of cilia and random left-right asymmetry. *J Clin Invest*. **102**(6): p. 1077-82 1998.

39. Chichester, C.H., R.M. Philpot, A.J. Weir, A.R. Buckpitt, and C.G. Plopper, Characterization of the cytochrome P-450 monooxygenase system in nonciliated bronchiolar epithelial (Clara) cells isolated from mouse lung. *Am J Respir Cell Mol Biol*. **4**(2): p. 179-86 1991.

40. Chilosi, M., V. Poletti, B. Murer, M. Lestani, A. Cancellieri, L. Montagna, P. Piccoli, G. Cangi, G. Semenzato, and C. Doglioni, Abnormal re-epithelialization and lung remodeling in idiopathic pulmonary fibrosis: the role of deltaN-p63. *Lab Invest*. **82**(10): p. 1335-45 2002.

41. Chilosi, M., V. Poletti, A. Zamo, M. Lestani, L. Montagna, P. Piccoli, S. Pedron, M. Bertaso, A. Scarpa, B. Murer, A. Cancellieri, R. Maestro, G. Semenzato, and C. Doglioni, Aberrant Wnt/beta-catenin pathway activation in idiopathic pulmonary fibrosis. *Am J Pathol*. **162**(5): p. 1495-502 2003.

42. Cho, T., W. Chan, and E. Cutz, Distribution and frequency of neuro-epithelial bodies in post-natal rabbit lung: quantitative study with monoclonal antibody against serotonin. *Cell Tissue Res*. **255**(2): p. 353-62 1989.

43. Clarke, D. and J. Frisen, Differentiation potential of adult stem cells. *Curr Opin Genet Dev*. **11**(5): p. 575-80 2001.

44. Clatworthy, J.P. and V. Subramanian, Stem cells and the regulation of proliferation, differentiation and patterning in the intestinal epithelium: emerging insights from gene expression patterns, transgenic and gene ablation studies. *Mech Dev*. **101**(1-2): p. 3-9 2001.

45. Cohn, L., J.A. Elias, and G.L. Chupp, Asthma: mechanisms of disease persistence and progression. *Annu Rev Immunol*. **22**: p. 789-815 2004.

46. Cutz, E., Neuroendocrine cells of the lung. An overview of morphologic characteristics and development. *Exp Lung Res*. **3**(3-4): p. 185-208 1982.

47. Cutz, E., J.E. Gillan, and A.C. Bryan, Neuroendocrine cells in the developing human lung: morphologic and functional considerations. *Pediatr Pulmonol*. **1**(3 Suppl): p. S21-9 1985.

48. Dang, T.P., S. Eichenberger, A. Gonzalez, S. Olson, and D.P. Carbone, Constitutive activation of Notch3 inhibits terminal epithelial differentiation in lungs of transgenic mice. *Oncogene*. **22**(13): p. 1988-97 2003.

49. DasGupta, R. and E. Fuchs, Multiple roles for activated LEF/TCF transcription complexes during hair follicle development and differentiation. *Development*. **126**(20): p. 4557-68 1999.

50. DasGupta, R., H. Rhee, and E. Fuchs, A developmental conundrum: a stabilized form of beta-catenin lacking the transcriptional activation domain triggers features of hair cell fate in epidermal cells and epidermal cell fate in hair follicle cells. *J Cell Biol*. **158**(2): p. 331-44 2002.

51. Davidson, D.J., F.M. Kilanowski, S.H. Randell, D.N. Sheppard, and J.R. Dorin, A primary culture model of differentiated murine tracheal epithelium. *Am J Physiol Lung Cell Mol Physiol*. **279**(4): p. L766-78 2000.

52. de la Pompa, J.L., A. Wakeham, K.M. Correia, E. Samper, S. Brown, R.J. Aguilera, T. Nakano, T. Honjo, T.W. Mak, J. Rossant, and R.A. Conlon, Conservation of the Notch signalling pathway in mammalian neurogenesis. *Development*. **124**(6): p. 1139-48 1997.

53. DeMarini, D.M., S. Landi, D. Tian, N.M. Hanley, X. Li, F. Hu, B.C. Roop, M.J. Mass, P. Keohavong, W. Gao, M. Olivier, P. Hainaut, and J.L. Mumford, Lung tumor KRAS and TP53 mutations in nonsmokers reflect exposure to PAH-rich coal combustion emissions. *Cancer Res*. **61**(18): p. 6679-81 2001.

54. Dodge, D.E., R.B. Rucker, K.E. Pinkerton, C.J. Haselton, and C.G. Plopper, Dose-dependent tolerance to ozone. III. Elevation of intracellular Clara cell 10-kDa protein in central acini of rats exposed for 20 months. *Toxicol Appl Pharmacol*. **127**(1): p. 109-23 1994.

55. Donnelly, G.M., D.G. Haack, and C.S. Heird, Tracheal epithelium: cell kinetics and differentiation in normal rat tissue. *Cell Tissue Kinet*. **15**(2): p. 119-30 1982.

56. Dowsley, T.F., J.B. Ulreich, J.L. Bolton, S.S. Park, and P.G. Forkert, CYP2E1-dependent bioactivation of 1,1-dichloroethylene in murine lung: formation of reactive intermediates and glutathione conjugates. *Toxicol Appl Pharmacol*. **139**(1): p. 42-8 1996.

57. Duan, D., A. Sehgal, J. Yao, and J.F. Engelhardt, Lef1 transcription factor expression defines airway progenitor cell targets for in utero gene therapy of submucosal gland in cystic fibrosis. *Am J Respir Cell Mol Biol*. **18**(6): p. 750-8 1998.

58. Duan, D., Y. Yue, W. Zhou, B. Labed, T.C. Ritchie, R. Grosschedl, and J.F. Engelhardt, Submucosal gland development in the airway is controlled by lymphoid enhancer binding factor 1 (LEF1). *Development*. **126**(20): p. 4441-53 1999.

59. Duman-Scheel, M., L. Weng, S. Xin, and W. Du, Hedgehog regulates cell growth and proliferation by inducing Cyclin D and Cyclin E. *Nature*. **417**(6886): p. 299-304 2002.

60. Dupuit, F., D. Gaillard, J. Hinnrasky, E. Mongodin, S. de Bentzmann, E. Copreni, and E. Puchelle, Differentiated and functional human airway epithelium regeneration in tracheal xenografts. *Am J Physiol Lung Cell Mol Physiol*. **278**(1): p. L165-76 2000.

61. Durand, R.E. and S.M. Brown, Combination adriamycin/misonidazole toxicity in V79 spheroids. *Int J Radiat Oncol Biol Phys*. **8**(3-4): p. 603-5 1982.

62. Eastman, Q. and R. Grosschedl, Regulation of LEF-1/TCF transcription factors by Wnt and other signals. *Curr Opin Cell Biol*. **11**(2): p. 233-40 1999.

63. Eaves, C.J., Manipulating hematopoietic stem cell amplification with Wnt. *Nat Immunol*. **4**(6): p. 511-2 2003.

64. Eberhart, C.G. and P. Argani, Wnt signaling in human development: beta-catenin nuclear translocation in fetal lung, kidney, placenta, capillaries, adrenal, and cartilage. *Pediatr Dev Pathol*. **4**(4): p. 351-7 2001.

65. Elias, J.A., Z. Zhu, G. Chupp, and R.J. Homer, Airway remodeling in asthma. *J Clin Invest*. **104**(8): p. 1001-6 1999.

66. Ellisen, L.W., J. Bird, D.C. West, A.L. Soreng, T.C. Reynolds, S.D. Smith, and J. Sklar, TAN-1, the human homolog of the Drosophila notch gene, is broken by chromosomal translocations in T lymphoblastic neoplasms. *Cell*. **66**(4): p. 649-61 1991.

67. Emmelin, A., L. Nystrom, and S. Wall, Diesel exhaust exposure and smoking: a case-referent study of lung cancer among Swedish dock workers. *Epidemiology*. **4**(3): p. 237-44 1993.

68. Engelhardt, J.F., E.D. Allen, and J.M. Wilson, Reconstitution of tracheal grafts with a genetically modified epithelium. *Proc Natl Acad Sci U S A*. **88**(24): p. 11192-6 1991.

69. Engelhardt, J.F., J.R. Yankaskas, S.A. Ernst, Y. Yang, C.R. Marino, R.C. Boucher, J.A. Cohn, and J.M. Wilson, Submucosal glands are the predominant site of CFTR expression in the human bronchus. *Nat Genet*. **2**(3): p. 240-8 1992.

70. Engelhardt, J.F., H. Schlossberg, J.R. Yankaskas, and L. Dudus, Progenitor cells of the adult human airway involved in submucosal gland development. *Development*. **121**(7): p. 2031-46 1995.

71. Engelhardt, J.F., Stem cell niches in the mouse airway. *Am J Respir Cell Mol Biol*. **24**(6): p. 649-52 2001.

72. Enver, T. and M. Greaves, Loops, lineage, and leukemia. *Cell*. **94**(1): p. 9-12 1998.
73. Erjefalt, J.S., I. Erjefalt, F. Sundler, and C.G. Persson, In vivo restitution of airway epithelium. *Cell Tissue Res*. **281**(2): p. 305-16 1995.

74. Evans, M.J. and J.D. Hackney, Cell proliferation in lungs of mice exposed to elevated concentrations of oxygen. *Aerosp Med*. **43**(6): p. 620-2 1972.

75. Evans, M.J., L.J. Cabral-Anderson, and G. Freeman, Effects of NO2 on the lungs of aging rats. II. Cell proliferation. *Exp Mol Pathol*. **27**(3): p. 366-76 1977.

76. Evans, M.J., L.J. Cabral-Anderson, and G. Freeman, Role of the Clara cell in renewal of the bronchiolar epithelium. *Lab Invest*. **38**(6): p. 648-53 1978.

77. Evans, M.J., N.P. Dekker, L.J. Cabral-Anderson, and G. Freeman, Quantitation of damage to the alveolar epithelium by means of type 2 cell proliferation. *Am Rev Respir Dis*. **118**(4): p. 787-90 1978.

78. Evans, M.J., S.G. Shami, L.J. Cabral-Anderson, and N.P. Dekker, Role of nonciliated cells in renewal of the bronchial epithelium of rats exposed to NO2. *Am J Pathol*. **123**(1): p. 126-33 1986.

79. Evans, M.J., S.G. Shami, and L.A. Martinez, Enhanced proliferation of pulmonary alveolar macrophages after carbon instillation in mice depleted of blood monocytes by strontium-89. *Lab Invest*. **54**(2): p. 154-9 1986.

80. Evans, M.J., R.A. Cox, S.G. Shami, and C.G. Plopper, Junctional adhesion mechanisms in airway basal cells. *Am J Respir Cell Mol Biol*. **3**(4): p. 341-7 1990.

81. Evans, M.J., L.S. Van Winkle, M.V. Fanucchi, and C.G. Plopper, Cellular and molecular characteristics of basal cells in airway epithelium. *Exp Lung Res*. **27**(5): p. 401-15 2001.

82. Evarts, R.P., P. Nagy, H. Nakatsukasa, E. Marsden, and S.S. Thorgeirsson, In vivo differentiation of rat liver oval cells into hepatocytes. *Cancer Res*. **49**(6): p. 1541-7 1989.

83. Fanucchi, M.V., A.R. Buckpitt, M.E. Murphy, and C.G. Plopper, Naphthalene cytotoxicity of differentiating Clara cells in neonatal mice. *Toxicol Appl Pharmacol*. **144**(1): p. 96-104 1997.

84. Fanucchi, M.V., A.R. Buckpitt, M.E. Murphy, D.H. Storms, B.D. Hammock, and C.G. Plopper, Development of phase II xenobiotic metabolizing enzymes in differentiating murine clara cells. *Toxicol Appl Pharmacol*. **168**(3): p. 253-67 2000.

85. Fitzgerald, K., A. Harrington, and P. Leder, Ras pathway signals are required for notch-mediated oncogenesis. *Oncogene*. **19**(37): p. 4191-8 2000.

86. Forkert, P.G., CYP2E1 is preferentially expressed in Clara cells of murine lung: localization by in situ hybridization and immunohistochemical methods. *Am J Respir Cell Mol Biol*. **12**(6): p. 589-96 1995.

87. Forkert, P.G., T.F. Dowsley, R.P. Lee, J.Y. Hong, and J.B. Ulreich, Differential formation of 1,1-dichloroethylene-metabolites in the lungs of adult and weanling male and female mice: correlation with severities of bronchiolar cytotoxicity. *J Pharmacol Exp Ther*. **279**(3): p. 1484-90 1996.

88. Forkert, P.G., Conjugation of glutathione with the reactive metabolites of 1, 1-dichloroethylene in murine lung and liver. *Microsc Res Tech*. **36**(4): p. 234-42 1997.

89. Forkert, P.G., 1,1-Dichloroethylene-induced Clara cell damage is associated with in situ formation of the reactive epoxide. Immunohistochemical detection of its glutathione conjugate. *Am J Respir Cell Mol Biol*. **20**(6): p. 1310-8 1999.

90. Forkert, P.G., S.M. Boyd, and J.B. Ulreich, Pulmonary bioactivation of 1,1-dichloroethylene is associated with CYP2E1 levels in A/J, CD-1, and C57BL/6 mice. *J Pharmacol Exp Ther*. **297**(3): p. 1193-200 2001.

91. Franklin, W.A., A.F. Gazdar, J. Haney, Wistuba, II, F.G. La Rosa, T. Kennedy, D.M. Ritchey, and Y.E. Miller, Widely dispersed p53 mutation in respiratory epithelium. A novel mechanism for field carcinogenesis. *J Clin Invest*. **100**(8): p. 2133-7 1997.

92. Fried, J., J. Doblin, S. Takamoto, A. Perez, H. Hansen, and B. Clarkson, Effects of Hoechst 33342 on survival and growth of two tumor cell lines and on hematopoietically normal bone marrow cells. *Cytometry*. **3**(1): p. 42-7 1982.

93. Frye, M., C. Gardner, E.R. Li, I. Arnold, and F.M. Watt, Evidence that Myc activation depletes the epidermal stem cell compartment by modulating adhesive interactions with the local microenvironment. *Development*. **130**(12): p. 2793-808 2003.

94. Gat, U., R. DasGupta, L. Degenstein, and E. Fuchs, De Novo hair follicle morphogenesis and hair tumors in mice expressing a truncated beta-catenin in skin. *Cell*. **95**(5): p. 605-14 1998.

95. Giangreco, A., S.D. Reynolds, and B.R. Stripp, Terminal Bronchioles Harbor a Unique Airway Stem Cell Population That Localizes to the Bronchoalveolar Duct Junction. *Am J Pathol*. **161**(1): p. 173-182 2002.

96. Giangreco, A., H. Shen, S.D. Reynolds, and B.R. Stripp, Molecular phenotype of airway side population cells. *Am J Physiol Lung Cell Mol Physiol*. **286**(4): p. L624-30 2004.

97. Goodell, M.A., K. Brose, G. Paradis, A.S. Conner, and R.C. Mulligan, Isolation and functional properties of murine hematopoietic stem cells that are replicating in vivo. *J Exp Med*. **183**(4): p. 1797-806 1996.

98. Goodell, M.A., M. Rosenzweig, H. Kim, D.F. Marks, M. DeMaria, G. Paradis, S.A. Grupp, C.A. Sieff, R.C. Mulligan, and R.P. Johnson, Dye efflux studies suggest that hematopoietic stem cells expressing low or undetectable levels of CD34 antigen exist in multiple species. *Nat Med*. **3**(12): p. 1337-45 1997.

99. Gottardi, C.J. and B.M. Gumbiner, Adhesion signaling: how beta-catenin interacts with its partners. *Curr Biol*. **11**(19): p. R792-4 2001.

100. Gould, V.E., R.I. Linnoila, V.A. Memoli, and W.H. Warren, Neuroendocrine cells and neuroendocrine neoplasms of the lung. *Pathol Annu*. **18 Pt 1**: p. 287-330 1983.

101. Hackett, B.P., S.L. Brody, M. Liang, I.D. Zeitz, L.A. Bruns, and J.D. Gitlin, Primary structure of hepatocyte nuclear factor/forkhead homologue 4 and characterization of gene expression in the developing respiratory and reproductive epithelium. *Proc Natl Acad Sci U S A*. **92**(10): p. 4249-53 1995.

102. Hatsell, S., T. Rowlands, M. Hiremath, and P. Cowin, Beta-catenin and Tcfs in mammary development and cancer. *J Mammary Gland Biol Neoplasia*. **8**(2): p. 145-58 2003.

103. Hayashi, T., A. Ishii, S. Nakai, and K. Hasegawa, Ultrastructure of goblet-cell metaplasia from Clara cell in the allergic asthmatic airway inflammation in a mouse model of asthma in vivo. *Virchows Arch*. **444**(1): p. 66-73 2004.

104. Hermans, C. and A. Bernard, Lung epithelium-specific proteins: characteristics and potential applications as markers. *Am J Respir Crit Care Med*. **159**(2): p. 646-78 1999.

105. Hogan, B.L., J. Grindley, S. Bellusci, N.R. Dunn, H. Emoto, and N. Itoh, Branching morphogenesis of the lung: new models for a classical problem. *Cold Spring Harb Symp Quant Biol*. **62**: p. 249-56 1997.

106. Hogan, B.L. and J.M. Yingling, Epithelial/mesenchymal interactions and branching morphogenesis of the lung. *Curr Opin Genet Dev*. **8**(4): p. 481-6 1998.

107. Hogan, B.L., Morphogenesis. *Cell*. **96**(2): p. 225-33 1999.

108. Holgate, S.T., Epithelial damage and response. *Clin Exp Allergy*. **30 Suppl 1**: p. 37-41 2000.

109. Holnthoner, W., M. Pillinger, M. Groger, K. Wolff, A.W. Ashton, C. Albanese, P. Neumeister, R.G. Pestell, and P. Petzelbauer, Fibroblast growth factor-2 induces Lef/Tcf-dependent transcription in human endothelial cells. *J Biol Chem*. **277**(48): p. 45847-53 2002.

110. Hong, K.U., S.D. Reynolds, A. Giangreco, C.M. Hurley, and B.R. Stripp, Clara cell secretory protein-expressing cells of the airway neuroepithelial body microenvironment include a label-retaining subset and are critical for epithelial renewal after progenitor cell depletion. *Am J Respir Cell Mol Biol*. **24**(6): p. 671-81 2001.

111. Hong, K.U., S.D. Reynolds, S. Watkins, E. Fuchs, and B.R. Stripp, Basal cells are a multipotent progenitor capable of renewing the bronchial epithelium. *Am J Pathol*. **164**(2): p. 577-88 2004.

112. Hong, K.U., S.D. Reynolds, S. Watkins, E. Fuchs, and B.R. Stripp, In vivo differentiation potential of tracheal basal cells: evidence for multipotent and unipotent subpopulations. *Am J Physiol Lung Cell Mol Physiol*. **286**(4): p. L643-9 2004.

113. Huelsken, J., R. Vogel, B. Erdmann, G. Cotsarelis, and W. Birchmeier, beta-Catenin controls hair follicle morphogenesis and stem cell differentiation in the skin. *Cell*. **105**(4): p. 533-45 2001.

114. Hyatt, B.A., X. Shangguan, and J.M. Shannon, BMP4 modulates fibroblast growth factor-mediated induction of proximal and distal lung differentiation in mouse embryonic tracheal epithelium in mesenchyme-free culture. *Dev Dyn*. **225**(2): p. 153-65 2002.

115. Hyde, D.M., C.G. Plopper, P.H. Kass, and J.L. Alley, Estimation of cell numbers and volumes of bronchiolar epithelium during rabbit lung maturation. *Am J Anat*. **167**(3): p. 359-70 1983.

116. Inayama, Y., G.E. Hook, A.R. Brody, G.S. Cameron, A.M. Jetten, L.B. Gilmore, T. Gray, and P. Nettesheim, The differentiation potential of tracheal basal cells. *Lab Invest*. **58**(6): p. 706-17 1988.

117. Inayama, Y., G.E. Hook, A.R. Brody, A.M. Jetten, T. Gray, J. Mahler, and P. Nettesheim, In vitro and in vivo growth and differentiation of clones of tracheal basal cells. *Am J Pathol*. **134**(3): p. 539-49 1989.

118. Israsena, N., M. Hu, W. Fu, L. Kan, and J.A. Kessler, The presence of FGF2 signaling determines whether beta-catenin exerts effects on proliferation or neuronal differentiation of neural stem cells. *Dev Biol*. **268**(1): p. 220-31 2004.

119. Ito, T., H. Kitamura, Y. Inayama, and M. Kanisawa, 4-Nitroquinoline 1-oxide-induced pulmonary endocrine cell hyperplasia in Syrian golden hamster. *Jpn J Cancer Res*. **77**(5): p. 441-5 1986.

120. Ito, T., H. Nogawa, N. Udaka, H. Kitamura, and M. Kanisawa, Development of pulmonary neuroendocrine cells of fetal hamster in explant culture. *Lab Invest*. **77**(5): p. 449-57 1997.

121. Ito, T., Differentiation and proliferation of pulmonary neuroendocrine cells. *Prog Histochem Cytochem*. **34**(4): p. 247-322 1999.

122. Ito, T., N. Udaka, T. Yazawa, K. Okudela, H. Hayashi, T. Sudo, F. Guillemot, R. Kageyama, and H. Kitamura, Basic helix-loop-helix transcription factors regulate the neuroendocrine differentiation of fetal mouse pulmonary epithelium. *Development*. **127**(18): p. 3913-21 2000.

123. Jackson, E.L., N. Willis, K. Mercer, R.T. Bronson, D. Crowley, R. Montoya, T. Jacks, and D.A. Tuveson, Analysis of lung tumor initiation and progression using conditional expression of oncogenic K-ras. *Genes Dev*. **15**(24): p. 3243-8 2001.

124. Jackson, K.A., T. Mi, and M.A. Goodell, Hematopoietic potential of stem cells isolated from murine skeletal muscle. *Proc Natl Acad Sci U S A*. **96**(25): p. 14482-6 1999.

125. Jamora, C., R. DasGupta, P. Kocieniewski, and E. Fuchs, Links between signal transduction, transcription and adhesion in epithelial bud development. *Nature*. **422**(6929): p. 317-22 2003.

126. Jensen, U.B., S. Lowell, and F.M. Watt, The spatial relationship between stem cells and their progeny in the basal layer of human epidermis: a new view based on whole-mount labelling and lineage analysis. *Development*. **126**(11): p. 2409-18 1999.

127. Jensen-Taubman, S.M., S.M. Steinberg, and R.I. Linnoila, Bronchiolization of the alveoli in lung cancer: pathology, patterns of differentiation and oncogene expression. *Int J Cancer*. **75**(4): p. 489-96 1998.

128. Jho, E.H., T. Zhang, C. Domon, C.K. Joo, J.N. Freund, and F. Costantini, Wnt/beta-catenin/Tcf signaling induces the transcription of Axin2, a negative regulator of the signaling pathway. *Mol Cell Biol*. **22**(4): p. 1172-83 2002.

129. Ji, C.M., C.G. Plopper, and K.E. Pinkerton, Clara cell heterogeneity in differentiation: correlation with proliferation, ultrastructural composition, and cell position in the rat bronchiole. *Am J Respir Cell Mol Biol*. **13**(2): p. 144-51 1995.

130. Ji, C.M., F.H. Royce, U. Truong, C.G. Plopper, G. Singh, and K.E. Pinkerton, Maternal exposure to environmental tobacco smoke alters Clara cell secretory protein expression in fetal rat lung. *Am J Physiol*. **275**(5 Pt 1): p. L870-6 1998.

131. Johnston, C.J., B.R. Stripp, B. Piedbeouf, T.W. Wright, G.W. Mango, C.K. Reed, and J.N. Finkelstein, Inflammatory and epithelial responses in mouse strains that differ in sensitivity to hyperoxic injury. *Exp Lung Res*. **24**(2): p. 189-202 1998.

132. Johnston, C.J., J.N. Finkelstein, G. Oberdorster, S.D. Reynolds, and B.R. Stripp, Clara cell secretory protein-deficient mice differ from wild-type mice in inflammatory chemokine expression to oxygen and ozone, but not to endotoxin. *Exp Lung Res*. **25**(1): p. 7-21 1999.

133. Johnston, C.J., B.R. Stripp, S.D. Reynolds, N.E. Avissar, C.K. Reed, and J.N. Finkelstein, Inflammatory and antioxidant gene expression in C57BL/6J mice after lethal and sublethal ozone exposures. *Exp Lung Res*. **25**(1): p. 81-97 1999.

134. Johnston, D., D. Hatzis, and M.E. Sunday, Expression of v-Ha-ras driven by the calcitonin/calcitonin gene-related peptide promoter: a novel transgenic murine model for medullary thyroid carcinoma. *Oncogene*. **16**(2): p. 167-77 1998.

135. Kiechle, F.L. and X. Zhang, Apoptosis: biochemical aspects and clinical implications. *Clin Chim Acta*. **326**(1-2): p. 27-45 2002.

136. Kiger, A.A., D.L. Jones, C. Schulz, M.B. Rogers, and M.T. Fuller, Stem cell self-renewal specified by JAK-STAT activation in response to a support cell cue. *Science*. **294**(5551): p. 2542-5 2001.

137. Kim, J.S., H. Crooks, T. Dracheva, T.G. Nishanian, B. Singh, J. Jen, and T. Waldman, Oncogenic beta-catenin is required for bone morphogenetic protein 4 expression in human cancer cells. *Cancer Res*. **62**(10): p. 2744-8 2002.

138. Kim, M., H. Turnquist, J. Jackson, M. Sgagias, Y. Yan, M. Gong, M. Dean, J.G. Sharp, and K. Cowan, The multidrug resistance transporter ABCG2 (breast cancer resistance protein 1) effluxes Hoechst 33342 and is overexpressed in hematopoietic stem cells. *Clin Cancer Res*. **8**(1): p. 22-8 2002.

139. Kim, S., J.J. Shim, P.R. Burgel, I.F. Ueki, T. Dao-Pick, D.C. Tam, and J.A. Nadel, IL-13-induced Clara cell secretory protein expression in airway epithelium: role of EGFR signaling pathway. *Am J Physiol Lung Cell Mol Physiol*. **283**(1): p. L67-75 2002.

140. Knight, D.A. and S.T. Holgate, The airway epithelium: structural and functional properties in health and disease. *Respirology*. **8**(4): p. 432-46 2003.

141. Korinek, V., N. Barker, P. Moerer, E. van Donselaar, G. Huls, P.J. Peters, and H. Clevers, Depletion of epithelial stem-cell compartments in the small intestine of mice lacking Tcf-4. *Nat Genet*. **19**(4): p. 379-83 1998.

142. Kuhnert, F., C.R. Davis, H.T. Wang, P. Chu, M. Lee, J. Yuan, R. Nusse, and C.J. Kuo, Essential requirement for Wnt signaling in proliferation of adult small intestine and colon revealed by adenoviral expression of Dickkopf-1. *Proc Natl Acad Sci U S A*. **101**(1): p. 266-71 2004.

143. Lawson, G.W., L.S. Van Winkle, E. Toskala, R.M. Senior, W.C. Parks, and C.G. Plopper, Mouse strain modulates the role of the ciliated cell in acute tracheobronchial airway injury-distal airways. *Am J Pathol*. **160**(1): p. 315-27 2002.

144. Lechner, A., C.A. Leech, E.J. Abraham, A.L. Nolan, and J.F. Habener, Nestin-positive progenitor cells derived from adult human pancreatic islets of Langerhans contain side population (SP) cells defined by expression of the ABCG2 (BCRP1) ATP-binding cassette transporter. *Biochem Biophys Res Commun*. **293**(2): p. 670-4 2002.

145. Lee, C., K.C. Watt, A.M. Chang, C.G. Plopper, A.R. Buckpitt, and K.E. Pinkerton, Site-selective differences in cytochrome P450 isoform activities. Comparison of expression in rat and rhesus monkey lung and induction in rats. *Drug Metab Dispos*. **26**(5): p. 396-400 1998.

146. Lee, C.G., R.J. Homer, L. Cohn, H. Link, S. Jung, J.E. Craft, B.S. Graham, T.R. Johnson, and J.A. Elias, Transgenic overexpression of interleukin (IL)-10 in the lung causes mucus metaplasia, tissue inflammation, and airway remodeling via IL-13-dependent and -independent pathways. *J Biol Chem*. **277**(38): p. 35466-74 2002.

147. Lee, R.P. and P.G. Forkert, Pulmonary CYP2E1 bioactivates 1,1-dichloroethylene in male and female mice. *J Pharmacol Exp Ther*. **273**(1): p. 561-7 1995.

148. Lehrer, M.S., T.T. Sun, and R.M. Lavker, Strategies of epithelial repair: modulation of stem cell and transit amplifying cell proliferation. *J Cell Sci*. **111 (Pt 19)**: p. 2867-75 1998.

149. Li, C., J. Xiao, K. Hormi, Z. Borok, and P. Minoo, Wnt5a participates in distal lung morphogenesis. *Dev Biol*. **248**(1): p. 68-81 2002.

150. Lickert, H., C. Domon, G. Huls, C. Wehrle, I. Duluc, H. Clevers, B.I. Meyer, J.N. Freund, and R. Kemler, Wnt/(beta)-catenin signaling regulates the expression of the homeobox gene Cdx1 in embryonic intestine. *Development*. **127**(17): p. 3805-13 2000.

151. Linnoila, R.I., A. Sahu, M. Miki, D.W. Ball, and F.J. DeMayo, Morphometric analysis of CC10-hASH1 transgenic mouse lung: a model for bronchiolization of alveoli and neuroendocrine carcinoma. *Exp Lung Res*. **26**(8): p. 595-615 2000.

152. Linnoila, R.I., B. Zhao, J.L. DeMayo, B.D. Nelkin, S.B. Baylin, F.J. DeMayo, and D.W. Ball, Constitutive achaete-scute homologue-1 promotes airway dysplasia and lung neuroendocrine tumors in transgenic mice. *Cancer Res*. **60**(15): p. 4005-9 2000.

153. Liou, G.I., S. Matragoon, S. Samuel, M.A. Behzadian, N.T. Tsai, X. Gu, P. Roon, D.M. Hunt, R.C. Hunt, R.B. Caldwell, and D.M. Marcus, MAP kinase and beta-catenin signaling in HGF induced RPE migration. *Mol Vis*. **8**: p. 483-93 2002.

154. Liu, J.Y., P. Nettesheim, and S.H. Randell, Growth and differentiation of tracheal epithelial progenitor cells. *Am J Physiol*. **266**(3 Pt 1): p. L296-307 1994.

155. Liu, Y., S. Lyle, Z. Yang, and G. Cotsarelis, Keratin 15 promoter targets putative epithelial stem cells in the hair follicle bulge. *J Invest Dermatol*. **121**(5): p. 963-8 2003.

156. Look, D.C., M.J. Walter, M.R. Williamson, L. Pang, Y. You, J.N. Sreshta, J.E. Johnson, D.S. Zander, and S.L. Brody, Effects of paramyxoviral infection on airway epithelial cell Foxj1 expression, ciliogenesis, and mucociliary function. *Am J Pathol*. **159**(6): p. 2055-69 2001.

157. Love, R., Beta-catenin, brains, and beyond. *Lancet Neurol*. **1**(5): p. 272 2002.

158. Lowell, S., P. Jones, I. Le Roux, J. Dunne, and F.M. Watt, Stimulation of human epidermal differentiation by delta-notch signalling at the boundaries of stem-cell clusters. *Curr Biol*. **10**(9): p. 491-500 2000.

159. Malik, T.H. and R.A. Shivdasani, Structure and expression of a novel frizzled gene isolated from the developing mouse gut. *Biochem J*. **349 Pt 3**: p. 829-34 2000.

160. Mariassy, A.T. and C.G. Plopper, Tracheobronchial epithelium of the sheep: I. Quantitative light-microscopic study of epithelial cell abundance, and distribution. *Anat Rec*. **205**(3): p. 263-75 1983.

161. Massaro, G.D., G. Singh, R. Mason, C.G. Plopper, A.M. Malkinson, and D.B. Gail, Biology of the Clara cell. *Am J Physiol*. **266**(1 Pt 1): p. L101-6 1994.

162. McKinney-Freeman, S.L., K.A. Jackson, F.D. Camargo, G. Ferrari, F. Mavilio, and M.A. Goodell, Muscle-derived hematopoietic stem cells are hematopoietic in origin. *Proc Natl Acad Sci U S A*. **99**(3): p. 1341-6 2002.

163. Mercer, R.R., M.L. Russell, V.L. Roggli, and J.D. Crapo, Cell number and distribution in human and rat airways. *Am J Respir Cell Mol Biol*. **10**(6): p. 613-24 1994.

164. Merrill, B.J., H.A. Pasolli, L. Polak, M. Rendl, M.J. Garcia-Garcia, K.V. Anderson, and E. Fuchs, Tcf3: a transcriptional regulator of axis induction in the early embryo. *Development*. **131**(2): p. 263-74 2004.

165. Miele, L., E. Cordella-Miele, G. Mantile, A. Peri, and A.B. Mukherjee, Uteroglobin and uteroglobin-like proteins: the uteroglobin family of proteins. *J Endocrinol Invest*. **17**(8): p. 679-92 1994.

166. Miller, L.A., S.E. Wert, and J.A. Whitsett, Immunolocalization of sonic hedgehog (Shh) in developing mouse lung. *J Histochem Cytochem*. **49**(12): p. 1593-604 2001.

167. Min, H., D.M. Danilenko, S.A. Scully, B. Bolon, B.D. Ring, J.E. Tarpley, M. DeRose, and W.S. Simonet, Fgf-10 is required for both limb and lung development and exhibits striking functional similarity to Drosophila branchless. *Genes Dev*. **12**(20): p. 3156-61 1998.

168. Minna, J.D., J.M. Kurie, and T. Jacks, A big step in the study of small cell lung cancer. *Cancer Cell*. **4**(3): p. 163-6 2003.

169. Moles, J.P. and F.M. Watt, The epidermal stem cell compartment: variation in expression levels of E-cadherin and catenins within the basal layer of human epidermis. *J Histochem Cytochem*. **45**(6): p. 867-74 1997.

170. Moon, R.T., B. Bowerman, M. Boutros, and N. Perrimon, The promise and perils of Wnt signaling through beta-catenin. *Science*. **296**(5573): p. 1644-6 2002.

171. Morrisey, E.E., Wnt signaling and pulmonary fibrosis. *Am J Pathol*. **162**(5): p. 1393-7 2003.

172. Mosca, L., M. Barbareschi, M.F. Mauri, J. Munguia-Barrera, B. Frigo, M. Muscara, L. Valentini, and C. Mariscotti, Neuroendocrine lung structures and tumours: immunohistochemical study by specific markers. *Histol Histopathol*. **3**(4): p. 367-76 1988.

173. Mucenski, M.L., S.E. Wert, J.M. Nation, D.E. Loudy, J. Huelsken, W. Birchmeier, E.E. Morrisey, and J.A. Whitsett, beta-Catenin is required for specification of proximal/distal cell fate during lung morphogenesis. *J Biol Chem*. **278**(41): p. 40231-8 2003.

174. Mulloy, K.B., D.S. James, K. Mohs, and M. Kornfeld, Lung cancer in a nonsmoking underground uranium miner. *Environ Health Perspect*. **109**(3): p. 305-9 2001.

175. Nacht, M., T. Dracheva, Y. Gao, T. Fujii, Y. Chen, A. Player, V. Akmaev, B. Cook, M. Dufault, M. Zhang, W. Zhang, M. Guo, J. Curran, S. Han, D. Sidransky, K. Buetow, S.L. Madden, and J. Jen, Molecular characteristics of non-small cell lung cancer. *Proc Natl Acad Sci U S A*. **98**(26): p. 15203-8 2001.

176. Niemann, C., D.M. Owens, J. Hulsken, W. Birchmeier, and F.M. Watt, Expression of DeltaNLef1 in mouse epidermis results in differentiation of hair follicles into squamous epidermal cysts and formation of skin tumours. *Development*. **129**(1): p. 95-109 2002.

177. Niemann, C. and F.M. Watt, Designer skin: lineage commitment in postnatal epidermis. *Trends Cell Biol*. **12**(4): p. 185-92 2002.

178. Niemann, C., A.B. Unden, S. Lyle, C. Zouboulis Ch, R. Toftgard, and F.M. Watt, Indian hedgehog and beta-catenin signaling: role in the sebaceous lineage of normal and neoplastic mammalian epidermis. *Proc Natl Acad Sci U S A*. **100 Suppl 1**: p. 11873-80 2003.

179. Nishimura, E.K., S.A. Jordan, H. Oshima, H. Yoshida, M. Osawa, M. Moriyama, I.J. Jackson, Y. Barrandon, Y. Miyachi, and S. Nishikawa, Dominant role of the niche in melanocyte stem-cell fate determination. *Nature*. **416**(6883): p. 854-60 2002.

180. Nord, M., J.A. Gustafsson, and J. Lund, Calcium-dependent binding of uteroglobin (PCB-BP/CCSP) to negatively charged phospholipid liposomes. *FEBS Lett*. **374**(3): p. 403-6 1995.

181. Nord, M., M. Lag, T.N. Cassel, M. Randmark, R. Becher, H.J. Barnes, P.E. Schwarze, J.A. Gustafsson, and J. Lund, Regulation of CCSP (PCB-BP/uteroglobin) expression in primary cultures of lung cells: involvement of C/EBP. *DNA Cell Biol*. **17**(5): p. 481-92 1998.

182. Nusse, R., Wnts and Hedgehogs: lipid-modified proteins and similarities in signaling mechanisms at the cell surface. *Development*. **130**(22): p. 5297-305 2003.

183. Ohira, T., R.M. Gemmill, K. Ferguson, S. Kusy, J. Roche, E. Brambilla, C. Zeng, A. Baron, L. Bemis, P. Erickson, E. Wilder, A. Rustgi, J. Kitajewski, E. Gabrielson, R. Bremnes, W. Franklin, and H.A. Drabkin, WNT7a induces E-cadherin in lung cancer cells. *Proc Natl Acad Sci U S A*. **100**(18): p. 10429-34 2003.

184. Ohishi, K., N. Katayama, H. Shiku, B. Varnum-Finney, and I.D. Bernstein, Notch signalling in hematopoiesis. *Semin Cell Dev Biol*. **14**(2): p. 143-50 2003.

185. Oshima, H., A. Rochat, C. Kedzia, K. Kobayashi, and Y. Barrandon, Morphogenesis and renewal of hair follicles from adult multipotent stem cells. *Cell*. **104**(2): p. 233-45 2001.

186. Otto, W.R., Lung stem cells. *Int J Exp Pathol*. **78**(5): p. 291-310 1997.

187. Otto, W.R., Lung epithelial stem cells. *J Pathol*. **197**(4): p. 527-35 2002.

188. Owens, D.M. and F.M. Watt, Contribution of stem cells and differentiated cells to epidermal tumours. *Nat Rev Cancer*. **3**(6): p. 444-51 2003.

189. Pack, R.J., L.H. Al-Ugaily, G. Morris, and J.G. Widdicombe, The distribution and structure of cells in the tracheal epithelium of the mouse. *Cell Tissue Res*. **208**(1): p. 65-84 1980.

190. Panin, V.M. and K.D. Irvine, Modulators of Notch signaling. *Semin Cell Dev Biol*. **9**(6): p. 609-17 1998.

191. Pardal, R., M.F. Clarke, and S.J. Morrison, Applying the principles of stem-cell biology to cancer. *Nat Rev Cancer*. **3**(12): p. 895-902 2003.

192. Pasca di Magliano, M. and M. Hebrok, Hedgehog signalling in cancer formation and maintenance. *Nat Rev Cancer*. **3**(12): p. 903-11 2003.

193. Peake, J.L., S.D. Reynolds, B.R. Stripp, K.E. Stephens, and K.E. Pinkerton, Alteration of pulmonary neuroendocrine cells during epithelial repair of naphthalene-induced airway injury. *Am J Pathol*. **156**(1): p. 279-86 2000.

194. Pear, W.S., J.C. Aster, M.L. Scott, R.P. Hasserjian, B. Soffer, J. Sklar, and D. Baltimore, Exclusive development of T cell neoplasms in mice transplanted with bone marrow expressing activated Notch alleles. *J Exp Med*. **183**(5): p. 2283-91 1996.

195. Pepicelli, C.V., P.M. Lewis, and A.P. McMahon, Sonic hedgehog regulates branching morphogenesis in the mammalian lung. *Curr Biol*. **8**(19): p. 1083-6 1998.

196. Perl, A.K. and J.A. Whitsett, Molecular mechanisms controlling lung morphogenesis. *Clin Genet*. **56**(1): p. 14-27 1999.

197. Petersen, B.E., Hepatic "stem" cells: coming full circle. *Blood Cells Mol Dis*. **27**(3): p. 590-600 2001.

198. Petersen, S., C. Heckert, J. Rudolf, K. Schluns, O.I. Tchernitsa, R. Schafer, M. Dietel, and I. Petersen, Gene expression profiling of advanced lung cancer. *Int J Cancer*. **86**(4): p. 512-7 2000.

199. Petkov, P.M., K. Kim, J. Sandhu, D.A. Shafritz, and M.D. Dabeva, Identification of differentially expressed genes in epithelial stem/progenitor cells of fetal rat liver. *Genomics*. **68**(2): p. 197-209 2000.

200. Phillips, R.L., R.E. Ernst, B. Brunk, N. Ivanova, M.A. Mahan, J.K. Deanehan, K.A. Moore, G.C. Overton, and I.R. Lemischka, The genetic program of hematopoietic stem cells. *Science*. **288**(5471): p. 1635-40 2000.

201. Pinkerton, K.E., C.G. Plopper, R.R. Mercer, V.L. Roggli, A.L. Patra, A.R. Brody, and J.D. Crapo, Airway branching patterns influence asbestos fiber location and the extent of tissue injury in the pulmonary parenchyma. *Lab Invest*. **55**(6): p. 688-95 1986.

202. Pinkerton, K.E., D.E. Dodge, J. Cederdahl-Demmler, V.J. Wong, J. Peake, C.J. Haselton, P.W. Mellick, G. Singh, and C.G. Plopper, Differentiated bronchiolar epithelium in alveolar ducts of rats exposed to ozone for 20 months. *Am J Pathol*. **142**(3): p. 947-56 1993.

203. Pinkerton, K.E., F.H. Green, C. Saiki, V. Vallyathan, C.G. Plopper, V. Gopal, D. Hung, E.B. Bahne, S.S. Lin, M.G. Menache, and M.B. Schenker, Distribution of particulate matter and tissue remodeling in the human lung. *Environ Health Perspect*. **108**(11): p. 1063-9 2000.

204. Pinto, D., A. Gregorieff, H. Begthel, and H. Clevers, Canonical Wnt signals are essential for homeostasis of the intestinal epithelium. *Genes Dev*. **17**(14): p. 1709-13 2003.

205. Plopper, C.G., L.H. Hill, and A.T. Mariassy, Ultrastructure of the nonciliated bronchiolar epithelial (Clara) cell of mammalian lung. III. A study of man with comparison of 15 mammalian species. *Exp Lung Res*. **1**(2): p. 171-80 1980.

206. Plopper, C.G., A.T. Mariassy, and L.H. Hill, Ultrastructure of the nonciliated bronchiolar epithelial (Clara) cell of mammalian lung: I. A comparison of rabbit, guinea pig, rat, hamster, and mouse. *Exp Lung Res*. **1**(2): p. 139-54 1980.

207. Plopper, C.G., A.T. Mariassy, and L.H. Hill, Ultrastructure of the nonciliated bronchiolar epithelial (Clara) cell of mammalian lung: II. A comparison of horse, steer, sheep, dog, and cat. *Exp Lung Res*. **1**(2): p. 155-69 1980.

208. Plopper, C.G., J.E. Halsebo, W.J. Berger, K.S. Sonstegard, and P. Nettesheim, Distribution of nonciliated bronchiolar epithelial (Clara) cells in intra- and extrapulmonary airways of the rabbit. *Exp Lung Res*. **5**(2): p. 79-98 1983.

209. Plopper, C.G., A.T. Mariassy, D.W. Wilson, J.L. Alley, S.J. Nishio, and P. Nettesheim, Comparison of nonciliated tracheal epithelial cells in six mammalian species: ultrastructure and population densities. *Exp Lung Res*. **5**(4): p. 281-94 1983.

210. Plopper, C.G., J. Macklin, S.J. Nishio, D.M. Hyde, and A.R. Buckpitt, Relationship of cytochrome P-450 activity to Clara cell cytotoxicity. III. Morphometric comparison of changes in the epithelial populations of terminal bronchioles and lobar bronchi in mice, hamsters, and rats after parenteral administration of naphthalene. *Lab Invest*. **67**(5): p. 553-65 1992.

211. Plopper, C.G., C. Suverkropp, D. Morin, S. Nishio, and A. Buckpitt, Relationship of cytochrome P-450 activity to Clara cell cytotoxicity. I. Histopathologic comparison of the respiratory tract of mice, rats and hamsters after parenteral administration of naphthalene. *J Pharmacol Exp Ther*. **261**(1): p. 353-63 1992.

212. Plopper, C.G., F.P. Chu, C.J. Haselton, J. Peake, J. Wu, and K.E. Pinkerton, Dose-dependent tolerance to ozone. I. Tracheobronchial epithelial reorganization in rats after 20 months' exposure. *Am J Pathol*. **144**(2): p. 404-20 1994.

213. Plopper, C.G., X. Duan, A.R. Buckpitt, and K.E. Pinkerton, Dose-dependent tolerance to ozone. IV. Site-specific elevation in antioxidant enzymes in the lungs of rats exposed for 90 days or 20 months. *Toxicol Appl Pharmacol*. **127**(1): p. 124-31 1994.

214. Plopper, C.G., G.E. Hatch, V. Wong, X. Duan, A.J. Weir, B.K. Tarkington, R.B. Devlin, S. Becker, and A.R. Buckpitt, Relationship of inhaled ozone concentration to acute tracheobronchial epithelial injury, site-specific ozone dose, and glutathione depletion in rhesus monkeys. *Am J Respir Cell Mol Biol*. **19**(3): p. 387-99 1998.

215. Plopper, C.G., A. Buckpitt, M. Evans, L. Van Winkle, M. Fanucchi, S. Smiley-Jewell, J. Lakritz, J. West, G. Lawson, R. Paige, L. Miller, and D. Hyde, Factors modulating the

epithelial response to toxicants in tracheobronchial airways. *Toxicology*. **160**(1-3): p. 173-80 2001.

216. Plopper, C.G., L.S. Van Winkle, M.V. Fanucchi, S.R. Malburg, S.J. Nishio, A. Chang, and A.R. Buckpitt, Early events in naphthalene-induced acute Clara cell toxicity. II. Comparison of glutathione depletion and histopathology by airway location. *Am J Respir Cell Mol Biol*. **24**(3): p. 272-81 2001.

217. Posthaus, H., L. Williamson, D. Baumann, R. Kemler, R. Caldelari, M.M. Suter, H. Schwarz, and E. Muller, beta-Catenin is not required for proliferation and differentiation of epidermal mouse keratinocytes. *J Cell Sci*. **115**(Pt 23): p. 4587-95 2002.

218. Potter, E., C. Bergwitz, and G. Brabant, The cadherin-catenin system: implications for growth and differentiation of endocrine tissues. *Endocr Rev*. **20**(2): p. 207-39 1999.

219. Prows, D.R., H.G. Shertzer, M.J. Daly, C.L. Sidman, and G.D. Leikauf, Genetic analysis of ozone-induced acute lung injury in sensitive and resistant strains of mice. *Nat Genet*. **17**(4): p. 471-4 1997.

220. Quesenberry, P.J. and P.S. Becker, Stem cell homing: rolling, crawling, and nesting. *Proc Natl Acad Sci U S A*. **95**(26): p. 15155-7 1998.

221. Radtke, F. and K. Raj, The role of Notch in tumorigenesis: oncogene or tumour suppressor? *Nat Rev Cancer*. **3**(10): p. 756-67 2003.

222. Reya, T., S.J. Morrison, M.F. Clarke, and I.L. Weissman, Stem cells, cancer, and cancer stem cells. *Nature*. **414**(6859): p. 105-11 2001.

223. Reya, T., A.W. Duncan, L. Ailles, J. Domen, D.C. Scherer, K. Willert, L. Hintz, R. Nusse, and I.L. Weissman, A role for Wnt signalling in self-renewal of haematopoietic stem cells. *Nature*. **423**(6938): p. 409-14 2003.

224. Reynolds, S.D., A. Giangreco, J.H. Power, and B.R. Stripp, Neuroepithelial bodies of pulmonary airways serve as a reservoir of progenitor cells capable of epithelial regeneration. *Am J Pathol*. **156**(1): p. 269-78 2000.

225. Reynolds, S.D., K.U. Hong, A. Giangreco, G.W. Mango, C. Guron, Y. Morimoto, and B.R. Stripp, Conditional clara cell ablation reveals a self-renewing progenitor function of pulmonary neuroendocrine cells. *Am J Physiol Lung Cell Mol Physiol*. **278**(6): p. L1256-63 2000.

226. Reynolds, S.D., P.R. Reynolds, G.S. Pryhuber, J.D. Finder, and B.R. Stripp, Secretoglobins SCGB3A1 and SCGB3A2 define secretory cell subsets in mouse and human airways. *Am J Respir Crit Care Med*. **166**(11): p. 1498-509 2002.

227. Rietjens, I.M., J.A. Dormans, P.J. Rombout, and L. van Bree, Qualitative and quantitative changes in cytochrome P-450-dependent xenobiotic metabolism in pulmonary microsomes and isolated Clara cell populations derived from ozone-exposed rats. *J Toxicol Environ Health*. **24**(4): p. 515-31 1988.

228. Ritchie, T.C., W. Zhou, E. McKinstry, M. Hosch, Y. Zhang, I. Nathke, and J.F. Engelhardt, Developmental expression of catenins and associated proteins during submucosal gland morphogenesis in the airway. *Exp Lung Res*. **27**(2): p. 121-41 2001.

229. Royce, F.H., L.S. Van Winkle, J. Yin, and C.G. Plopper, Comparison of regional variability in lung-specific gene expression using a novel method for RNA isolation from lung subcompartments of rats and mice. *Am J Pathol*. **148**(6): p. 1779-86 1996.

230. Saam, J.R. and J.I. Gordon, Inducible gene knockouts in the small intestinal and colonic epithelium. *J Biol Chem*. **274**(53): p. 38071-82 1999.

231. Sato, N., L. Meijer, L. Skaltsounis, P. Greengard, and A.H. Brivanlou, Maintenance of pluripotency in human and mouse embryonic stem cells through activation of Wnt signaling by a pharmacological GSK-3-specific inhibitor. *Nat Med*. **10**(1): p. 55-63 2004.

232. Sawaya, P.L., B.R. Stripp, J.A. Whitsett, and D.S. Luse, The lung-specific CC10 gene is regulated by transcription factors from the AP-1, octamer, and hepatocyte nuclear factor 3 families. *Mol Cell Biol*. **13**(7): p. 3860-71 1993.

233. Scharenberg, C.W., M.A. Harkey, and B. Torok-Storb, The ABCG2 transporter is an efficient Hoechst 33342 efflux pump and is preferentially expressed by immature human hematopoietic progenitors. *Blood*. **99**(2): p. 507-12 2002.

234. Sharpe, C., N. Lawrence, and A. Martinez Arias, Wnt signalling: a theme with nuclear variations. *Bioessays*. **23**(4): p. 311-8 2001.

235. Shimizu, T., M. Nishihara, S. Kawaguchi, and Y. Sakakura, Expression of phenotypic markers during regeneration of rat tracheal epithelium following mechanical injury. *Am J Respir Cell Mol Biol*. **11**(1): p. 85-94 1994.

236. Shu, W., H. Yang, L. Zhang, M.M. Lu, and E.E. Morrisey, Characterization of a new subfamily of winged-helix/forkhead (Fox) genes that are expressed in the lung and act as transcriptional repressors. *J Biol Chem*. **276**(29): p. 27488-97 2001.

237. Shu, W., Y.Q. Jiang, M.M. Lu, and E.E. Morrisey, Wnt7b regulates mesenchymal proliferation and vascular development in the lung. *Development*. **129**(20): p. 4831-42 2002.

238. Shultz, M.A., P.V. Choudary, and A.R. Buckpitt, Role of murine cytochrome P-450 2F2 in metabolic activation of naphthalene and metabolism of other xenobiotics. *J Pharmacol Exp Ther*. **290**(1): p. 281-8 1999.

239. Sims, D.E. and M.M. Horne, Heterogeneity of the composition and thickness of tracheal mucus in rats. *Am J Physiol*. **273**(5 Pt 1): p. L1036-41 1997.

240. Slack, J.M., Stem cells in epithelial tissues. *Science*. **287**(5457): p. 1431-3 2000.

241. Smiley-Jewell, S.M., S.J. Nishio, A.J. Weir, and C.G. Plopper, Neonatal Clara cell toxicity by 4-ipomeanol alters bronchiolar organization in adult rabbits. *Am J Physiol*. **274**(4 Pt 1): p. L485-98 1998.

242. Smiley-Jewell, S.M., F.J. Liu, A.J. Weir, and C.G. Plopper, Acute injury to differentiating Clara cells in neonatal rabbits results in age-related failure of bronchiolar epithelial repair. *Toxicol Pathol*. **28**(2): p. 267-76 2000.

243. Smiley-Jewell, S.M. and C.G. Plopper, Proliferation during early phases of bronchiolar repair in neonatal rabbits following lung injury by 4-ipomeanol. *Toxicol Appl Pharmacol*. **192**(1): p. 69-77 2003.

244. Smythe, W.R., J.P. Williams, M.J. Wheelock, K.R. Johnson, L.R. Kaiser, and S.M. Albelda, Cadherin and catenin expression in normal human bronchial epithelium and non-small cell lung cancer. *Lung Cancer*. **24**(3): p. 157-68 1999.

245. Spradling, A., D. Drummond-Barbosa, and T. Kai, Stem cells find their niche. *Nature*. **414**(6859): p. 98-104 2001.

246. Sridhar, K.S. and W.A. Raub, Jr., Present and past smoking history and other predisposing factors in 100 lung cancer patients. *Chest*. **101**(1): p. 19-25 1992.

247. Sriuranpong, V., M.W. Borges, R.K. Ravi, D.R. Arnold, B.D. Nelkin, S.B. Baylin, and D.W. Ball, Notch signaling induces cell cycle arrest in small cell lung cancer cells. *Cancer Res*. **61**(7): p. 3200-5 2001.

248. Sriuranpong, V., M.W. Borges, C.L. Strock, E.K. Nakakura, D.N. Watkins, C.M. Blaumueller, B.D. Nelkin, and D.W. Ball, Notch signaling induces rapid degradation of achaete-scute homolog 1. *Mol Cell Biol*. **22**(9): p. 3129-39 2002.

249. Stevens, T.P., J.T. McBride, J.L. Peake, K.E. Pinkerton, and B.R. Stripp, Cell proliferation contributes to PNEC hyperplasia after acute airway injury. *Am J Physiol*. **272**(3 Pt 1): p. L486-93 1997.

250. Stripp, B.R., K. Maxson, R. Mera, and G. Singh, Plasticity of airway cell proliferation and gene expression after acute naphthalene injury. *Am J Physiol*. **269**(6 Pt 1): p. L791-9 1995.

251. Stripp, B.R., J. Lund, G.W. Mango, K.C. Doyen, C. Johnston, K. Hultenby, M. Nord, and J.A. Whitsett, Clara cell secretory protein: a determinant of PCB bioaccumulation in mammals. *Am J Physiol*. **271**(4 Pt 1): p. L656-64 1996.

252. Stump, R.J., S. Ang, Y. Chen, T. von Bahr, F.J. Lovicu, K. Pinson, R.U. de Iongh, T.P. Yamaguchi, D.A. Sassoon, and J.W. McAvoy, A role for Wnt/beta-catenin signaling in lens epithelial differentiation. *Dev Biol*. **259**(1): p. 48-61 2003.

253. Summer, R., D.N. Kotton, X. Sun, B. Ma, K. Fitzsimmons, and A. Fine, SP (Side Population) Cells and Bcrp1 Expression in Lung. *Am J Physiol Lung Cell Mol Physiol*, 2003.

254. Sunday, M.E., C.G. Willett, S.A. Graham, V.I. Oreffo, R.I. Linnoila, and H. Witschi, Histochemical characterization of non-neuroendocrine tumors and neuroendocrine cell hyperplasia induced in hamster lung by 4-(methylnitrosamino)-1-(3-pyridyl)-1-butanone with or without hyperoxia. *Am J Pathol*. **147**(3): p. 740-52 1995.

255. Sunday, M.E., K.J. Haley, K. Sikorski, S.A. Graham, R.L. Emanuel, F. Zhang, Q. Mu, A. Shahsafaei, and D. Hatzis, Calcitonin driven v-Ha-ras induces multilineage pulmonary epithelial hyperplasias and neoplasms. *Oncogene*. **18**(30): p. 4336-47 1999.

256. Szabo, E., A. Goheer, H. Witschi, and R.I. Linnoila, Overexpression of CC10 modifies neoplastic potential in lung cancer cells. *Cell Growth Differ*. **9**(6): p. 475-85 1998.

257. Tabassian, A.R., E.S. Nylen, R.I. Linnoila, R.H. Snider, M.M. Cassidy, and K.L. Becker, Stimulation of hamster pulmonary neuroendocrine cells and associated peptides by repeated exposure to cigarette smoke. *Am Rev Respir Dis*. **140**(2): p. 436-40 1989.

258. Tang, W., G.P. Geba, T. Zheng, P. Ray, R.J. Homer, C. Kuhn, 3rd, R.A. Flavell, and J.A. Elias, Targeted expression of IL-11 in the murine airway causes lymphocytic inflammation, bronchial remodeling, and airways obstruction. *J Clin Invest*. **98**(12): p. 2845-53 1996.

259. Taylor, G., M.S. Lehrer, P.J. Jensen, T.T. Sun, and R.M. Lavker, Involvement of follicular stem cells in forming not only the follicle but also the epidermis. *Cell*. **102**(4): p. 451-61 2000.

260. Tebar, M., O. Destree, W.J. de Vree, and A.A. Ten Have-Opbroek, Expression of Tcf/Lef and sFrp and localization of beta-catenin in the developing mouse lung. *Mech Dev*. **109**(2): p. 437-40 2001.

261. Terskikh, A.V., M.C. Easterday, L. Li, L. Hood, H.I. Kornblum, D.H. Geschwind, and I.L. Weissman, From hematopoiesis to neuropoiesis: evidence of overlapping genetic programs. *Proc Natl Acad Sci U S A*. **98**(14): p. 7934-9 2001.

262. Tichelaar, J.W., L. Lim, R.H. Costa, and J.A. Whitsett, HNF-3/forkhead homologue-4 influences lung morphogenesis and respiratory epithelial cell differentiation in vivo. *Dev Biol*. **213**(2): p. 405-17 1999.

263. Tiddens, H., M. Silverman, and A. Bush, The role of inflammation in airway disease: remodeling. *Am J Respir Crit Care Med*. **162**(2 Pt 2): p. S7-S10 2000.

264. Tokiwa, H., N. Sera, A. Nakashima, K. Nakashima, Y. Nakanishi, and N. Shigematu, Mutagenic and carcinogenic significance and the possible induction of lung cancer by nitro aromatic hydrocarbons in particulate pollutants. *Environ Health Perspect*. **102 Suppl 4**: p. 107-10 1994.

265. Tropepe, V., B.L. Coles, B.J. Chiasson, D.J. Horsford, A.J. Elia, R.R. McInnes, and D. van der Kooy, Retinal stem cells in the adult mammalian eye. *Science*. **287**(5460): p. 2032-6 2000.

266. Tumbar, T., G. Guasch, V. Greco, C. Blanpain, W.E. Lowry, M. Rendl, and E. Fuchs, Defining the epithelial stem cell niche in skin. *Science*. **303**(5656): p. 359-63 2004.

267. Tuveson, D.A. and T. Jacks, Modeling human lung cancer in mice: similarities and shortcomings. *Oncogene*. **18**(38): p. 5318-24 1999.

268. Uchida, N., F.Y. Leung, and C.J. Eaves, Liver and marrow of adult mdr-1a/1b(-/-) mice show normal generation, function, and multi-tissue trafficking of primitive hematopoietic cells. *Exp Hematol*. **30**(8): p. 862-9 2002.

269. van de Wetering, M., E. Sancho, C. Verweij, W. de Lau, I. Oving, A. Hurlstone, K. van der Horn, E. Batlle, D. Coudreuse, A.P. Haramis, M. Tjon-Pon-Fong, P. Moerer, M. van den Born, G. Soete, S. Pals, M. Eilers, R. Medema, and H. Clevers, The beta-catenin/TCF-4 complex imposes a crypt progenitor phenotype on colorectal cancer cells. *Cell*. **111**(2): p. 241-50 2002.

270. van den Brink, G.R., S.A. Bleuming, J.C. Hardwick, B.L. Schepman, G.J. Offerhaus, J.J. Keller, C. Nielsen, W. Gaffield, S.J. van Deventer, D.J. Roberts, and M.P. Peppelenbosch, Indian Hedgehog is an antagonist of Wnt signaling in colonic epithelial cell differentiation. *Nat Genet*. **36**(3): p. 277-82 2004.

271. Van Eerdewegh, P., R.D. Little, J. Dupuis, R.G. Del Mastro, K. Falls, J. Simon, D. Torrey, S. Pandit, J. McKenny, K. Braunschweiger, A. Walsh, Z. Liu, B. Hayward, C. Folz, S.P. Manning, A. Bawa, L. Saracino, M. Thackston, Y. Benchekroun, N. Capparell, M. Wang, R. Adair, Y. Feng, J. Dubois, M.G. FitzGerald, H. Huang, R. Gibson, K.M. Allen, A. Pedan, M.R. Danzig, S.P. Umland, R.W. Egan, F.M. Cuss, S. Rorke, J.B. Clough, J.W. Holloway, S.T. Holgate, and T.P. Keith, Association of the ADAM33 gene with asthma and bronchial hyperresponsiveness. *Nature*. **418**(6896): p. 426-30 2002.

272. Van Lommel, A., T. Bolle, W. Fannes, and J.M. Lauweryns, The pulmonary neuroendocrine system: the past decade. *Arch Histol Cytol*. **62**(1): p. 1-16 1999.

273. van Tuyl, M. and M. Post, From fruitflies to mammals: mechanisms of signalling via the Sonic hedgehog pathway in lung development. *Respir Res*. **1**(1): p. 30-5 2000.

274. Van Winkle, L.S., A.R. Buckpitt, S.J. Nishio, J.M. Isaac, and C.G. Plopper, Cellular response in naphthalene-induced Clara cell injury and bronchiolar epithelial repair in mice. *Am J Physiol*. **269**(6 Pt 1): p. L800-18 1995.

275. Van Winkle, L.S., J.M. Isaac, and C.G. Plopper, Repair of naphthalene-injured microdissected airways in vitro. *Am J Respir Cell Mol Biol*. **15**(1): p. 1-8 1996.

276. Van Winkle, L.S., J.M. Isaac, and C.G. Plopper, Distribution of epidermal growth factor receptor and ligands during bronchiolar epithelial repair from naphthalene-induced Clara cell injury in the mouse. *Am J Pathol*. **151**(2): p. 443-59 1997.

277. Van Winkle, L.S., Z.A. Johnson, S.J. Nishio, C.D. Brown, and C.G. Plopper, Early events in naphthalene-induced acute Clara cell toxicity: comparison of membrane permeability and ultrastructure. *Am J Respir Cell Mol Biol*. **21**(1): p. 44-53 1999.

278. Van Winkle, L.S., M.J. Evans, C.D. Brown, N.H. Willits, K.E. Pinkerton, and C.G. Plopper, Prior exposure to aged and diluted sidestream cigarette smoke impairs bronchiolar injury and repair. *Toxicol Sci*. **60**(1): p. 152-64 2001.

279. Van Winkle, L.S., A.D. Gunderson, J.A. Shimizu, G.L. Baker, and C.D. Brown, Gender differences in naphthalene metabolism and naphthalene-induced acute lung injury. *Am J Physiol Lung Cell Mol Physiol*. **282**(5): p. L1122-34 2002.

280. Veeman, M.T., J.D. Axelrod, and R.T. Moon, A second canon. Functions and mechanisms of beta-catenin-independent Wnt signaling. *Dev Cell*. **5**(3): p. 367-77 2003.

281. Velilla, E., M. Lopez-Bejar, E. Rodriguez-Gonzalez, F. Vidal, and M.T. Paramio, Effect of Hoechst 33342 staining on developmental competence of prepubertal goat oocytes. *Zygote*. **10**(3): p. 201-8 2002.

282. Vermeer, P.D., R. Harson, L.A. Einwalter, T. Moninger, and J. Zabner, Interleukin-9 induces goblet cell hyperplasia during repair of human airway epithelia. *Am J Respir Cell Mol Biol*. **28**(3): p. 286-95 2003.

283. Vessey, C.J. and P.M. de la Hall, Hepatic stem cells: a review. *Pathology*. **33**(2): p. 130-41 2001.

284. Wagenaar, R.A., H.C. Crawford, and L.M. Matrisian, Stabilized beta-catenin immortalizes colonic epithelial cells. *Cancer Res*. **61**(5): p. 2097-104 2001.

285. Wagers, A.J., R.I. Sherwood, J.L. Christensen, and I.L. Weissman, Little evidence for developmental plasticity of adult hematopoietic stem cells. *Science*. **297**(5590): p. 2256-9 2002.

286. Warburton, D., C. Wuenschell, G. Flores-Delgado, and K. Anderson, Commitment and differentiation of lung cell lineages. *Biochem Cell Biol*. **76**(6): p. 971-95 1998.

287. Warburton, D., M. Schwarz, D. Tefft, G. Flores-Delgado, K.D. Anderson, and W.V. Cardoso, The molecular basis of lung morphogenesis. *Mech Dev*. **92**(1): p. 55-81 2000.

288. Warren, D.L., D.L. Brown, Jr., and A.R. Buckpitt, Evidence for cytochrome P-450 mediated metabolism in the bronchiolar damage by naphthalene. *Chem Biol Interact*. **40**(3): p. 287-303 1982.

289. Watkins, D.N., D.M. Berman, S.G. Burkholder, B. Wang, P.A. Beachy, and S.B. Baylin, Hedgehog signalling within airway epithelial progenitors and in small-cell lung cancer. *Nature*. **422**(6929): p. 313-7 2003.

290. Watt, F.M., Epidermal stem cells: markers, patterning and the control of stem cell fate. *Philos Trans R Soc Lond B Biol Sci*. **353**(1370): p. 831-7 1998.

291. Watt, F.M. and B.L. Hogan, Out of Eden: stem cells and their niches. *Science*. **287**(5457): p. 1427-30 2000.

292. Watt, F.M., Stem cell fate and patterning in mammalian epidermis. *Curr Opin Genet Dev*. **11**(4): p. 410-7 2001.

293. Watt, F.M., The stem cell compartment in human interfollicular epidermis. *J Dermatol Sci*. **28**(3): p. 173-80 2002.

294. Wattiez, R., C. Hermans, A. Bernard, O. Lesur, and P. Falmagne, Human bronchoalveolar lavage fluid: two-dimensional gel electrophoresis, amino acid microsequencing and identification of major proteins. *Electrophoresis*. **20**(7): p. 1634-45 1999.

295. Wattiez, R., C. Hermans, C. Cruyt, A. Bernard, and P. Falmagne, Human bronchoalveolar lavage fluid protein two-dimensional database: study of interstitial lung diseases. *Electrophoresis*. **21**(13): p. 2703-12 2000.

296. Weaver, M., N.R. Dunn, and B.L. Hogan, Bmp4 and Fgf10 play opposing roles during lung bud morphogenesis. *Development*. **127**(12): p. 2695-704 2000.

297. Wechsler-Reya, R. and M.P. Scott, The developmental biology of brain tumors. *Annu Rev Neurosci*. **24**: p. 385-428 2001.

298. Weidenfeld, J., W. Shu, L. Zhang, S.E. Millar, and E.E. Morrisey, The WNT7b Promoter Is Regulated by TTF-1, GATA6, and Foxa2 in Lung Epithelium. *J Biol Chem*. **277**(23): p. 21061-70 2002.

299. Weissman, I.L., D.J. Anderson, and F. Gage, Stem and progenitor cells: origins, phenotypes, lineage commitments, and transdifferentiations. *Annu Rev Cell Dev Biol*. **17**: p. 387-403 2001.

300. Welm, B.E., S.B. Tepera, T. Venezia, T.A. Graubert, J.M. Rosen, and M.A. Goodell, Sca-1(pos) cells in the mouse mammary gland represent an enriched progenitor cell population. *Dev Biol*. **245**(1): p. 42-56 2002.

301. Wert, S.E., S.W. Glasser, T.R. Korfhagen, and J.A. Whitsett, Transcriptional elements from the human SP-C gene direct expression in the primordial respiratory epithelium of transgenic mice. *Dev Biol*. **156**(2): p. 426-43 1993.

302. West, J.A., A.R. Buckpitt, and C.G. Plopper, Elevated airway GSH resynthesis confers protection to Clara cells from naphthalene injury in mice made tolerant by repeated exposures. *J Pharmacol Exp Ther*. **294**(2): p. 516-23 2000.

303. West, J.A., C.H. Chichester, A.R. Buckpitt, N.K. Tyler, P. Brennan, C. Helton, and C.G. Plopper, Heterogeneity of clara cell glutathione. A possible basis for differences in cellular responses to pulmonary cytotoxicants. *Am J Respir Cell Mol Biol*. **23**(1): p. 27-36 2000.

304. West, J.A., K.J. Williams, E. Toskala, S.J. Nishio, C.A. Fleschner, H.J. Forman, A.R. Buckpitt, and C.G. Plopper, Induction of tolerance to naphthalene in Clara cells is dependent on a stable phenotypic adaptation favoring maintenance of the glutathione pool. *Am J Pathol*. **160**(3): p. 1115-27 2002.

305. Whitsett, J.A., J.C. Clark, L. Picard, J.W. Tichelaar, S.E. Wert, N. Itoh, A.K. Perl, and M.T. Stahlman, Fibroblast growth factor 18 influences proximal programming during lung morphogenesis. *J Biol Chem*. **277**(25): p. 22743-9 2002.

306. Widdicombe, J.G. and R.J. Pack, The Clara cell. *Eur J Respir Dis*. **63**(3): p. 202-20 1982.

307. Wine, J.J., The genesis of cystic fibrosis lung disease. *J Clin Invest*. **103**(3): p. 309-12 1999.

308. Wong, M.H., J. Huelsken, W. Birchmeier, and J.I. Gordon, Selection of multipotent stem cells during morphogenesis of small intestinal crypts of Lieberkuhn is perturbed by stimulation of Lef-1/beta-catenin signaling. *J Biol Chem*. **277**(18): p. 15843-50 2002.

309. Wright, D.E., A.J. Wagers, A.P. Gulati, F.L. Johnson, and I.L. Weissman, Physiological migration of hematopoietic stem and progenitor cells. *Science*. **294**(5548): p. 1933-6 2001.

310. Wu, R., Y.H. Zhao, C.G. Plopper, M.M. Chang, K. Chmiel, J.J. Cross, A. Weir, J.A. Last, and B. Tarkington, Differential expression of stress proteins in nonhuman primate lung and conducting airway after ozone exposure. *Am J Physiol*. **277**(3 Pt 1): p. L511-22 1999.

311. Wulf, G.G., K.L. Luo, K.A. Jackson, M.K. Brenner, and M.A. Goodell, Cells of the hepatic side population contribute to liver regeneration and can be replenished with bone marrow stem cells. *Haematologica*. **88**(4): p. 368-78 2003.

312. Xu, Y., D. Banerjee, J. Huelsken, W. Birchmeier, and J.M. Sen, Deletion of beta-catenin impairs T cell development. *Nat Immunol*. **4**(12): p. 1177-82 2003.

313. You, Y., E.J. Richer, T. Huang, and S.L. Brody, Growth and differentiation of mouse tracheal epithelial cells: selection of a proliferative population. *Am J Physiol Lung Cell Mol Physiol*. **283**(6): p. L1315-21 2002.

314. Youngson, C., C. Nurse, H. Yeger, and E. Cutz, Oxygen sensing in airway chemoreceptors. *Nature*. **365**(6442): p. 153-5 1993.

315. Zechner, D., Y. Fujita, J. Hulsken, T. Muller, I. Walther, M.M. Taketo, E.B. Crenshaw, 3rd, W. Birchmeier, and C. Birchmeier, beta-Catenin signals regulate cell growth and the balance between progenitor cell expansion and differentiation in the nervous system. *Dev Biol*. **258**(2): p. 406-18 2003.

316. Zepeda, M.L., M.R. Chinoy, and J.M. Wilson, Characterization of stem cells in human airway capable of reconstituting a fully differentiated bronchial epithelium. *Somat Cell Mol Genet*. **21**(1): p. 61-73 1995.

317. Zhou, S., J.D. Schuetz, K.D. Bunting, A.M. Colapietro, J. Sampath, J.J. Morris, I. Lagutina, G.C. Grosveld, M. Osawa, H. Nakauchi, and B.P. Sorrentino, The ABC transporter Bcrp1/ABCG2 is expressed in a wide variety of stem cells and is a molecular determinant of the side-population phenotype. *Nat Med*. **7**(9): p. 1028-34 2001.

318. Zhou, S., J.J. Morris, Y. Barnes, L. Lan, J.D. Schuetz, and B.P. Sorrentino, Bcrp1 gene expression is required for normal numbers of side population stem cells in mice, and confers relative protection to mitoxantrone in hematopoietic cells in vivo. *Proc Natl Acad Sci U S A*. **99**(19): p. 12339-44 2002.

319. Zhu, Z., C.G. Lee, T. Zheng, G. Chupp, J. Wang, R.J. Homer, P.W. Noble, Q. Hamid, and J.A. Elias, Airway inflammation and remodeling in asthma. Lessons from interleukin 11 and interleukin 13 transgenic mice. *Am J Respir Crit Care Med*. **164**(10 Pt 2): p. S67-70 2001.